ADDIS ABABA UNIVERSITY
ADDIS ABABA INSTITUTE OF TECHMNOLOGY

ROLLOVER OPTIMIZATION AND RIDE COMFORT VERIFICATION OF FOUR-WHEELER BAJAJ QUTE

BY: - MUKEREM GETAHUN

FINAL THESIS PAPER SUBMITTED FOR THE PARTIAL FULFILLMENT OF THE DEGREE OF MASTER OF SCIENCE IN MECHANICAL ENGINEEERING

(MECHANICAL DESIGN)

ADVISOR: - Ermiase g. Koricho (PhD)

ADDIS ABABA, ETHIOPIA

FEBRUARY 28, 2020

Table of content

LIST OF TABLES

LIST OF FIGURES

Acknowledgment

Firstly, I am grateful to the Almighty God (Allah) for the good health and wellbeing that were necessary to complete this thesis. Next, I would like to express my sincere gratitude to my advisor Dr Ermiase g. Koricho for the continuous support of my research, for his patience, motivation, and immense knowledge. His guidance helped me in all the time of research and writing of this thesis.

Besides my advisor, I would like to thank for the rest of mechanical engineering staff members, for their insightful comments and encouragement, and also for the critical question which incented me to widen my research from various perspectives.

I thank my colleagues for stimulating discussions for the times we were working together before deadlines, and for all the fun we have had in the last two and half years.

Last but not the least, I would like to thank my family: my parents and to my brothers and siters for supporting me.

ABSTRACT

Bajaj qute is four-wheeler type of bajaj which is categorized under small utility vehicles (LTV). In our country (Ethiopia) Bajaj qutes are the main transportation system in transport industry. Passenger cars had the lowest rollover fatality rate (23 percent of fatalities were in vehicles that rolled over), while SUVs had the highest, 59 percent. Clearly, rollover crashes are a major safety problem for all classes of light vehicles, particularly LTVs. Except on static stability factor (SSF) approach for the analysis, there is no enough research paper which worked particularly on rollover propensity of Bajaj qute. SSF ignored the effect of suspension system. In reality vehicle suspension allowed for significant movements of wheels with respect to the body. And it had significant effect on lateral behavior of bajaj qute. The lateral forces are transmitted between the body and the wheels by rigid suspension arms. The suspension arm should also be analyzed by FEA to ensure that the part is strong enough to with stand the applied loads. In addition, varying the rollover behavior of a car could have an effect on ride comfort behavior of the passenger occupant. It is needed to verify the effect on ride comfort behavior of Bajaj After the rollover behavior of the car is changed. The whole suspension system of bajaj qute was modelled in ANSYS and ADAMS/CAR for structural and dynamic analysis respectively. The part with worst loading was selected for structural analysis to ensure that the part is strong enough to with stand the load applied. For dynamic analysis, the full vehicle was modelled for roll over analysis. Hence, both suspension system and full vehicles are optimized by ADAMS/INSIGHT for suspension parameter and rollover respectively. Sprung mass RMs values for different bajaj qute speeds were calculated to check ride comfort behavior of original and optimized model. From the structural analysis the lower control arm was strong enough to with stand the load applied. Furthermore, the analysis showed that the arm carries extra strength which takes us to additional weight. So that, topology optimization is done with constant fatigue life. Using topology optimization, the mass of the vehicle was reduced and resulted in to reduction of carbon emission of Bajaj qute by 1.4%. using the rollover optimization, the fishhook speed of car was increased from 50km/hr to 60km/hr. Ride comfort analysis showed that, even if both the original and optimized models are within the standard limit, the optimized model was more comfortable for the passenger occupant than the original one. Finally, as a conclusion, suspension systems parameters had invaluable effect on the lateral behavior of car.

Key words: Bajaj qute, rollover, ADAMS/CAR, Ride comfort, SSF, ADAMS/INSIGHT

CHAPTER 1 INTRODUCTION

1.1 BACKGROUND OF THE STUDY

Baja qute earlier called bajaj RE60, is rear wheel-drive, four-passenger quadricycle built by the Indian company Bajaj auto. Bajaj qutes are the main transportation system in transport industry. The vehicle has independent suspension on front and rear as well. Suspension system is the term given to the system of springs, shock absorbers and linkages that connect a vehicle to its wheels. When a tire hits an obstruction, there is a reaction force and the suspension system try to reduce this force. A suspension system is comprised of an arrangement of springs, shock absorbers, and linkages, which allow a vehicle's body to be controlled. If the suspension system of the vehicle is not robust, and the driver cannot control it, the power produced by the engine is worthless. Further, to ensure smooth movement, a vehicle needs to absorb all of the bumps and holes on the surface of a road using its suspension system. Without this system, even the smallest of bumps, which may appear negligible to a passenger, will disrupt the smoothness of a journey. Different types of springs and suspension systems are used depending on the type of vehicle. Independent Suspensions. To provide the best possible ride quality, many vehicles use fully independent front Dependent Suspensions. Still found on the rear of many vehicles and on the front of most heavy-duty vehicles, dependent suspensions sacrifice ride quality for strength. Since the movement of one wheel affects the opposite wheel, ride quality and handling suffer on these systems. A large, straight I-beam is often used on the front of heavy-duty vehicles, such as buses and semi-truck[1].

The most important assembly designs of the automobile are suspension, engine, and transmission. The design of suspension system influences a variety of performances. Vehicle suspension is the important structure linked to the frame and tires. Suspension system design is sensitive to vehicle parameters. Bajaj qute car are four-wheel type light weight vehicles. Most of the existed models use simple independent coil spring type suspension system. Varying the parameters like, suspension geometry (hard point location) directly affect the performance and cornering behavior of a car. It needs to be optimized to develop compatible and robust suspension system for better lateral stable and ride comfort the bajaj qute.

In this paper, a relevant type of optimization approach is selected and analyzed for improving the vehicle performances under different loading conditions. Structural optimization for lower control arm of front suspension system, dynamic optimization for front and rear suspension system, and verification of ride comfort are amongst the main issues addressed in this paper.

1.2 STATEMENTS OF THE PROBLEM

Now a day in our country (Ethiopia) Bajaj qutes are one of the main transportation systems in transport industry. Bajaj qute is four-wheeler type of vehicles which is categorized under light vehicles.

Passenger cars had the lowest rollover fatality rate (23 percent of fatalities were in vehicles that rolled over), while SUVs had the highest, 59 percent[2], [3]. Clearly, rollover crashes are a major safety problem for all classes of light vehicles, particularly LTVs and small passenger cars [3].

According to the above description on rollover fatalities, light vehicles are more prone to rollover relative to other class of cars. But there is no enough research paper which works particularly on rollover propensity of bajaj qute. Debebe[4] studied the rollover behavior of Bajaj Qute using a static stability factor approach. Static stability factor is a ratio of half-track width to the height of vehicle center of gravity above ground[5]. This measure of rollover propensity reflects only the most fundamental relationship. It is obtained under the assumption that a vehicle is a rigid body and ignores all higher order effects, in particular the effects of suspension and tire compliance. In reality vehicle suspension allows for significant movements of wheels with respect to the body.

There exists a variety of models, which predict vehicle rollover propensity and in particular lateral acceleration at the rollover threshold. They range from a simplistic static stability factor ground at one side of the spectrum to complex computer models on the other. None of these extremes provides significant insights into the effects of vehicle suspension design on rollover propensity[6]. However, recent published literature has shown significant insights by relating a suspension design parameters with lateral behavior of a car to combat rollover fatalities [2], [5]–[8].

Neglecting the compliances of suspensions and tires leads to overestimation of rollover threshold. During cornering vehicle body rolls about the roll axis, resulting in the lateral shift of vehicle center of gravity towards outside of turn. At the same time lateral forces of the outside tires cause lateral deformation of the tires and camber. This lateral movement is determined primarily by suspension kinematics. Debebe varied track width for better tilt angle in optimum static Stability factor ranges. The angle of tilt of bajaj Qute increased from 53.25^0 to 56.65^0 with the increment in track width of 200mm. Finally, Debebe also recommended to work on lateral behavior of the car and topology optimization for weight reduction.

In this paper the rollover propensity of bajaj qute is studied based on primary factor called suspension parameters. In addition to the lateral dynamic behavior, the lateral forces are transmitted between the body and the wheels by rigid suspension arms. Hence the worst loaded arm should be analyzed and optimized. FEA is applied to ensure that the part is strong enough to withstand the workloads. FEA results such as the stresses, fatigue life and deflections of parts, were considered to ensure reliability of the vehicle for the intended uses.

Furthermore, varying the rollover behavior of a car could have an effect on ride comfort behavior of the passenger occupant. It is needed to verify the effect on ride comfort behavior of bajaj due to changing of the rollover behavior caused by various suspension parameters, and finally taking corrective measure if the ride comfort is not comfortable according to ISO 2635.

1.3 OBJECTIVES OF THE STUDY

1.3.1 MAIN OBJECTIVES OF THE STUDY

The main objective of the thesis is, rollover optimization of Bajaj qute based on suspension parameters to overcome lateral instability of Bajaj qute and to improve ride comfort behavior.

1.3.2 SPECIFIC OBJECTIVES OF THE STUDY

- Rollover optimization is done to overcome lateral instability.
- Structural analysis of front suspension system is done to ensure the performance of the arm withstanding of the load applied
- Ride comfort verification is done to check whether the rollover optimization affects the ride comfort behavior of bajaj qute or not. Rms (root mean square) values of sprung mass acceleration is a deciding factor.

CHAPTER TWO LITERATURE REVIEW

Rollovers are among the most severe traffic crashes and are of particular concern for occupant of light trucks and vans (Ltv) including pickup trucks, sport utility vehicles (SUV)[3]. Vehicle roll dynamics are strongly influenced by suspension properties[6].

Suspension systems have evolved significantly since the earliest adaptations from horse-drawn buggies to self- powered automobiles, but the basic requirements remain the same[9]. Just as in the horse and buggy days, today's suspension systems must provide for safe handling and maximum traction while being able to sustain passenger comfort. To accomplish these goals, modern suspension systems rely on various types of springs, shock absorbers, control arms, and other components. All of the components of the suspension system must work together to provide the proper ride quality and handling characteristics expected by the driver and passengers[10]. Each component is engineered to work as a part of the overall system. If one part of the system fails, it can lead to faster wear or damage to other components. Therefore, a complete understanding of each component and how it functions as part of the whole suspension system is critical[11] .

Currently, there are three types of automotive suspensions commonly used namely passive, semi active, and active. All of the systems are based by either pneumatic or hydraulic operation[12]. It was asserted that some of these suspension systems cannot fully solve automobile oscillations problem, because they are very costly and lend towards vehicle energy consumption increment[13]-[16].

Automotive manufacturers often compete against each other to develop dependable and comfortable drive characteristics while at the same time also producing best stability during braking and cornering[17]. In a vehicle, problems happen while driving on bumpy road condition. The shock absorber is one of the suspension systems is designed to handle shock impulse and dissipate kinetic energy. It decreases amplitude of disturbances leading to increase in comfort and improved ride[18].

The spring is compressed when the wheel strikes a bump. The compressed spring rebound to its normal dimension which causes the body to lift up. The spring goes down below its normal length when the weight of the vehicle pushes the spring down. The spring bouncing process occurs again and again, until the up-and-down movement finally stops. Hence, spring design in a suspension system is utmost crucial[17].

Conventionally, the design practice of vehicle suspensions has been based on trial and error approaches, where designers iteratively change the values of the design variables and reanalyze the system until acceptable design criteria are achieved[19]. This is both time-consuming and tedious.

Due to advances in computational power and theoretical methods, the focus of vehicle suspension design has switched from pure numerical analysis to extensive design synthesis using optimization approaches[20]–[23]. A number of optimization algorithms have been used to determine optimal suspension characteristics [24]. Research reveals[25]–[27] that suspension system design is iterative process. Good suspension system improves ride quality, cornering and braking efficiency. Bajaj qute cars uses independent type suspension systems. Modification for any parameter can affect the performance of suspension system and needs analysis and verification.

Considering the pollution is originated from automotive, one of the solutions for reducing produced fumes by cars and factories could be mass reduction[28]–[31]. This approach leads to less energy and fossil fuel consumption. Different optimization methods help engineers and designers produce automotive components with low mass and high performance[30]. This paper [32]presents a survey of manufacturing-oriented topology optimization methods.. Efficient implementation of manufacturing constraints is still a critical problem in topology optimization. Even though the topology optimization method has been widely accepted in recent years in the industrial design process for delivering optimized designs on weight, materials, functionality and cost, the results are typically considered conceptual due to loosely defined topologies and the necessary interpretation and post- processing steps. Imposing manufacturing constraints[33] should be approached with caution because it can affect the performance and functionality of the optimized design, potentially crippling the optimality of the solution. From an industrial point of view, the complexity of a topology optimization design should be such that existing manufacturing techniques can be applied. This has been a long-standing problem since the beginning of the topology optimization method. [34] discussed a systematic methodology of structural bionics is presented and utilized in design case. The type spectrum is developed for the “top-down” approach of mechanical lightweight design, based on the structure, load and function similarities. The structural bionic method can increase the structural efficiency and produce innovative ideas or conceptual solutions, which is valuable and meaningful compared with conventional design method. This research could eventually lead to the lightweight design of new bio-inspired mechanical structures.

Every automotive suspension has two goals, passenger comfort and vehicle control. Comfort is provided by isolating the vehicle's passengers from road disturbances like bumps or potholes. Control is achieved by keeping the car body from rolling and pitching excessively, and maintaining good contact between the tire and the road[35].

Present automotive market demands low cost and light weight component to meet the need of fuel efficient and cost-effective vehicle. This in turn gives the rise to more effective use of materials for automotive parts which can reduce the mass of vehicle. Since automotive components are under dynamic loads which cause fatigue damage, considering fatigue criteria seems to be essential in designing automotive components[30], [32], [35]. Then, the topology optimization is performed based on fatigue life criterion. Topology optimization allows designers to start with a design that already has the advantage of optimal material distribution and is ready for design fine tuning with shape or size optimization[30].

During the car crash accidents, when the car is damaged from front side, it was seen that the lower suspension arm is the strongest and is just slightly damaged[36]. Therefore, it can be said that the lower suspension arm carries over strength. From this observation the material optimization team from Tata Motors found the scope to optimize lower suspension arm. So that, bajaj qute also needs analysis of lower control arm as well.

There exists a variety of models, which predict vehicle rollover propensity and in particular lateral acceleration at the rollover threshold. They range from a simplistic static stability factor ground (Garrot et al., 1999) at one side of the spectrum to complex computer models (Allen et al. 1999) on the other. None of these extremes provides significant insights into the effects of vehicle suspension design on rollover propensity[5]. This paper presents a method for systematic investigations on dynamic roll behavior and improvement to the stability dynamics based on varying hard points of suspension system.

Suspension system is one of the important components to connect a vehicle body and its wheel, which does not only affects the vehicle ride comfort, but also has the negative effects on the road surface as well as safe driving [37]. Parameters matching, and optimization of suspension system are an important approach to improve vehicle ride comfort. Changing the suspension parameters have significant effect on the ride comfort of a car.

CHAPTER THREE

RESEARCH METHODS FOR STRUCTURAL ANALYSIS

3.1 DATA COLLECTION

3.1.1 PRIMARY DATA COLLECTION

Internal data related to this paper are collected in different ways. Materials related properties, and standard are assessed from published journals. But the specifications, which are mainly related to bajaj qute, are assessed from maintenance company and importers manuals. Some of the main data are described in Table 3.1. The other data mainly applied for analysis and simulation like engine power, gear specification, electricity, and vehicle properties are listed in table form in appendix A

Table 3. 1 specification data of bajaj qute[4]

Data	Measurement
Length*width*height	2752mm*1312mm*1652
Kerb weight	390kg (weight of the motor car without an occupant
Wheelbase	1925mm
Suspension front	Independent suspension twin leading arm
Suspension rear	Independent suspension coil spring semi-trailing arm
Turning radius	3.5mm
Frame type	Monocoque chassis

3.1.2 SECONDARY DATA COLLECTION

The basic constraint that happened in data collection was finding the specification of the geometry of the suspension system. But it was very difficult because there is no local manufacturing company here in Ethiopia. Assembly system information and the dimension of each element was the main input to model the suspension system for further analysis of structural as well as dynamic system.

It was not easy to get the geometrical dimension, the assembly guides and of the material structure. Hence, the only option to model and virtualize the system is reverse engineering. To reverse engineering the external data, have incredible uses. We start first manually reverse-engineering the whole suspension system with the help of special tools like Vernier gauge, radius gauge and divider etc. All the dimensions which are measured have been recorded on the drawing (as shown in fig 3.1). based on the collected dimensions, modelling of suspension system is done in solid work software.

3.2 STRUCTURAL MODELING OF FRONT SUSPENSION SYSTEM

The vehicle has an independent suspension on the front and rear as well. Independent suspension allows each wheel on the same axle to move independently(vertically) of each other. Note that "independent" refers to the motion or path of movement of the wheel/suspension.

Figure 3. 1 Sample photos from Hora Bajaj (Goro branch Addis Ababa)

We start first manually reverse-engineering the whole suspension system with the help of measuring tools like Vernier gauge, radius gauge and divider etc. All the dimensions, which are

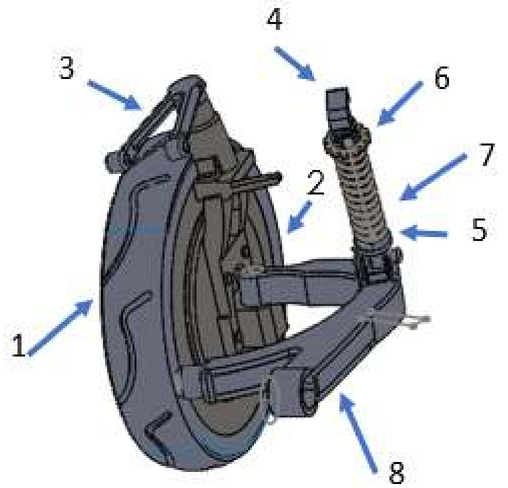

ITEM NO.	PART NUMBER	DESCRIPTION	QTY.
1	tire design		1
2	rim-suspension system		1
3	ed upper control arm		1
4	ed top rod		1
5	ED BASE		1
6	ed nut		1
7	ed spring		1
8	lower control arm for analysis		1

Figure 3. 2 Solid work modelling of front suspension system

measured, have been recorded on the drawing. Now by taking the dimensions from the drawing modeling of the suspension system is done in solid work software (depicted in fig 3.2).

3.3 WORKING ANALYSIS FOR WORST LOADED PART AND CONDITIONS

Due to its various functions, the control arm is one of the critical components in the suspension system. When the vehicle takes turn various types of forces are acting on the wheels which are transmitted to the control arm through attachments such as ball joint assembly and so on, to the wheel[38]. These torque and force values can be mentioned in the load case. Here in this analysis, the main concern is to find out the maximum stress region and stress values in the control arm and compare this value with the yield strength of materials and working for topological optimization.

In the above model, it is visible that the worst loaded part is the lower control arm. Lower control arm carries all the loads such as weight of the car, braking force, cornering forces, bump forces and accelerating forces. All these loads make lower control arm vulnerable for failures. So that the structural analysis of the lower control arm can confirm as the structural stability of the suspension system. Structural analysis is used to calculate the stresses, deformation, and fatigue life that are generated by the mechanical loads. It is done to determine the effect of loads on the physical structure. The lower control arm is connected to the wheel and chassis of a car. The lower control arm experiences several loads. Due to these loads, the lower control arm undergoes deformation.

Due to deformation and cyclic loads the lower control arm fails. To overcome the shortcomings and prolong life, automotive manufactures makes lower control arm stronger[36]. During the car crash accidents, when the car is damaged from front side, it was seen that the lower suspension arm is the strongest and is just slightly damaged[36]. Therefore, it can be said that the lower suspension arm carries over strength. So, it is necessary to calculate the stresses acting on the lower arm before the manufacturing of arm. FEA is used to ensure that all parts, linkages, and systems, which make up a vehicle, are strong enough to withstand the workloads[39]. Table 3.2 describes the material properties of structural steel. This material is one of the most used to manufacture this mechanical part in commercial automobiles[40].

Table 3. 2 Material properties of the lower control arm[4]

parameter	values	units
density	7850	Kg/m3
Youngs modules	2E+05	MPa
Poisson's ratio	0.3	
Yield tensile strength	250	MPa
weight	19.15	kg

3.3.2 IMPORTING FRONT LOWER ARM SUSPENSION SYSTEM IN TO ANSYS WORKBENCH

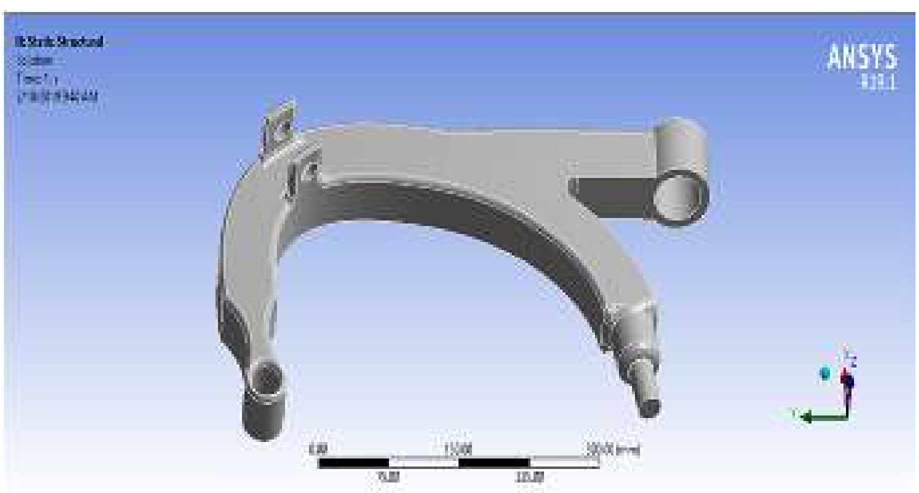

Figure 3. 3 Imported model to Ansys workbench

3.3.3 MESHING THE MODEL

In meshing the element type, the quadratic tetrahedron is also called ten node tetrahedron is used. It is a second-order complete polynomial adherent of the isoparametric tetrahedron family. In this element, the stress calculation is considerably better than the four nodes. This element proceeds the compensations of the existence of fully automatic tetrahedral mashers. The meshing method used is patch conforming second order tetra element. Tetra elements are solid elements which have been extracted from 2D tri elements. This type of meshing is used as it consists of additional mid nodes due to which the deformation can be captured more accurately[41].

Figure 3. 4 Meshed model

Fig 3.4 describes the quality of the mesh. Low Orthogonal Quality or high skewness values are not recommended. Generally, it is recommended to keep minimum orthogonal quality > 0.1, or maximum skewness < 0.95.

Table 3. 3 skewness mesh metric spectrum

excellent	Very good	good	acceptable	bad	unacceptable
0-0.25	0.25-0.5	0.5-0.8	0.8-0.94	0.95-0.97	0.98-1.00

Table 3. 4 orthogonal quality mesh metric spectrum

unacceptable	bad	acceptable	good	very good	excellent
0-0.001	0.001-0.14	0.15-0.2	0.2-0.69	0.70-0.95	0.95-1.00

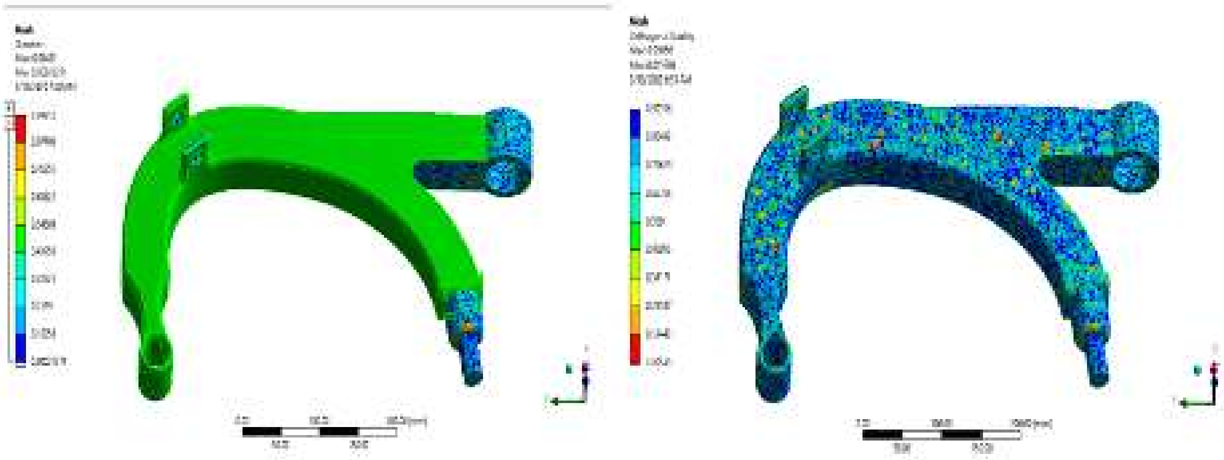

(a) skewness (b) Orthogonal quality

Figure 3. 5 mesh quality spectrum (a) skewness (b) orthogonal quality

3.3.4 APPLYING THE BOUNDARY CONDITION

As it is displayed in the modelling (Table 3.2) left-hand end is connected to the ball joint where it moves in a vertical direction i.e. z and this vertical load is from the ground (bump force) and it is calculated as shown below. It is fixed in the x-and y-directions, such that there is no motion in x- and y-direction. Where the right-hand front and rear end are fixed in z-direction so that it cannot move in vertical direction since they are connected to chassis. And it can rotate only in x-direction but rotation is fixed in y and z-direction. Cornering and braking loads are calculated to be applied for both ends.

Figure 3. 6 Applying boundary conditions

3.4 CALCULATING AND APPLYING THE LOADS ON THE MESHED CONSTRAINED MODEL

3.4.1 BUMP FORCE

Bump force especially for a formula-one car can go up to 10G which means the load on every wheel can become 10 times the static load on that wheel[42]. However, since Bajaj qute has no large aerodynamics forces and speeds are much lower than the go-kart circuit, the bumps are taken slower. Hence, in this work, the acceleration is assumed to be 2G or smaller.

The car mass is 400kg, together with driver and passenger of the average mass of 65 kg is 660 kg.

Without load transfer, 40% of the load is on the front wheels,

$$weight\ on\ thee\ front\ wheels = \frac{40}{100}(660kg) = 264kg$$

$$static\ load\ on\ each\ wheel\ of\ front\ axle = 132kg$$

$$bump\ forces = 2G = 2 * 132kg * \frac{9.81m}{sec^2}$$

$$bump\ force = 2589.84 \qquad equation\ 3.1$$

3.4.2 BRAKING FORCES

During braking or accelerating the front or rear load distribution will change. While the braking load is transferred to the front axle and when accelerating the load is transferred to the rear axle. In driving, one should always brake and accelerate as fast as possible. This is limited by the tire longitudinal friction coefficient $\mu_{long.}$

When breaking all tires are producing friction forces: this gives forces equilibrium shown as follows

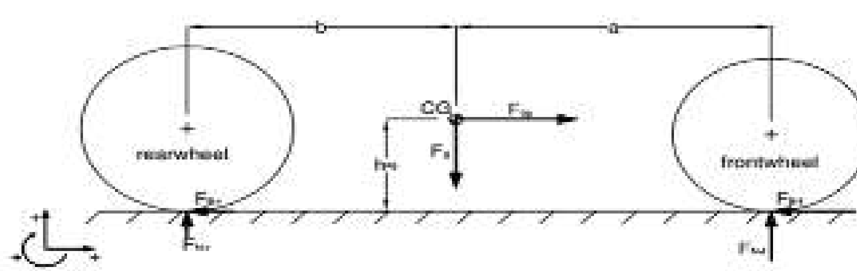

Figure 3. 7 Force equilibrium during braking [42]

With:

F_g $force\ of\ gravity$

F_{cg} $inertia\ force$

$F_{N-f,r}$$norma\ force\ front\ and\ rear\ wheel$

a, b $distances\ rear\ and\ front\ axle\ to\ center\ of\ gravity$

h_{cg} $height\ center\ of\ gravity$

It is required to solve four equations to find the brake distribution during maximum braking.

The equilibrium of moments around CG:

$\sum M_{cg} = 0$

$b * F_{Nr} + h_{cg} * (F_{B-f} + F_{B-r}) - a * F_{N-f} = 0$ $equation\ 3.2$

And the force the equilibrium in vertical direction

$\sum F_y = 0$

$F_{N-f} + F_{N-r} - F_g = 0$ $equation\ 3.3$

F_{Bf} and F_{Br} can be written as a function of F_{Nf} and F_{Nr}

$F_{B-f} = \mu long_f * F_{N-f}$ $equation\ 3.4$

$F_{B-r} = \mu long_r * F_{N-r}$ $equation\ 3.5$

$F_g = m * g = 660kg * 9.81\ {}^{m}/_{sec^2} = 6474.6N$

$F_{N-f} + F_{N-r} = F_g = 6474.6N$ $equation\ 3.6$

μlong for the front tire = 0.7, for the tire normal force of 1249N

for the rear tire on dry road

μlat − r = μlong = 0.8

simplifying all the equation and we get,

$Fnf = 4840N$

$Fnr = 1634.4N$

3.4.3 APPLYING LOADS WHEN THE QUTE IS IN BRAKING MANEUVER

Figure 3. 8 Load histories in a braking maneuver

3.4.4 CORNERING FORCES

Lateral load transferring takes place when cornering. The force equilibrium on the front of the car during cornering at constant speed is shown as follows.

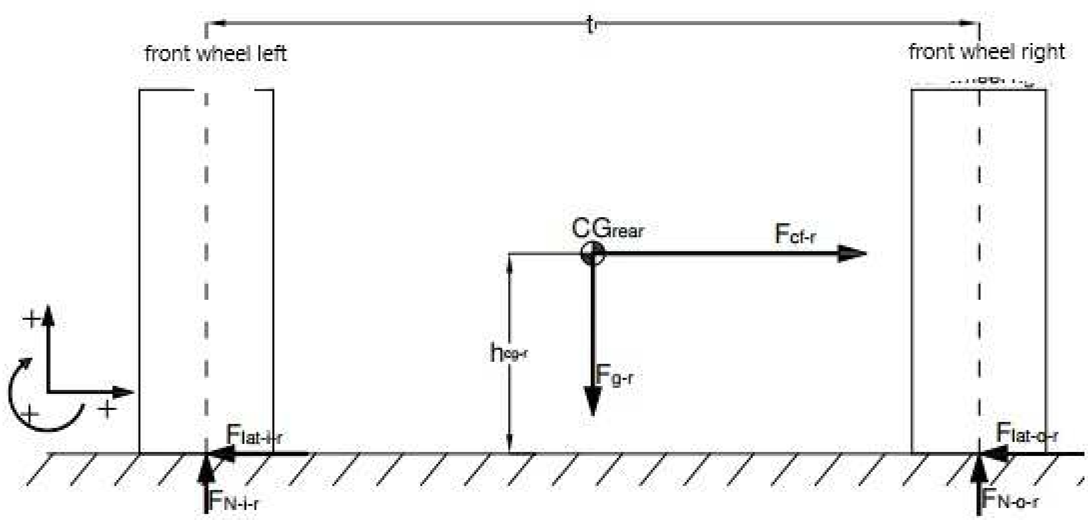

Figure 3. 9 Force equilibrium during cornering maneuver [42]

F_{g-f} $gravity\ force\ front (40\%\ of\ total\ gravity\ force)$

F_{cf-f} $centrifugal\ force\ front(40\%\ total\ centrifugal\ force)$

$F_{N-i-o-f}$ $normal\ force\ inner\ and\ outer\ front\ wheels$

t_r $track\ width$

h_{cg-r} $height\ center\ of\ gravity\ front$

The equilibrium of moments around CG:

$\sum M_{cg-f} = 0$

$\frac{1}{2} * t_f * F_{N-i-f} + h_{cg-f} * (F_{lat-i-f} + F_{lat-o-f}) - \frac{1}{2} * t_r * F_{N-o-f} = 0$

The equilibrium in the vertical direction:

$\sum F_y = 0$

$F_{N-i-f} + F_{N-o-f} - F_{g-f} = 0$

$F_{lati-f} and\ F_{lat-o-f} canbe\ written\ as\ functions\ of\ F_{N-i-f}\ and\ F_{N-o-f}$

$F_{lat-i-f} = \mu_{lat-f} * F_{N-i-f}$

$F_{lat-o-f} = \mu_{lat-f} * F_{N-o-f}$

μ_{lat} $is\ a\ function\ of\ the\ tire\ normal\ force\ and\ is\ calculated\ in\ paragraph$

Simplifying all the equation for cornering force and we get

$F_{lat-i-f} = 355.9N$

$F_{lat-o-f} = 1456.3N$

The control arm chassis points are exposed to 728.5N force at each point.

3.4.5 APPLYING THE LOADS WHEN THE QUTE IS IN CORNERING MANEUVER

Figure 3. 10 Load histories in a cornering maneuver

3.5.5 FATIGUE LOADING IN BRAKING AND CORNERING MANEUVER

Fatigue failure is defined as the tendency of a material to fracture by means of progressive brittle cracking under repeated alternating or cyclic stresses of an intensity considerably below the normal strength. Although the fracture is of a brittle type, it may take some time to propagate, depending on both the intensity and frequency of the stress cycles.

Fatigue analysis itself usually refers to one of two methodologies. The local-strain or strain-life (E-N) method, commonly referred to as the crack initiation method was more recently developed and is intended to describe only the ‘initiation’ of a crack. This approach is best suited for low cycle fatigue problems, where the applied stresses have a significant plastic component.

The stress-life (or S-N method), is commonly referred to as the total life method since it makes no distinction between initiating or growing a crack. This was the first fatigue analysis method to be developed over 100 years ago. It assumes the structure to be fully elastic (even in local fatigue-related details like notches). The initiation or growing phase of a crack is not considered. Applicable to high cycle fatigue problems (low load-long life). This approach should not be used to estimate fatigue lives below 10,000 cycles. The structural analysis for the lower control arm is characterized by low loading and high cyclic fatigue lives. The stress life approach is best suited and adopted in this paper.

Mathematical description of the material S-N curve[35]:

$$S_a = \sigma_a = A.N_f^{-B} \qquad \text{equation 3.7}$$

where

σa – applied alternating stress
A – constant, value of σa at one cycle
B – Basquin's exponent, the slope of the log-log curve
Nf - the number of cycles of stress that a specimen sustains before failure occurs

3.6 TOPOLOGY OPTIMIZATION

From the above analysis, it implies that stress and deformation are below the yield limit of structural steel even though the fatigue life of the lower control arm at constant throughout the arm. It is needed to remove the material by increasing the compliance of the structure and taking the fatigue life in to consideration by using the topology optimization tool. Topology optimization has become a popular topic in the field of optimal design is necessary to apply mathematical and mechanical tools for a solution even in case of simple structures. Hence, it requires an iterative solution technique to be adopted[43].

The topology optimization process aims at distributing a specified amount of materials in a given design domain by minimizing an objective function and fulfilling the asset of constraints[44]. Here the focus is on density-based formulations. Topology optimization can be implemented through the use of finite element methods for the analysis and optimization technique based on the homogenization method, optimality criteria method, level set, moving asymptotes, genetic algorithms.

To formulate the structural optimization problem, an objective function, design variables and state variables need to be introduced. The objective function (f), represents an objective that could either be minimized or maximized. A typical objective could be the stiffness or volume of a structure. Furthermore, some structural design domain and state variables associated with the objective function needs to be defined. The design variables (x) describes the design of the structure, it may represent the geometry. The state variables (y) represents the structural response which can, for example, be recognized as stress, strain or displacement. Furthermore, the state variables depend on the design variables y(x). The objective function is subjected to the design and state variable constraints to steer the optimization to a sought solution[28].

$$\begin{cases} \min x \quad f\big(x, y(x)\big) \\ \text{subject} \begin{cases} \text{design constraint on } x \\ \text{state constraint on } y(x) \\ \text{equilibrum constraint} \end{cases} \end{cases}$$

In the present problem, ANSYS software, which is robust and with built-in topology optimization module, is used to model, analyze and perform a topology optimization.

The optimization process consists of the following process, as shown in Figure 3.10. In addition to this fig 4.7 describes convergency process.

Figure 3. 11 Topology optimization process

There are two options available in the ANSYS 19.1 topology optimization module, optimal criteria module, which is the default, and sequential convex programming optimization approach.

3.6.1 GENERAL MATHEMATICAL APPROACH FOR TOPOLOGY OPTIMIZATION

The goal of the topology optimization is to find the optimal use of material for vehicle body such that an objective criterion (i.e. global stiffness, natural frequency etc.) is achieved subject to given constraints (i.e. Volume reduction).

In topological optimization objective function (f) is minimized or maximized subject to the defined constraints (gj). Densities of each finite element(i) are treated as design variables (ηi) in the topological problem. The pseudo density for each element varies from 0 to 1; where ηi ≈0 represents material to be removed; and ηi ≈1 represents material that should be kept. Mathematically the optimization problem expressed as:

$$f = \text{minimize or maximize with respect to } \eta_i$$

Subjected to

$$0 \leq \eta_i \leq 1 \qquad \text{where } i = 1,2,3 \ldots N$$

$g_{j1} < g_j < g_{ju}$ where $j = 1,2,3 \ldots \ldots . M$

$N =$ number of finite elements

$M =$ number of constraints

$g_j =$ computed j^{th}constraintg value

$g_{j-1,u} =$ lower, upper bound forjthconstraint

3.6.2 OPTIMAL CRITERIA METHOD IN ANSYS 19.1 MODULE

In structural topology optimization problem, the purpose is to determine material distribution which optimizes a certain objective function (e.g. minimum compliance, maximum force, maximum displacement) for structure with a given load and support subjected to prescribed volume or mass. the distribution of material is limited to the design domain, **Ω** which forms apart of from the large domain which can include areas prescribed to be solid or void.

For example, one seeks to minimize the energy of the structural static compliance (UC) for a given load case subject to a given volume reduction. Minimizing compliance is equivalent to maximizing the global structural static stiffness. Minimum compliance topology optimization problems impose a constraint on the amount of material that can be utilized. In this case, the optimization problem is formulated as follow. For our analysis, in order to reduce the mass of the control arm, the element density is the design variable, fatigue life is a design constraint and compliance is considered as objective function which is supposed to be minimized.

$UC = a\ minimum\ witht\ respect\ to\ \eta i$

Subjected to

$0 \leq \eta i \leq 1\ \ where\ i = 1,2,3 \ldots \ldots N$

$V \leq Vo - V^*$

Where, $V = computed\ volume$

$V0 = orginal\ volume$

$V^* = amount\ material\ to\ be\ removed$

3.7 DESIGN REALIZATION

The objective of the design process is to create a cost-effective design that meets certain expectations towards functionality and appearance. The design is created in an iterative process where the analysis of the structural behavior leads to changes in the design. It is very common that these changes are obtained using a trial and error approach. The use of optimization technology will change the design process into a process-driven directly by computational analysis. The design problem can be given as a structural optimization problem. The application of structural optimization allows an efficient search for the right combination of design variables for a certain design.

Very little attention has been paid to manufacturing aspects in optimal structural design. Most automotive structures are manufactured by sheet metal components welded together[29]. Spot and seam welding are applied. The welding process is very labor-intensive. Hence, saving a number of welds drive down the labor cost. Also, the manufacturing methods, such as casting, forming have not been taken into consideration so far, but can if applied in the conceptual design phase lead to substantial cost savings.

3.7.1 CONSIDERING SHAPE OPTIMIZATION BASED ON BIOLOGICAL GROWTH

The Biological Growth Method (BGM) is a shape optimization method focused on the stress of structural parts[45]. This method is based on the observation that biological structures as tree trunks and animal bones evolve by adding new layers of biological material at the surface with stress promoted growth rate. Structural bionics is a highly interdisciplinary science, which now involves understanding and application of biological structure principles for technical developments. A systematic approach is therefore necessary for lightweight design of mechanical structures[34].

It has been shown that biological structures self-optimize their shapes by growth with respect to the natural loading applied. The word optimum in this case means that in all the structures considered (tree butts, branch joints, deer antlers, antelope horns, tiger claws, camel thorns, etc.)

a state of constant stress at the surface of the biological 'component" was always given for the

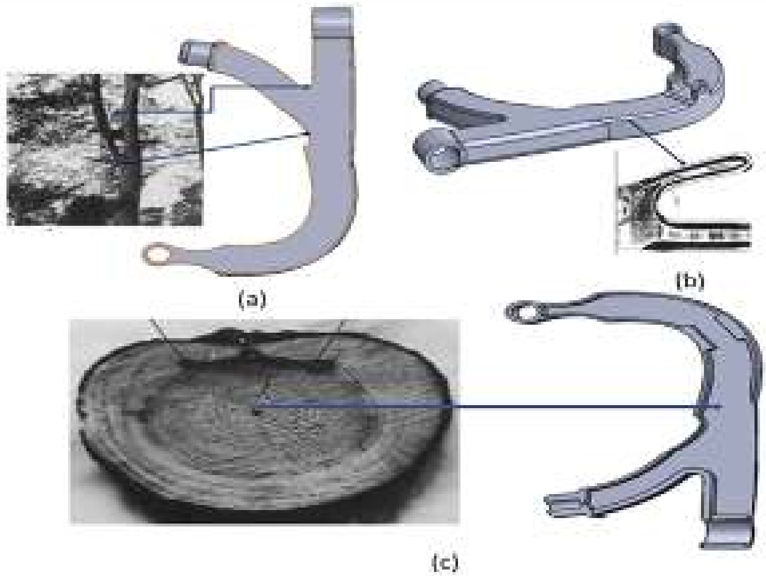

Figure 3. 12 consideration of biological growth (a) tree elongation for constant stress natural optimization(b) further increase in lateral diameter only above the lateral bridge (c) outer most growth ring adapts to external loading [46]

natural loading case applied. The idea was proposed by [47] to copy the mechanism of the tree growth in order to optimize mechanical engineering structures. It is based on the unproven but plausible assumption that biological load carriers can survive only if they are mechanically optimized, lightweight and fatigue resistant. It also relies on the law that not only the full-grown biological specimen is optimized but also the mechanism by which this optimum is reached the mechanism of biological growth. Because the growth behavior of trees is easier to simulate on a computer than the growth of bones, the method copies tree growth in order to provide the manufacturer with lightweight constructions with minimized notch stresses to guarantee a long fatigue life. In trees, only the outermost growth ring adapts to external loading (Fig 3.11).

3.7.2 IMPORTING THE EDITED MODEL AND MESHING FOR ANALYSIS

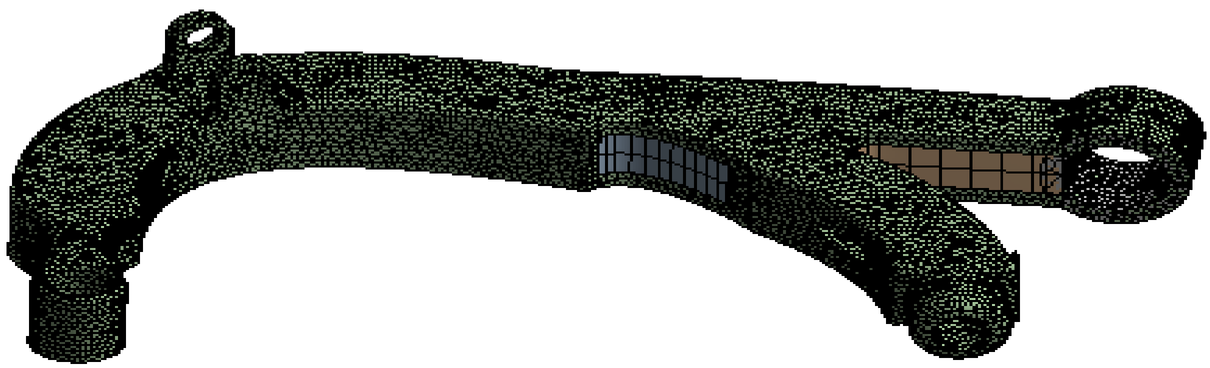

Figure 3. 13 Mesh for optimized model

Figure 3.18 shows optimized model after topology optimizations. The model is refined and the loads are applied on the model (Fig 3.12) based on the loading conditions discussed in the previous topic to validate if the optimized model is still in the working condition. The concept for the biological growth mechanisms are included in the design realization process.

3.7.3 LOAD AND BOUNDARY CONDITION FOR BRAKING AND CORNERING MANEUVER

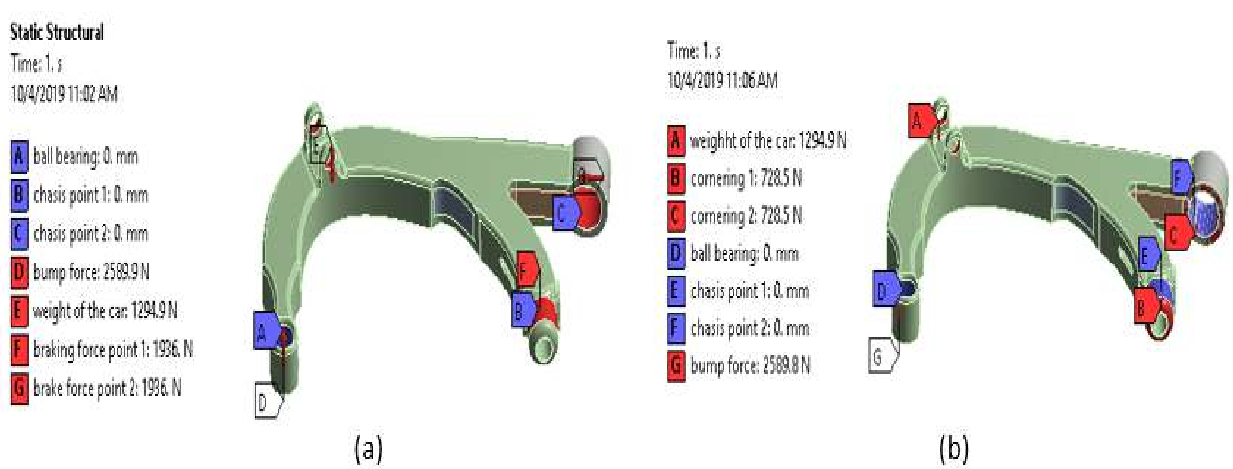

Figure 3. 14 Load and boundary condition (a) braking maneuver (b) cornering maneuver

CHAPTER FOUR
RESULTS AND DISCUSSION FOR STRUCTURAL ANALYSIS

4.1 TOTAL DEFORMATION, STRESS (VON MISES) AND FATIGUE LIFE OF LOWER CONTROL ARM BEFORE OPTIMIZATION

4.1.1 TOTAL DEFORMATION (BRAKING MANEUVER)

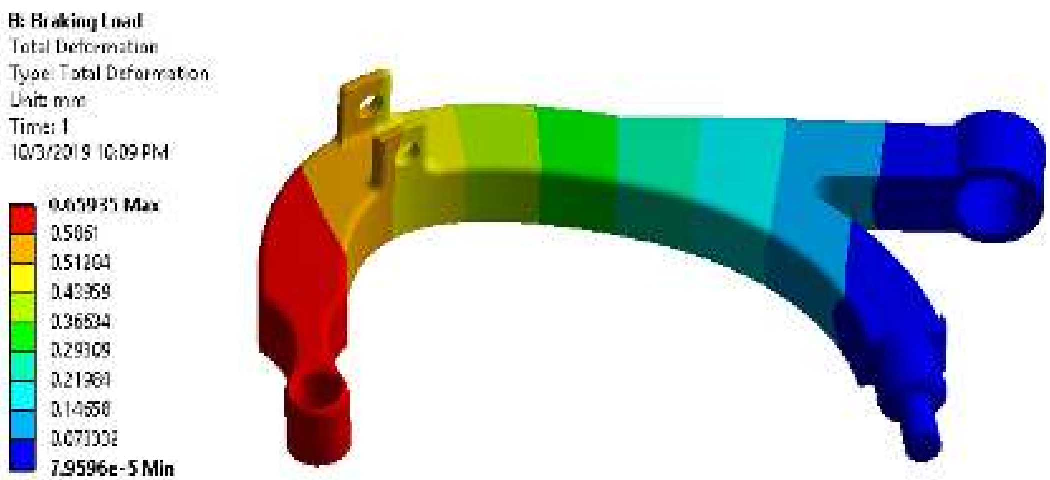

Figure 4. 1 Total deformations in a braking maneuver

4.1.2 STRESS ANALYSIS (BRAKING MANEUVER)

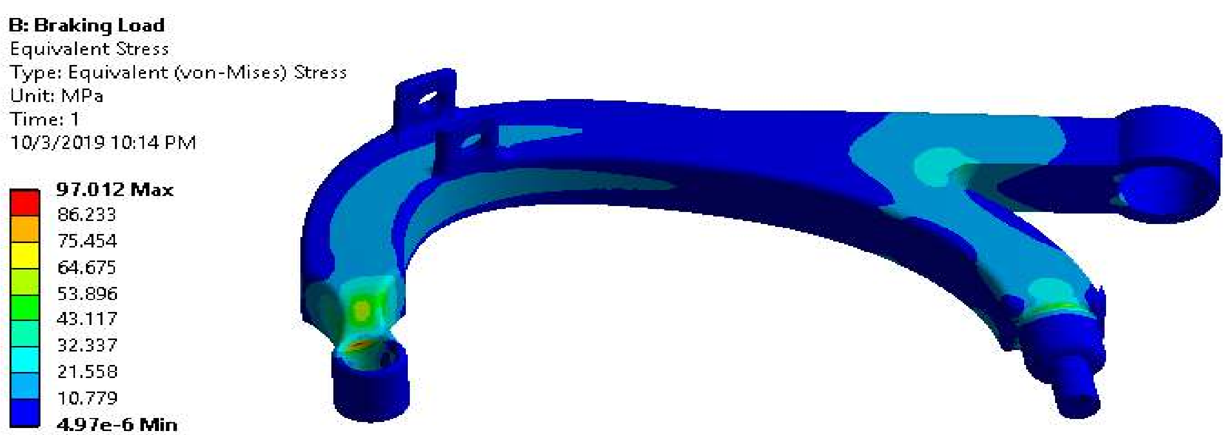

Figure 4. 2 Stress distribution in braking maneuver

4.1.3 TOTAL DEFORMATION (CORNERING MANEUVER)

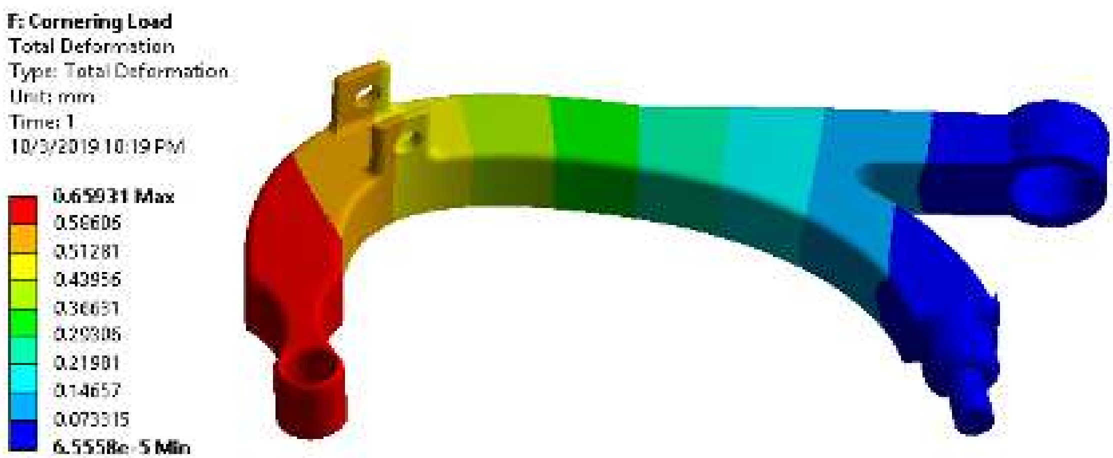

Figure 4. 3 Total deformations in a cornering maneuver

4.1.4 STRESS ANALYSIS (CORNERING MANEUVER)

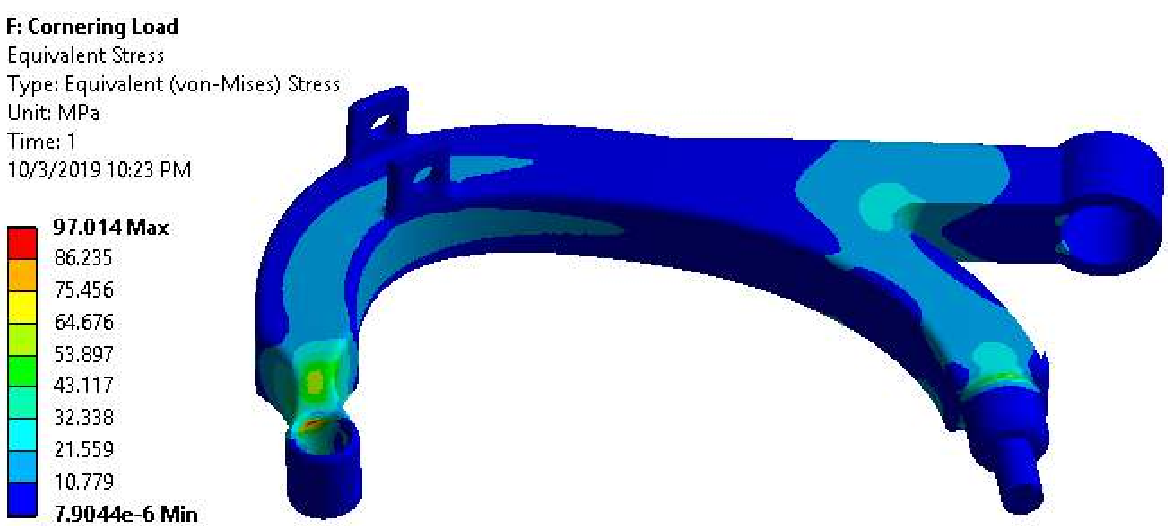

Figure 4. 4 Stress distribution in a cornering maneuver

4.1.5 FATIGUE LIFE FOR CORNERING AND BRAKING MANEUVER

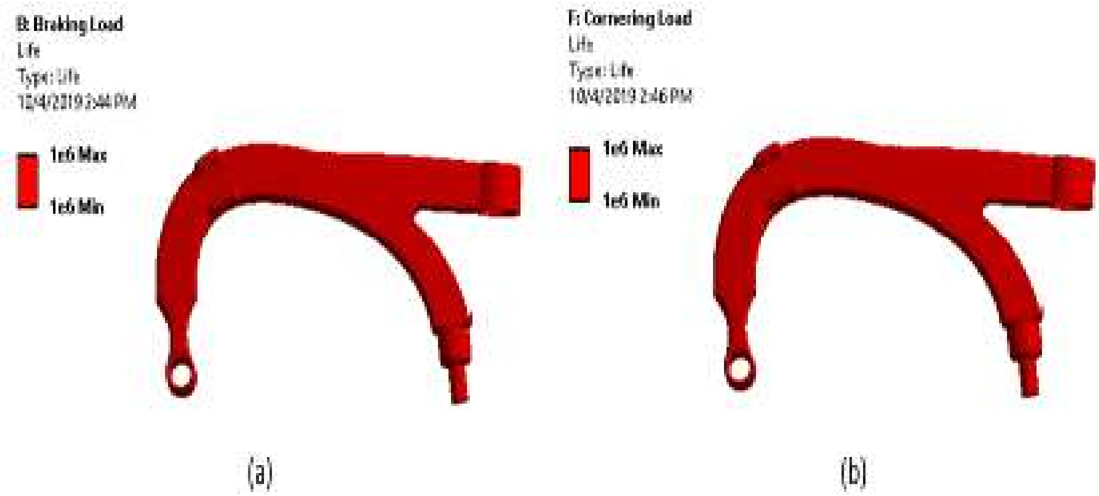

Figure 4. 5 Fatigue life (a) cornering maneuver (b) braking maneuver

4.2 OPTIMIZED MODEL

Figure 4. 6 Optimized model

4.3 OBJECTIVE (COMPLIANCE) AND MASS RESPONSE CONVERGENCE

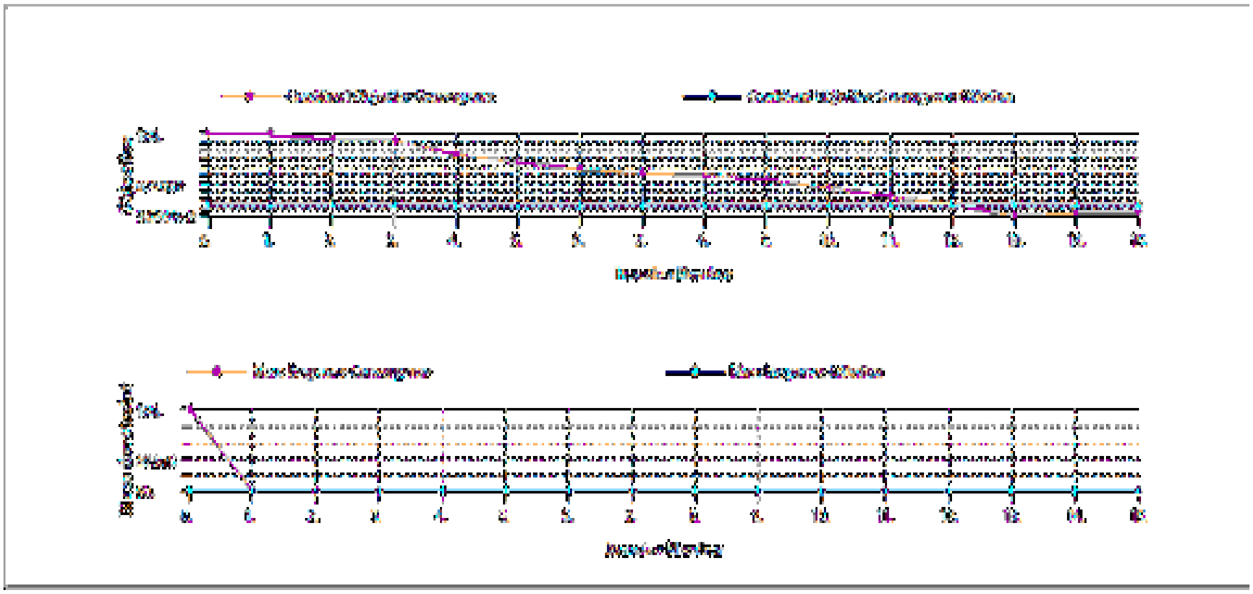

Figure 4. 7 Objective and design variable convergence

4.4 TOTAL DEFORMATION, STRESS (VON MISES) AND FATIGUE LIFE OF LOWER CONTROL ARM AFTER OPTIMIZATION

4.4. 1 STRESS AND DEFORMATION IN BRAKING MANEUVER FOR OPTIMIZED MODEL

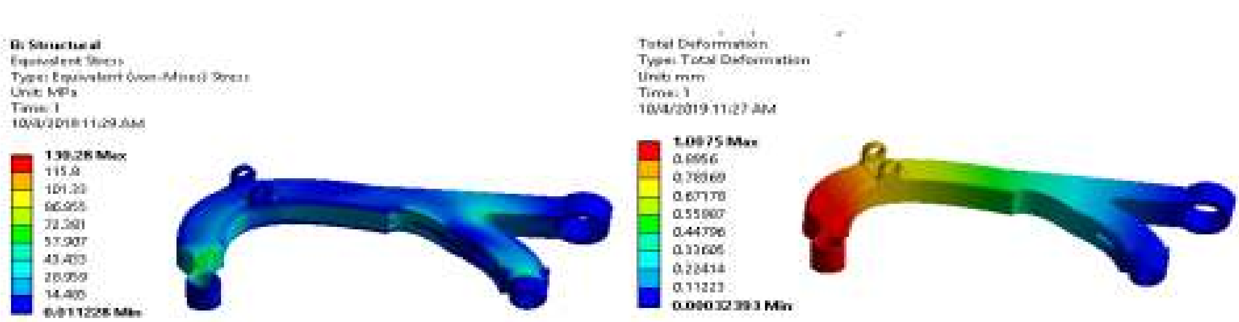

Figure 4. 8 Optimized model (a) stress analysis (b) deformation analysis in braking maneuver

4.4.2 STRESS AND DEFORMATION IN CORNERING MANEUVER FOR OPTIMIZED MODEL

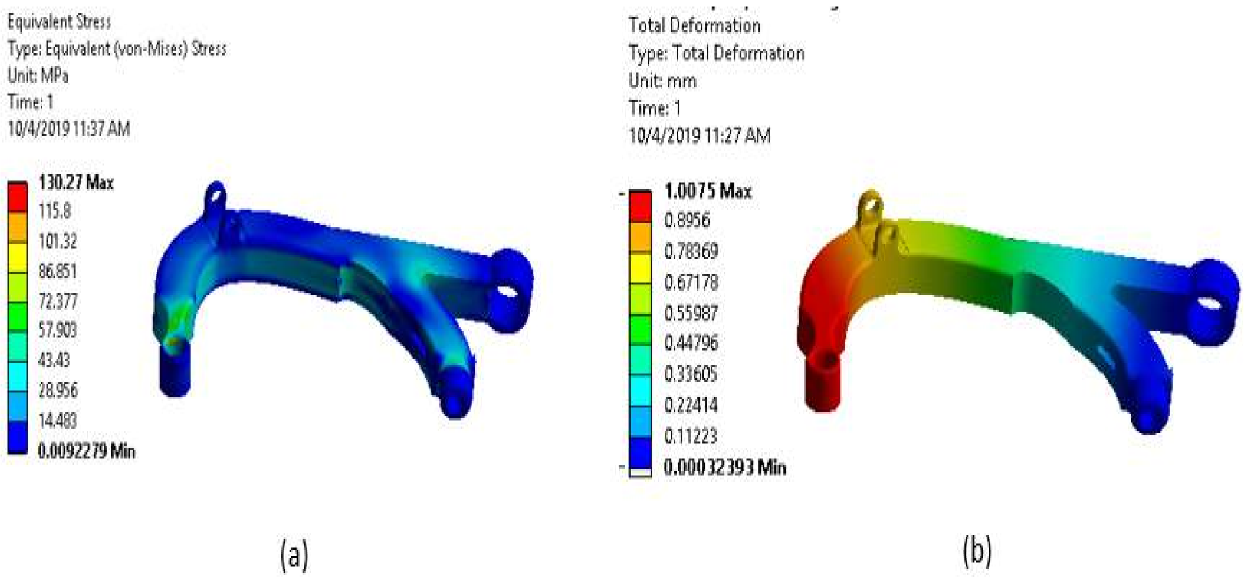

Figure 4. 9 Optimized model stress analysis deformation analysis

4.4.3 FATIGUE LIFE FOR OPTIMIZED MODEL

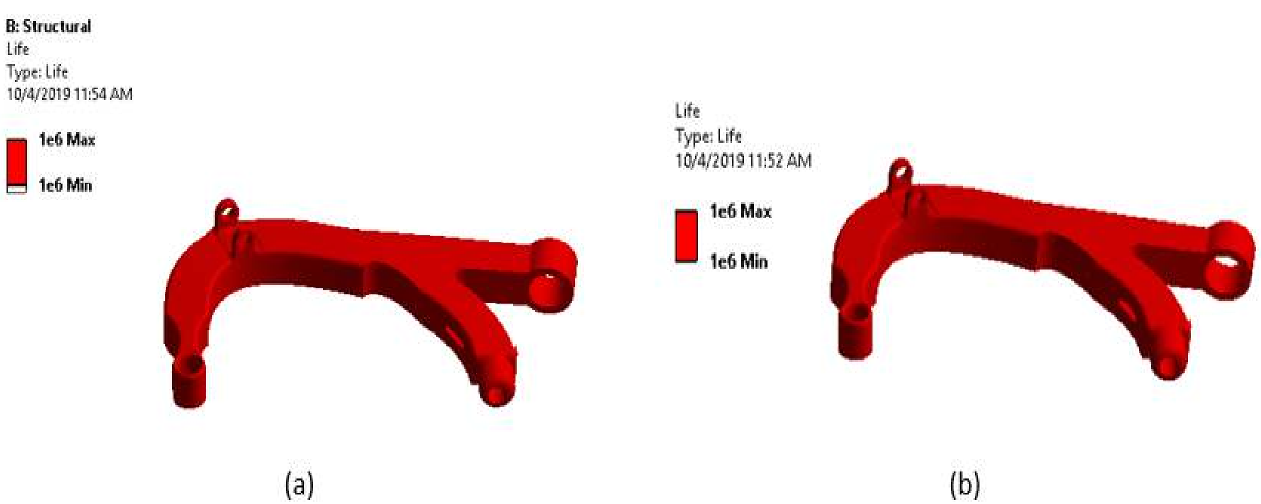

Figure 4. 10 Fatigue life for fatigue constrained optimized model (a) braking (b) cornering maneuver

4.5 DISCUSSION

After optimization, the weight of the lower control arm is reduced. Due to this, stress induced in the arm is increased but still in the working limit. The stress value analysis for an optimized suspension system shows that the maximum principal stress is within yield limit and fatigue life is constant (shown in Fig 4.11). So that the design is safe. The geometry of an optimized lower control arm saves 9kg weight form each arm. Considering the pollution is originated from automotive, one of the solutions for reducing produced fumes by cars and factories could be mass reduction[30]. This approach leads to less energy and fossil fuel consumption. Reduction in the weight of the car has a direct relationship with carbon emission reduction. Even from this analysis, it is shown that there is a 2.8% reduction of weight. The weight reduction has significant effect on carbon emission which is not less than 2.8% of carbon emission reduction from the total amount.

The von mise stress, deformation, and also fatigue life for existing and optimized lower control arm are shown comparatively below.

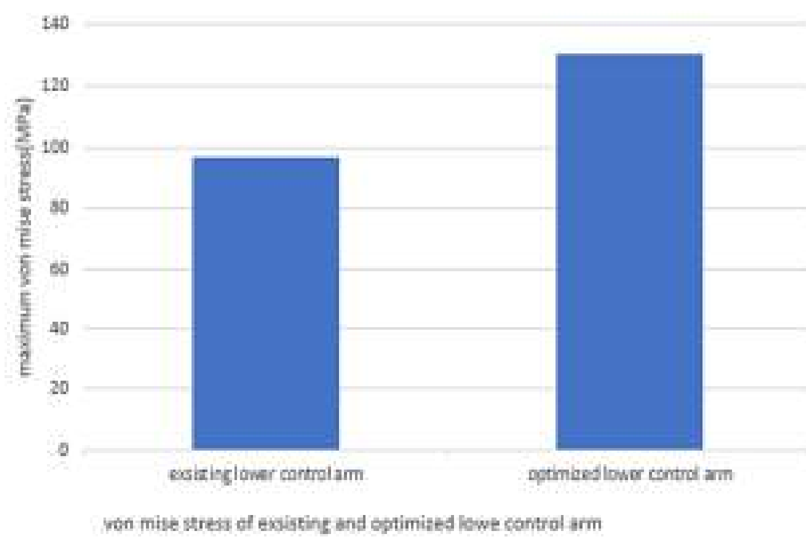

(a)

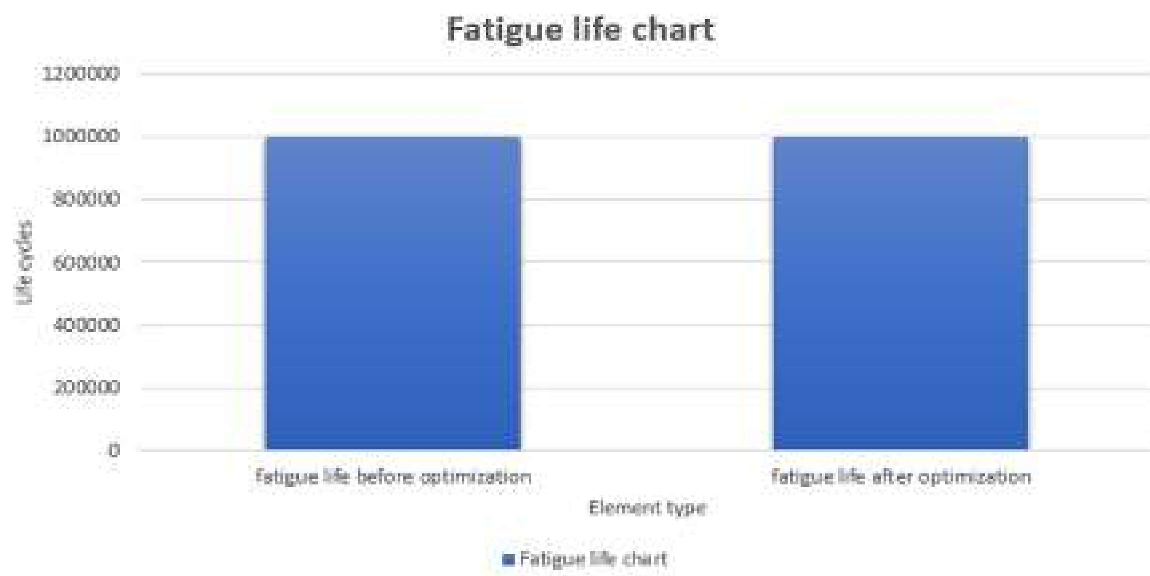

(b)

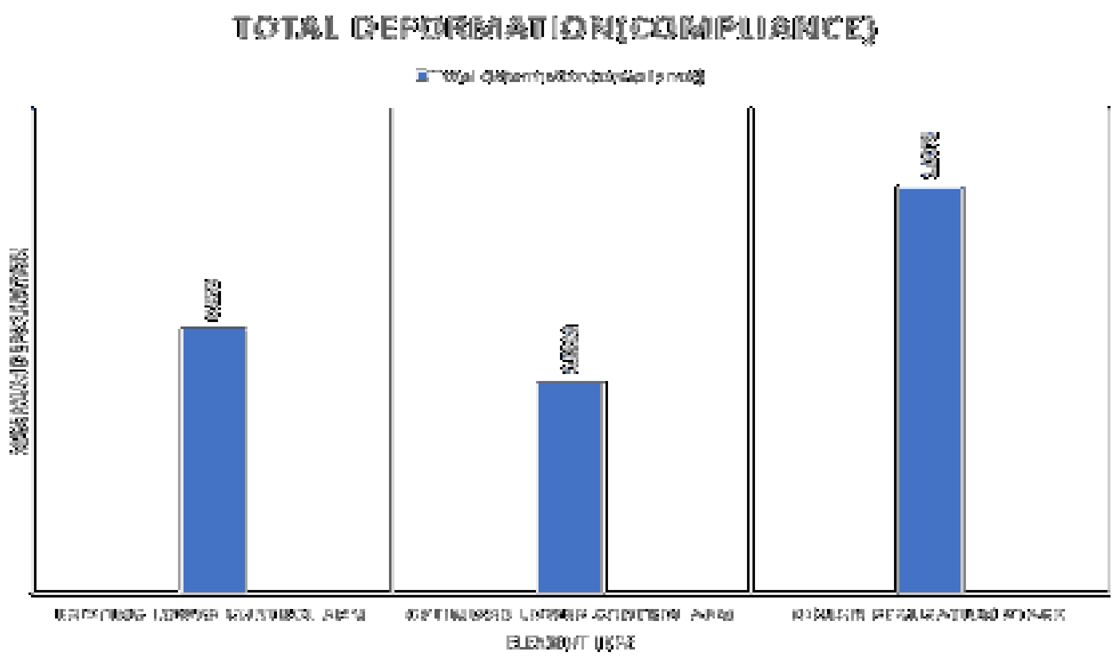

(c)

Figure 4. 11 Comparison of design parameters before and after optimization (a) vonmises stress (b) fatigue life (c) total deformation

The existing lower control arm is subjected to the load due to which stress and deformation are developed which are in the desired range of fatigue life and strength (as shown in Figure 4.11).

The maximum stress and deformation developed for the optimized model are depicted from Figure 4.8 to Figure 4.10 which are less than the yield point allowable deformation of the material.

FEA analysis shows that the maximum von mises stress value of an optimized component is 130.27Mpa which is below the yield limit as shown in the Figure 4.9 According to Fig 4.9 the safety factor of the optimal design is 1.92. There is no cutoff decision to specify the minimum permissible safety factor. According to many enthusiasts, the recommended factor of safety for this mechanical part (as it is ductile material) should be greater than 1.2. Hence the optimization process is safe[48]–[50].

After analysis of the new optimized model results revealed that

- ❖ The presented methodology approximately uniform for life cycle time for design of lower control arm.
- ❖ The mass reduction of the lower control arm was found to be 45% compared to the original model with desired fatigue life and strength.
- ❖ The approach used in this paper can be applied to other vehicle components to reduce vehicle weight.
- ❖ Therefore, there is potential to contribute towards environmental sustainability by better conserving worlds metal resources and reducing carbon emission through improved overall vehicle fuel efficiency

CHAPTER FIVE
RESEARCH METHODS FOR DYNAMIC ANALYSIS

The process for this study involved several important steps. It starts with modelling of front twin leading arm suspension system and rear trailing arm suspension system using MSC/ADAMS car, employing simulation analysis of the current model and generated for the kinematic and compliance data for selected output and optimization is done to ensure rollover stability.

5.1 MODELING OF FRONT SUSPENSION SYSTEM

The multibody models of suspension systems are built using MSC ADAMS/CAR based on actual Bajaj qute car suspension system named as twin leading arm suspension system. In order to replicate the actual suspension system, the model must be built using the same parameter as the actual suspension such as hardpoints, geometry, damper profiles, spring stiffness, material selection of components, joint types and orientation as well as bushing properties. There was a total of 13 components hard point in x, y, z direction for both suspension models with specific joining type and orientation.

	loc_x	loc_y	loc_z
hpl_lower_arm_front	0.0	-556.0	0.0
hpl_lower_arm_rear	350.0	-556.0	0.0
hpl_lower_control_arm_inner	350.0	-256.0	0.0
hpl_spring_lower	62.0	-406.0	50.0
hpl_strut_lower	40.0	-406.0	0.0
hpl_strut_upper	220.0	-406.0	420.0
hpl_sub_frame_inner	500.0	-256.0	0.0
hpl_sub_frame_rear	500.0	-556.0	0.0
hpl_tierod_inner	-150.0	-250.0	420.0
hpl_tierod_outer	-100.0	-474.0	420.0
hpl_upper_control_arm_inner	180.0	-330.0	420.0
hpl_upper_control_arm_outer	180.0	-506.0	420.0
hpl_wheel_carier_upper	0.0	-506.0	420.0
hpl_wheel_center	0.0	-606.0	100.0

(a)

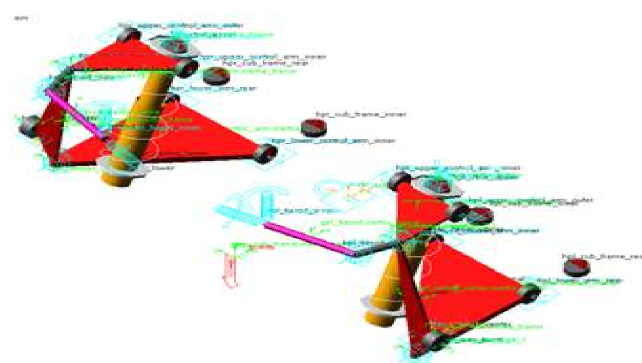

(b)

Figure 5. 1 Front suspension template (a) hardpoints or key location for modeling (b) modeled template

The modeling stage is started by generating the suspension model template in the template view in MSC/ADAMS car (shown in Fig 5.1)

The coordinates basically define the key points to generate a template in ADAMS/CAR. The hard point coordinates for the front suspension system are as per table 5.1. these points belong to left hand side of front suspension system. As the suspension is symmetrical about the vertical center plane of the vehicle, the right-hand side hard points are found out by putting negative valve for the y-coordinate.

Table 5. 1 Hard point coordinate for front suspension system

	loc_x	loc_y	loc_z
hpl_lower_arm_front	0.0	-556.0	0.0
hpl_lower_arm_rear	350.0	-556.0	0.0
hpl_lower_control_arm_inner	350.0	-256.0	0.0
hpl_spring_lower	62.0	-406.0	50.0
hpl_strut_lower	40.0	-406.0	0.0
hpl_strut_upper	220.0	-406.0	420.0
hpl_sub_frame_inner	500.0	-256.0	0.0
hpl_sub_frame_rear	500.0	-556.0	0.0
hpl_tierod_inner	-150.0	-250.0	420.0
hpl_tierod_outer	-100.0	-474.0	420.0
hpl_upper_control_arm_inner	180.0	-330.0	420.0
hpl_upper_control_arm_outer	180.0	-506.0	420.0
hpl_wheel_carier_upper	0.0	-506.0	420.0
hpl_wheel_center	0.0	-606.0	100.0

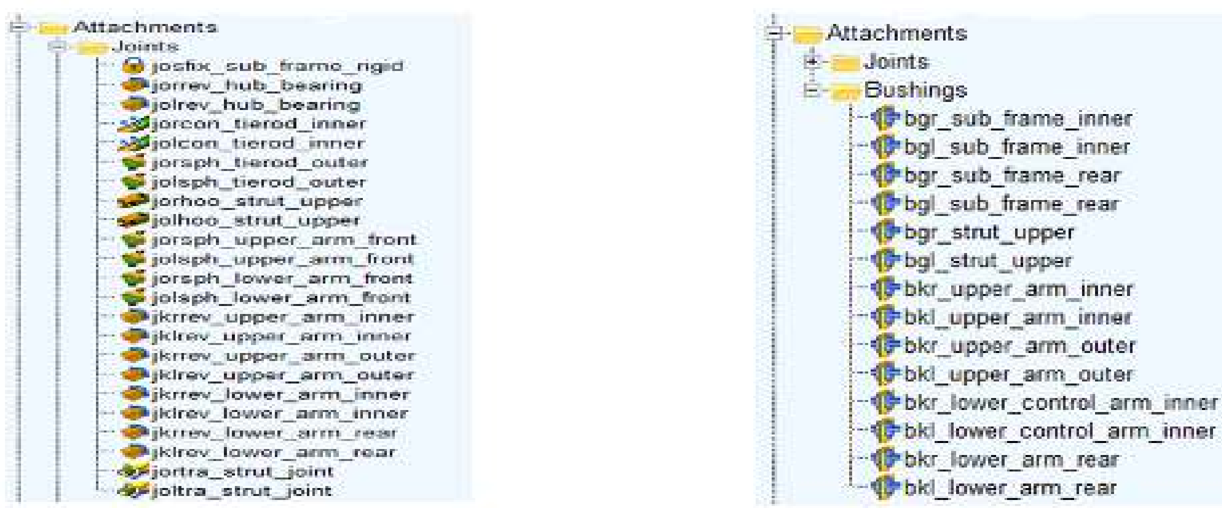

(a) Joint attachments (b) Bushing attachments

Figure 5. 2 Attachments in front suspension system (a) joint attachments (b) bushing attachments

This stage is important since it determines the accuracy and working behavior of a suspension as an actual suspension. Once the template is done, it must save as a subsystem. At this point, not so much parameter can be changed as the template stage can do[51]. There were three subsystems used for this study for front suspension assembly, which are twin leading arm suspension, steering system and MDI TEST RIG. Finally, the subsystems are assembled as one working suspension system assembly. Note that, only the complete assembly system can be analyzed and tested using MSC/ADAMS Car.

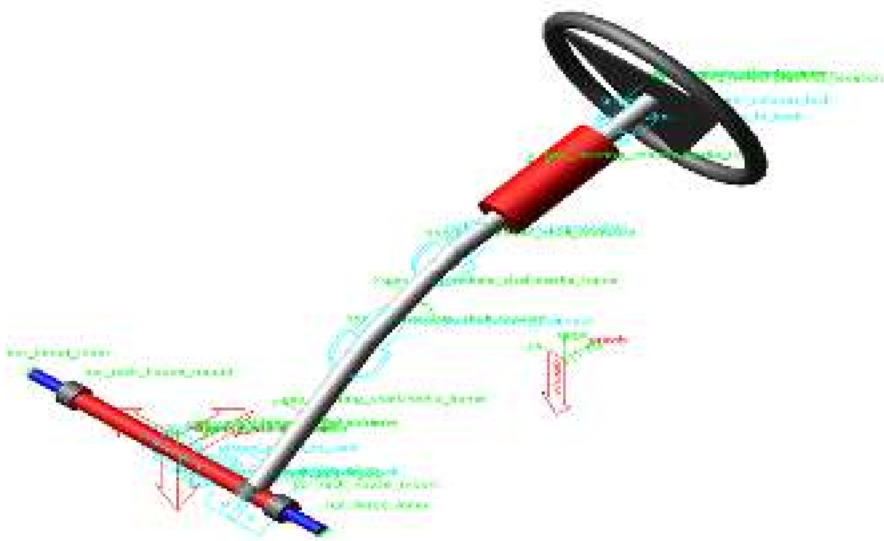

Figure 5. 3 Steering subsystem for the front suspension system

A test rig is a special subsystem that is connected to all of the other subsystems that make up the model, forming an assembly[51]. A test rig in ADAMS/ car (fig 5.3) is the part of the model that imposes motion on the vehicle. Depending on the model and event, different test rigs must be used.

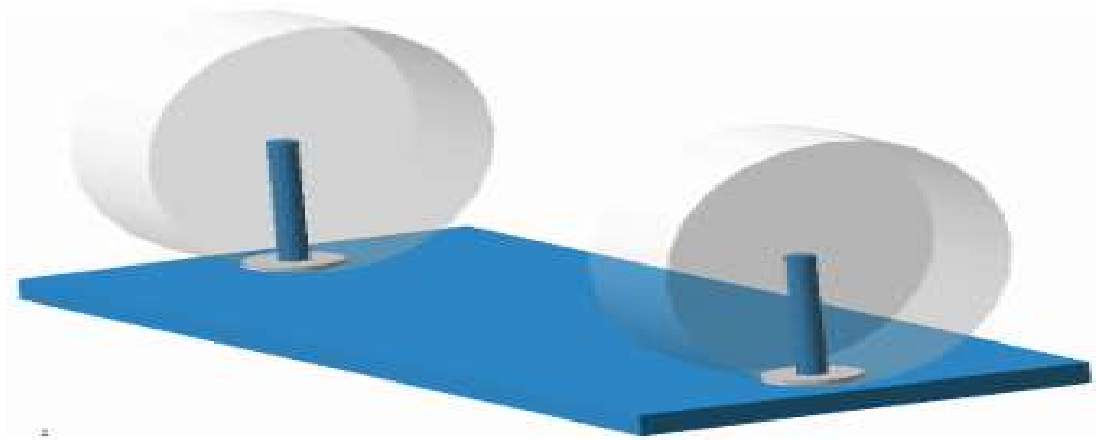

Figure 5. 4 Suspension test rig

In Adams/Car, a steering subsystem and a front suspension subsystem, plus a suspension test rig, form the basis of a suspension assembly (Fig 5.4) that is analyzed for kinematic behavior.

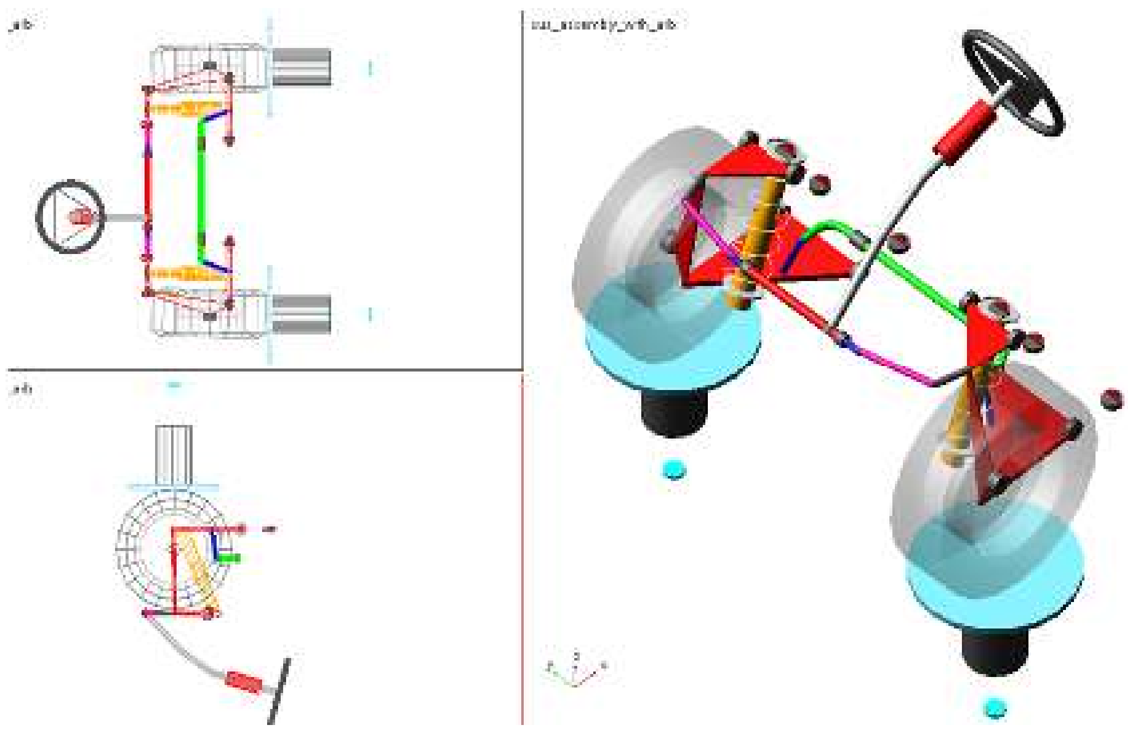

Figure 5. 5 Full front suspension system assembly

5.3 MODELLING OF REAR SUSPENSION SYSTEM

Trailing arm rear suspension is modeled in a similar way as explained in the front suspension. The template generated as shown in Fig 5.6 in rear suspension has not to tie rod link instead it has a power transmission line, since the Bajaj qute is rear-wheel drive.

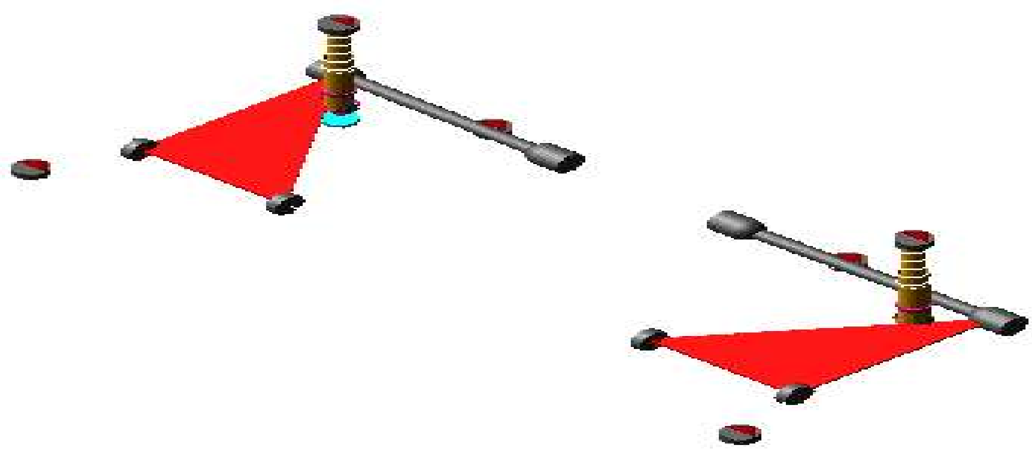

Figure 5. 6 Rear suspension templates

Table 5. 2 Hard point coordinate for the rear suspension system

	loc_x	loc_y	loc_z
hpl_arm_inner_pivot	1545.0	-365.0	100.0
hpl_arm_outer_pivot	1505.0	-676.0	100.0
hpl_arm_strut_bushing	1865.0	-576.0	80.0
hpl_arm_strut_bushing_x	1762.5	-580.0	120.0
hpl_arm_strut_bushing_z	1762.5	-595.0	100.0
hpl_drive_shaft_inr	1902.5	-180.0	150.0
hpl_spring_lower_seat	1865.0	-576.0	220.0
hpl_spring_upper_seat	1865.0	-576.0	380.0
hpl_subframe_front	1362.5	-690.0	120.0
hpl_subframe_rear	1952.5	-356.0	80.0
hpl_top_mount	1845.0	-576.0	420.0
hpl_wheel_center	1905.0	-656.0	120.0
hps_subframe_fixed	1925.0	0.0	100.0

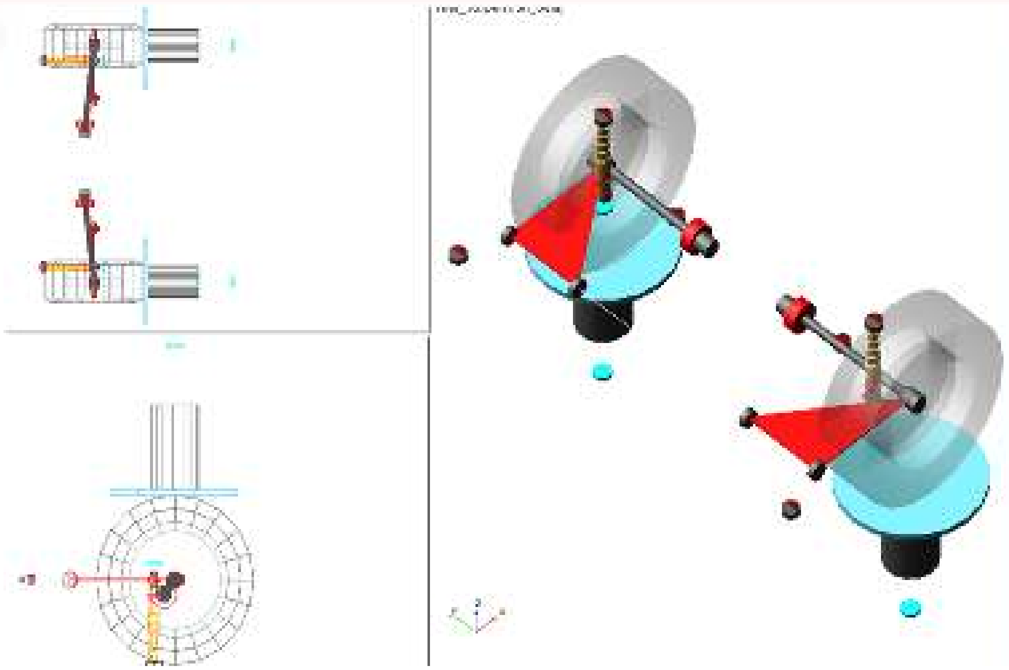

Figure 5. 7 Rear suspension assembly of Bajaj qute for kinematic and compliance analysis

As discussed in front suspension assembly hardpoints are used to model the parts, attachment, and construction frames for correct manipulation of the coordinate system. Once the template is generated with the correct communicator, it is saved to the subsystem. There are three subsystems for suspension assembly; suspension subsystem, driveline, and suspension test rig. A combination of all these subsystems for rear gives us a correct suspension assembly as shown in Fig 5.7 for kinematic and compliance analysis.

5.4 MODELLING OF SPRING AND DAMPER FOR THE SUSPENSION SYSTEM

Springs and shocks are an integral part of any suspension system. But the total suspension system must be considered as a coordinated package, so just changing springs and/or shocks will not always give the desired results. Generally, for light vehicles, coil springs are used as suspension system[17]. Spring is an elastic object used to store mechanical energy and it can be twisted, pulled (or) stretched by some force and can return to their original shape when the force is released. Where the springs are mounted is as important as their rate. Either an existing car or a newly designed car must take these factors into consideration. For the front spring to minimize the linkage ratio effects, it is usually best to mount the front springs as close to the ball joint as possible[52]. There are obvious clearance considerations that must be resolved, but in general, the closer the better. For the rear suspension system, it is often possible to mount rear coil springs directly on the axle housing. This configuration produces wheel rates equal to the spring rates. The rear springs can also be mounted on the rear control arms, but since this introduces linkage ratio considerations, the wheel rate will not be the same as the spring rate.

When creating a spring, two coordinates are needed to attach the two ends for the spring. The coordinates can be either hardpoints or construction frame. Then, to define the spring it must specify[53]:

- Two bodies between which you want the force to act and two reference frames (points at which the spring is attached to the bodies).
- Installed length of the spring, which will be used to derive the design preload on the spring.
- Property file, which contains the free length information, as well as the force/ deflection characteristics.

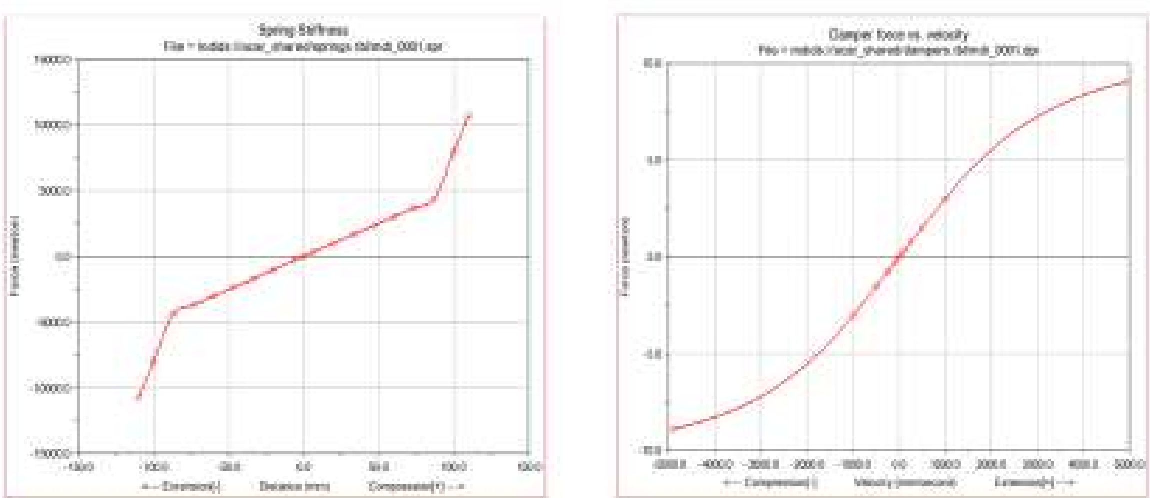

(a) (b)

Figure 5. 8 Front suspension system (twin leading arm suspension system) (a) spring (b) damper

Adams car calculate the force exerted by the spring using the equation [51]

$$Force = -k\left(C - DM(i,j)\right) \qquad equation\ 5.5$$

$$C = FL - IL + DM(i,j) * \qquad equation\ 5.6$$

Where,

C is a constant

FL is the is the free length of the spring, as defined in the property file

IL is the defined installed length

DM (i, j) * is the initial displacement between the I and J coordinate reference points. If you enter a smaller value for DM (i, j) *, ADAMS/Car calculates an increased preload for the spring; conversely, a decreased preload.

Force represents the spring force.

k is the nonlinear spring stiffness derived from the property file.

When creating dampers specify the two ends points and the property file. Unlike spring damper doesn't need a preload.

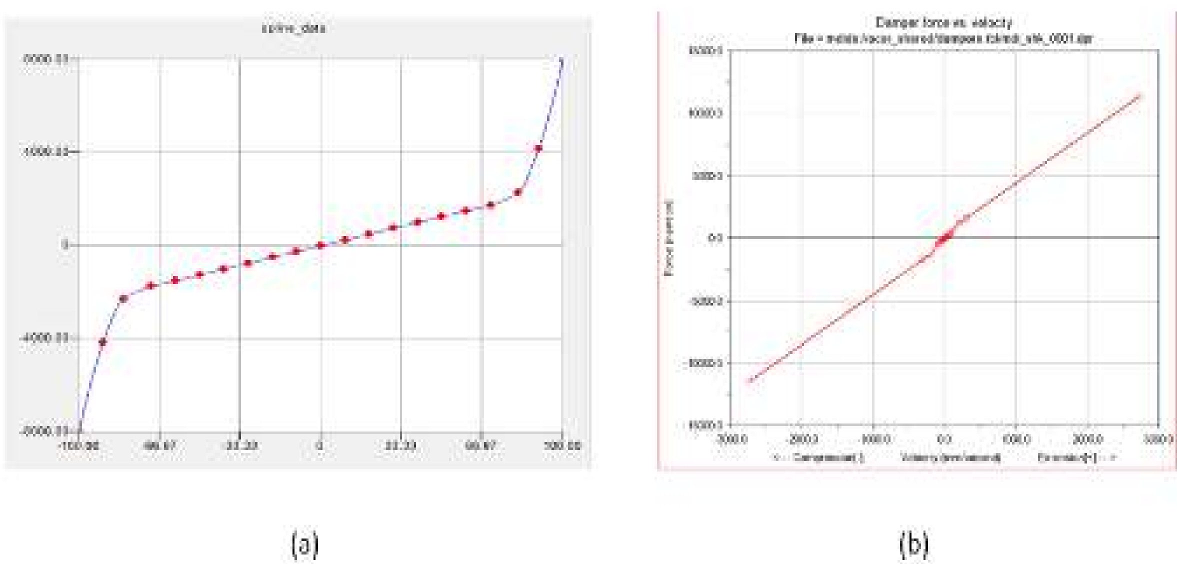

Figure 5. 9 Rear suspension system (trailing arm suspension system) (a) spring profile (b) damper profile

5.5 SIMULATION BEFORE OPTIMIZATION

5.5.1 ASSUMPTIONS AND SIMPLIFICATIONS

Suspension of all parts are regarded as rigid body, (not including elasticity, rubber components) wheel deformation does not occur when jumping up and down; The friction between the parts is negligible, at the same time for the seamless connection between parts; Analysis software does not consider the deformation of the wheel[54][55].

5.5.2 KINEMATIC ANALYSIS

Suspension kinematics strongly influences the handling and stability of a vehicle. The kinematic design of a suspension system involves determining the positions of hardpoints or kinematic design points. Suspension static design factors such as toe, camber, and caster are decided by the location of hardpoints[6].

5.5.2.1 DEFINING VEHICLE PARAMETERS AND PERFORMING ANALYSIS

Before performing a suspension analysis, it must be specified several parameters about the vehicle in which it is intended to use the suspension and steering subsystems. These parameters include the vehicle’s wheelbase and sprung mass, whether or not the suspension is front- or rear-wheel drive, and the braking ratio. For this analysis, we enter the parameters to indicate rear-wheel drive and a brake ratio of 100% front and 0% rear.

Now that we’ve defined the vehicle parameters, we can run the parallel wheel travel analysis. During the analysis, the test rig applies either forces or displacements to the assembly, as defined in a load case file. For this analysis, ADAMS/Car generates a temporary load case file based on the inputs we specify.

The parallel wheel travel analysis moves the wheel centers from -50mm to +50 mm relative to their input position while holding the steering fixed. During the wheel motion, ADAMS/Car calculates many suspension characteristics, such as camber and toe angle, wheel rate, and roll center height.

5.5.2.2 PLOTTING THE RESULTS

Toe is (as shown in Fig 5.9) defined as the angular deflection from the vehicle’s centerline and the centerline of the rim. Positive toe (toe-out) is defined as a wheel splaying out from the direction of travel. A “toe-in” occurs when the front part of wheel is turned inward, and a “toe-out” occurs when the wheel is turned outward. Rolling resistance and braking forces push the wheel slightly backward resulting in toe-out situations, and when traction pulls the wheel forward, it results in a toe-in situation.

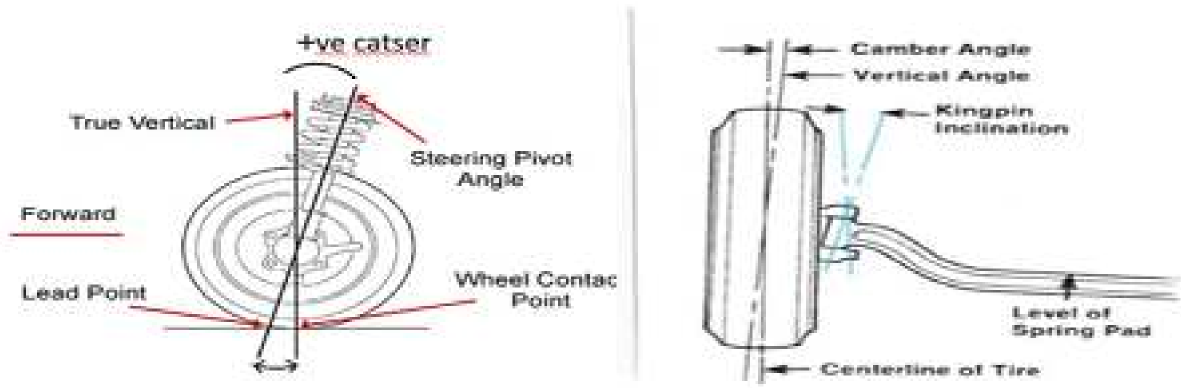

Figure 5. 10 Geometry of suspension parameters

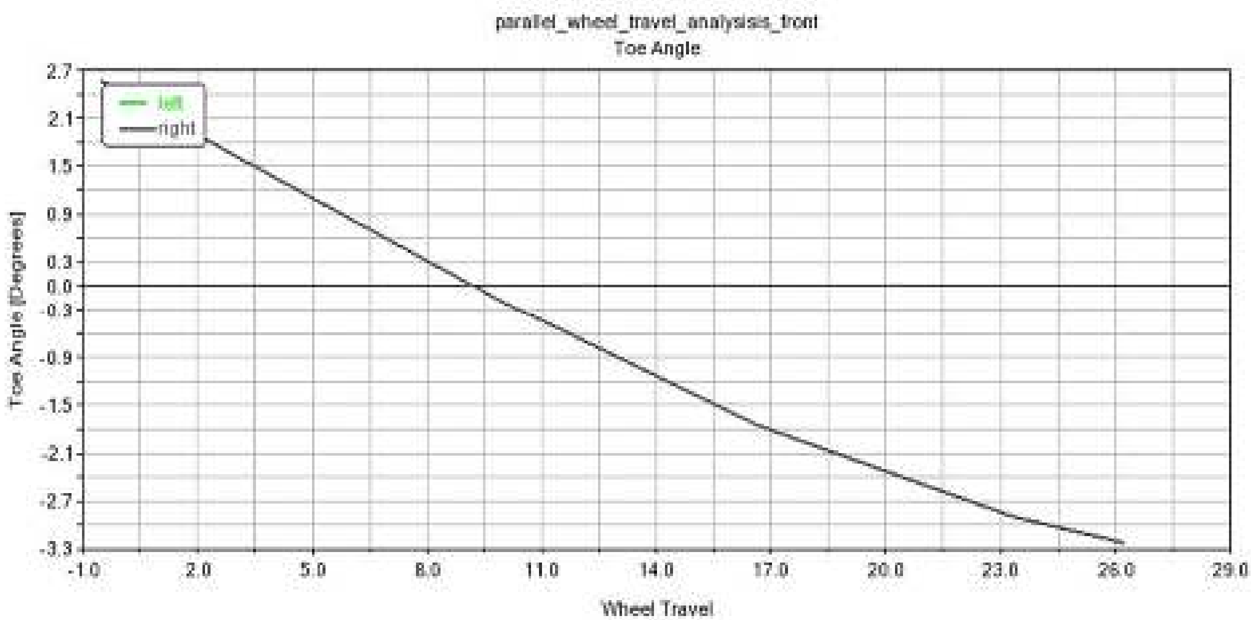

Figure 5. 11 Toe angle Vs wheel travel for the front suspension system

The toe angle should ideally be zero for the lowest amount of tire wear and rolling resistance. Therefore, manufacturers tend to define a toe angle on a static wheel that goes to zero under working conditions. Usually, to offset the braking forces on the front axle that normally results in toe-out situations, manufacturers set the front axle with toe-in angles (negative toe angle). This is done because the vehicle may be unstable if the absolute value of the angle presents as a toe-out.

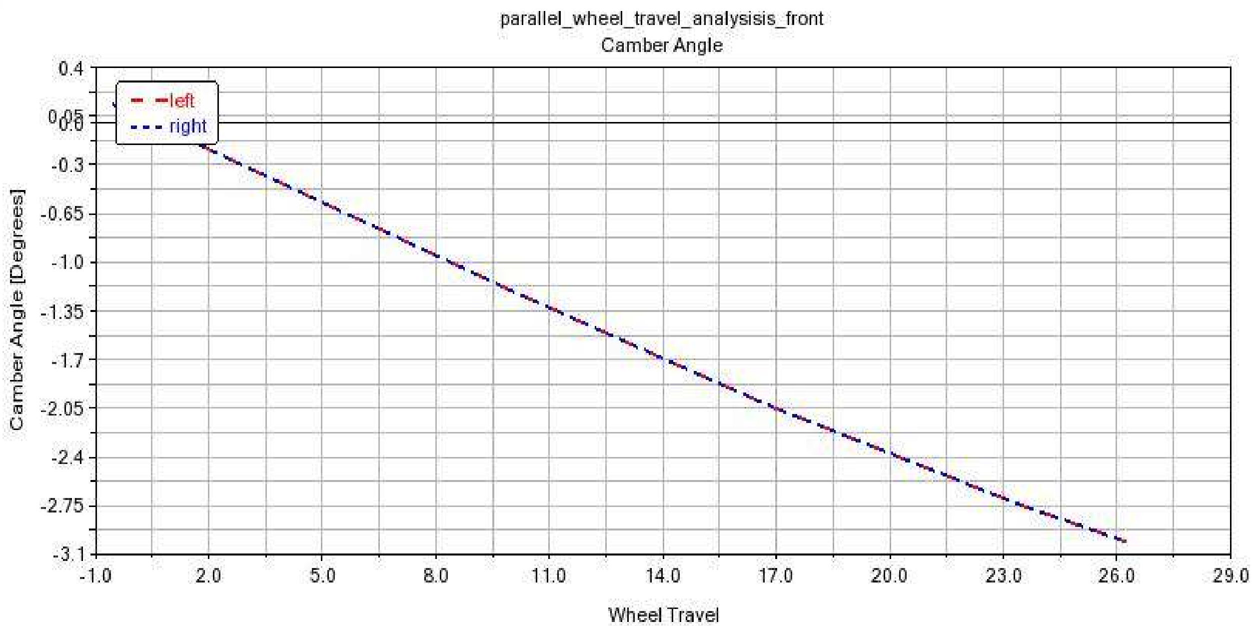

Figure 5. 12 Camber angle Vs wheel travel for front suspension system

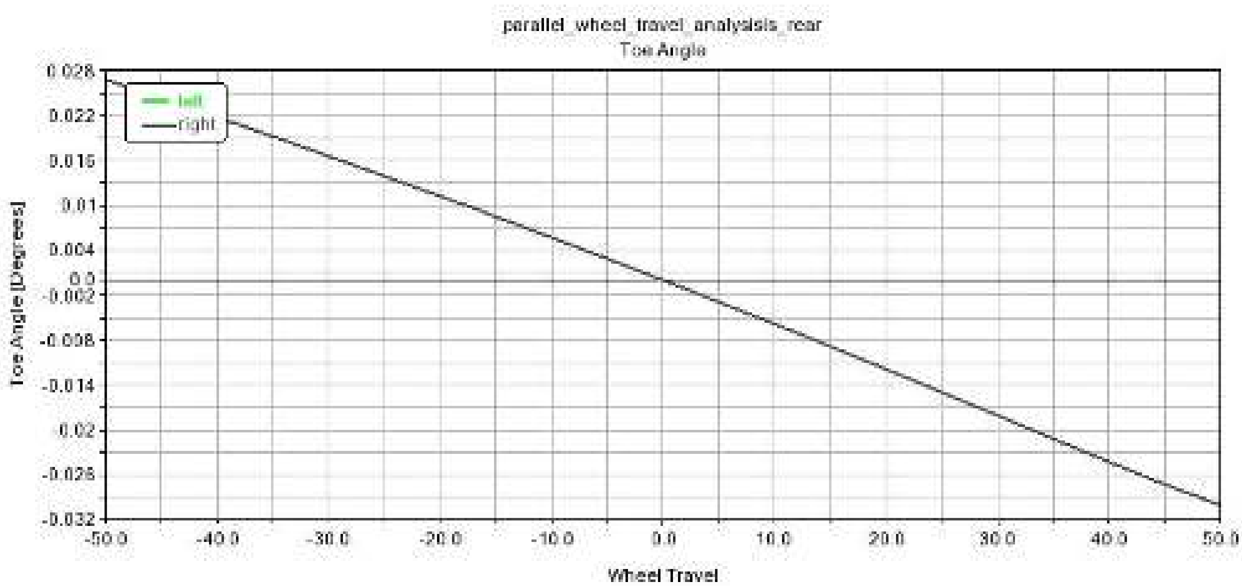

Figure 5. 13 Toe angle Vs wheel travel for rear suspension system

from the plotting, we can see that the toe angle for the front suspension as shown in Fig 5.10 varies between 2.7 degrees of toe out to 3.3 degrees of toe-in and the rear suspension (fig 5.12)[56] variation is approximately equal to zero. The rear suspension is statically positioned to zero and

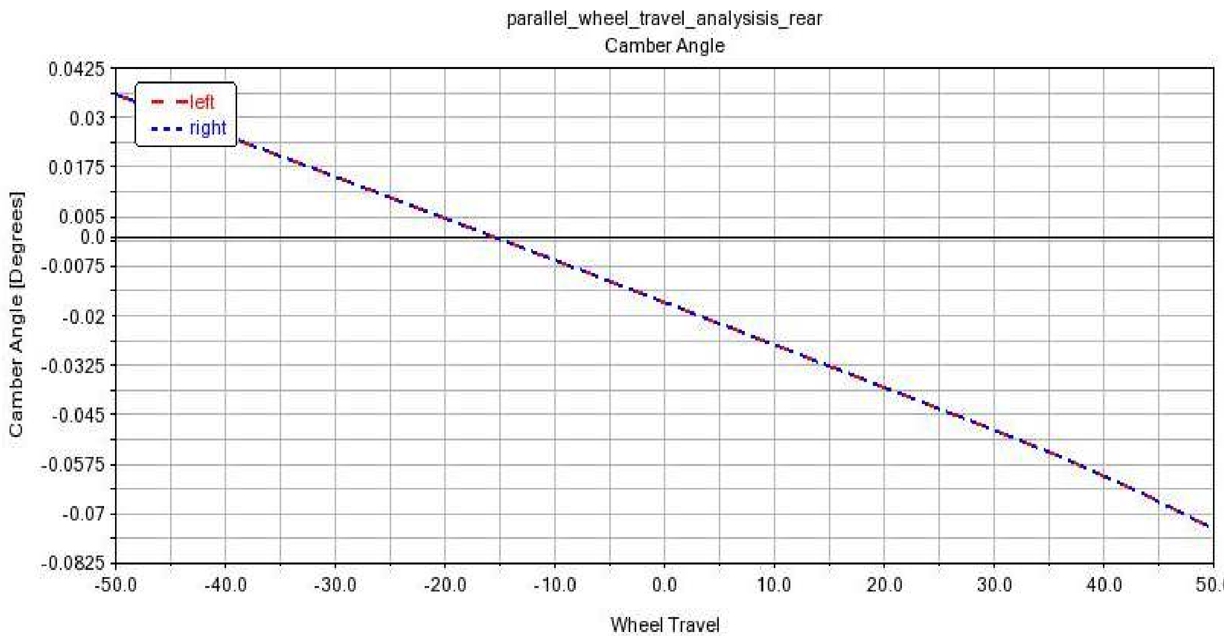

Figure 5. 14 Camber angle Vs wheel travel for rear suspension system

designed to attain zero toe angle in working condition. But it is necessary to optimize the front suspension system to decrease the variance and as it may cause bump steer which is undesirable for off-road cars.

Camber is defined (as shown in Fig 5.9) as the inclination angle between the side plane (vertical-longitudinal plane) and the rim plane lying on the centerline of the rim. Appositive camber is defined as the tops of the wheels tipping away from the vehicle. A tire will provide the maximum traction at any given. Vertical load when it is perpendicular to the ground. This is called zero camber angle.

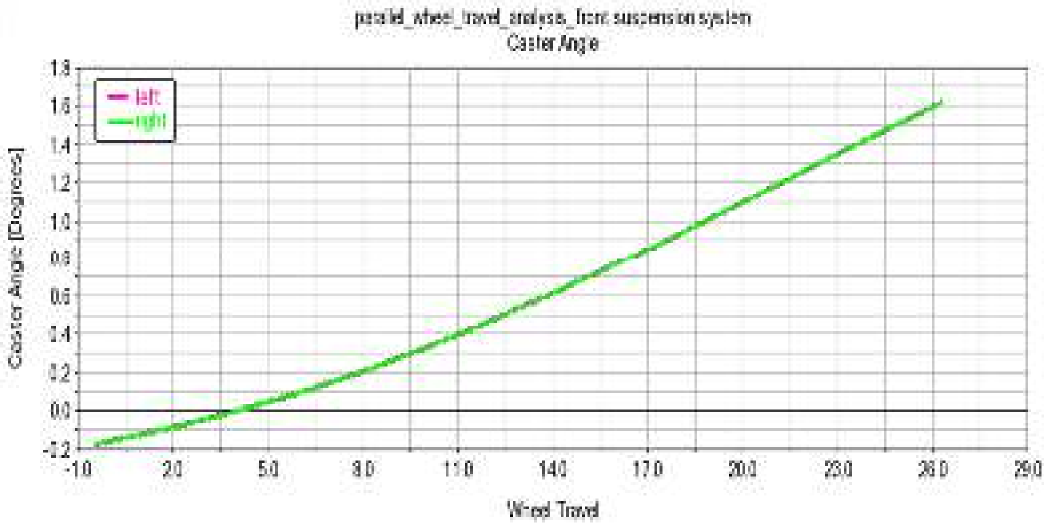

Figure 5. 15 Caster angle vs wheel travel for front suspension

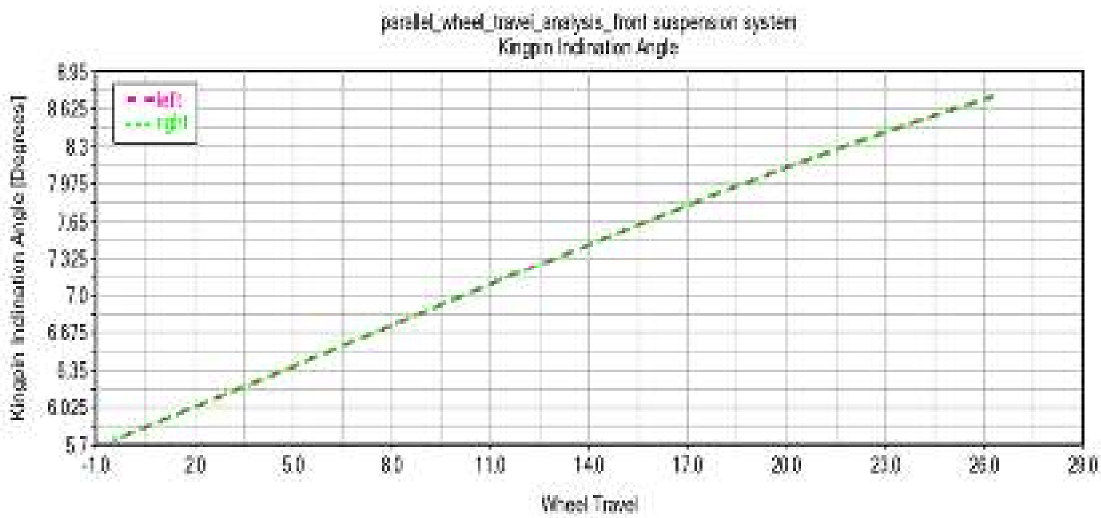

Figure 5. 16 kingpin inclination Vs wheel travel in front suspension

When the tire is perpendicular to the ground, its contact patch is bigger than when it is at any other angle[52]. Contact patch is the area of the tire in direct contact with the road surface. If a tire is tilted out at the top, it has positive camber. Even though this condition reduces the tire contact patch and the tire will not provide as much traction as when it is perpendicular, positive camber would be useful for a reduction in tire wear due to the road profile[57]. Negative camber, when the top of the tire is tilted inward, is often dialed in to compensate for the moving or bending (known as deflection) of suspension parts. When it is used, the result is to have a zero-camber angle when maximum tire traction is needed. Fig 5.11 shows that the camber angle variation in the front suspension system is from 0.4 degree of positive camber to 3.1 degree of negative camber. The variation of the camber angle as depicted in Fig 5.13 in the rear suspension system is approximately equal to zero. Negative cambered car has more effective cornering stiffness. The lateral capabilities of tire are increased when its effective cornering stiffness is increased. Since it can handle more amount of lateral force it corners smoothly and effectively without loss of traction. So, a negative camber of -1 to -3 degree is preferred at static for off-road conditions. The camber gain should limit within 8 degrees during bump and rebound[23] , because too much of camber degrades the tire performance and results in increased tire wear.

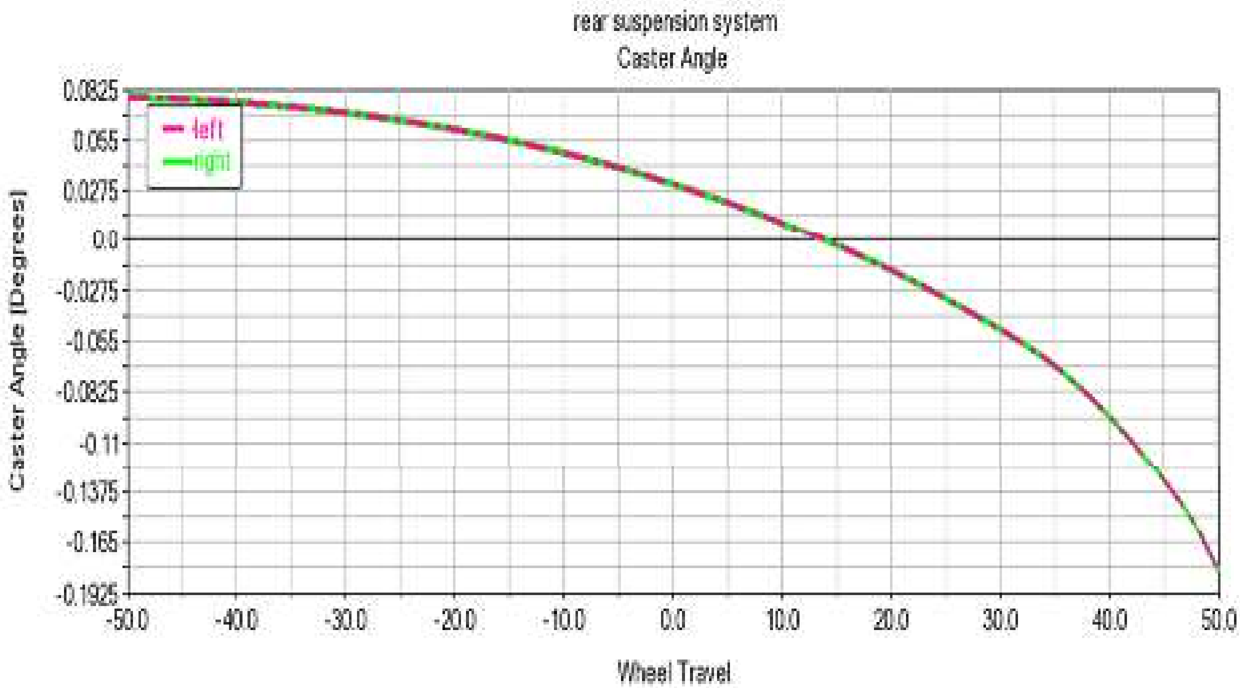

Figure 5. 17 Caster angle Vs wheel travel for rear suspension system

Caster is defined (as shown in Fig 5.9) as the angle between the steering axis and the wheel centerline extending perpendicular from the contact patch, viewed perpendicular to the side view (vertical longitudinal plane). When you turn the steering wheel, the front wheels respond by turning on a pivot attached to the suspension system. Caster is the angle of this steering pivot, measured in degrees, when viewed from the side of the vehicle. If the top of the pivot is leaning toward the rear of the car, then the caster is positive, if it is leaning toward the front, it is negative. If the caster is out of adjustment, it can cause problems in straight-line tracking. If the caster is different from side to side, the vehicle will pull to the side with the less positive caster. If the caster is equal but too negative, the steering will be light and the vehicle will wander and be difficult to keep in a straight line. If the caster is equal but too positive, the steering will be heavy and the steering wheel may kick when you hit a bump. Caster has little effect on tire wear. Simulated result for caster angle in front suspension (as shown in Fig 5.15) is from -0.2 to 1.8. For the rear suspension (as shown in the Fig 5.17) caster angle is zero except for only small uncertainty since there is no any steering axis assembly in the rear suspension system making caster angle negative makes the steering axis light and becomes very difficult to control and to perform straight-line maneuver. The optimal setting helps for better steering and rollover the behavior of the car. Different companies use different result for the caster angle in the acceptable range. Such as Citroën C5-3.1, Audi A4-3.4, Renault Clio II -2.1, Peugeot 307 -4.6 and Volkswagen Tourane uses 7.5.

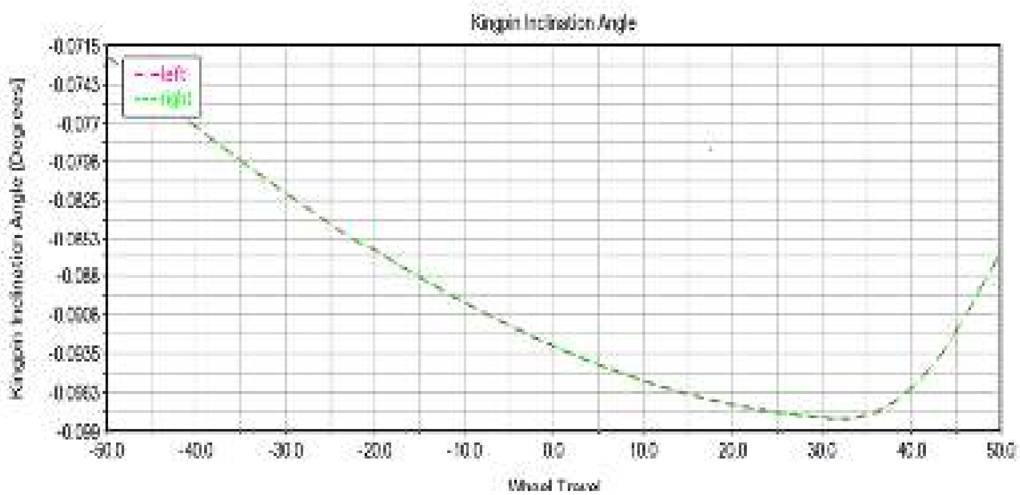

Figure 5. 18 Kingpin inclination Vs wheel travel in rear suspension

Kingpin inclination angle (shown in Fig 5.9) is the measurement in degrees of the steering pivot line when viewed from the front of the vehicle. This angle causes the vehicle to lift slightly when you turn the wheel away from a straight-ahead position. This action uses the weight of the vehicle to cause the steering wheel to return to the center when you let go of it after making a turn. Typically, this angle is between 5 and 10 degrees. more king pin inclination will also reduce the scrub radius. Increasing the king pin inclination also helps to center the steering, so why not use a lot of king pin angle? The reason is another compromise situation. With excessive king pin angle, the tire tends to flop from side to side as it is steered[52]. This causes the tire contact patch to run up the edge of the tire as it is turned. The acceptable range in king pin angle is between 7 and 9 degrees. The variation in the front suspension system from the Fig 5.15 is shown that, it is from 5.7 degrees to 8.97 degrees. For the rear suspension by default it is zero degree (Fig 5.17) since there is no steering axis in the rear suspension system.

5.5.3 FULL VEHICLE ASSEMBLY BY MBS (ADAMS CAR)

Multibody system is the group of bodies interconnected by joints, influenced by forces, and restricted by constraints. And the field of studying the classical mechanical properties (especially motion) of these systems is known as Multibody dynamics. A Multibody system is used to model the dynamic behavior of interconnected rigid or flexible bodies. The key feature of a system that makes it suitable for Multibody treatment is the observation that the motion is localized, that is, it

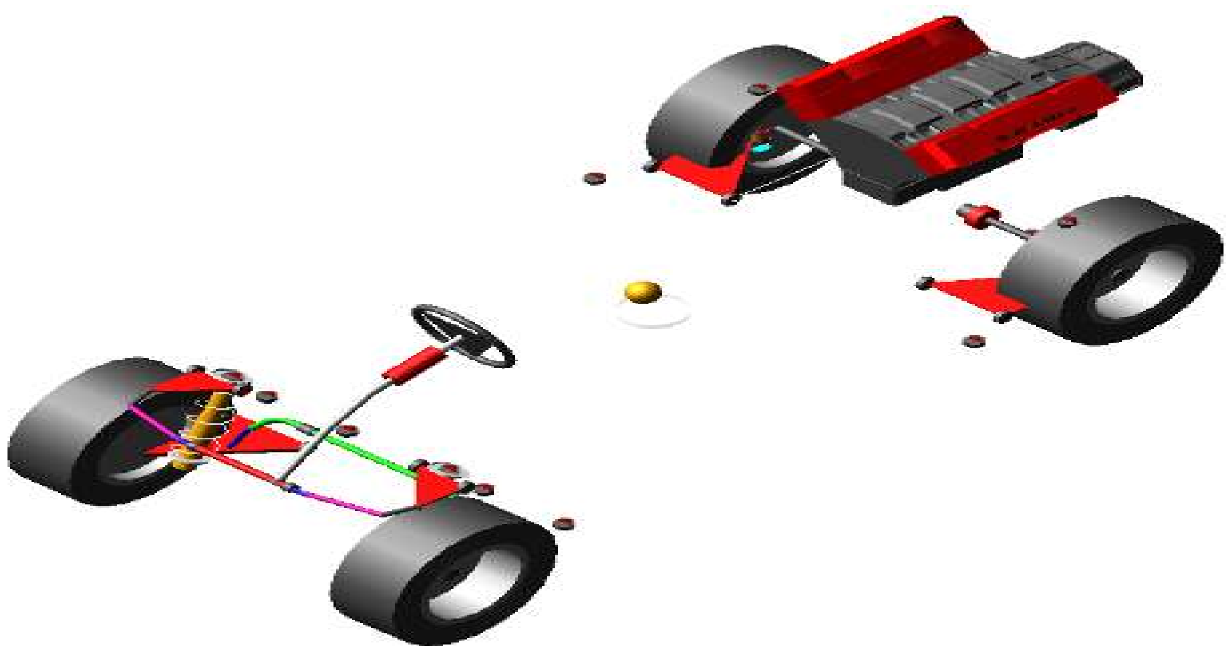

Figure 5. 19 Bajaj qute full vehicle assembly

is well described as a set of composite parts, which undergo large motion with respect to one another, but are themselves nearly rigid [58].

MSC.ADAMS program is typical of the range of multi-body analysis software described as numeric where the user is concerned with assembling a physical description of the problem rather than writing equations of motions. Here, the equations are generated in numerical format and are solved directly using numerical integration routine embedded in the package. To create full vehicle assembly in Adams car, it requires all the sub system that the vehicle made up of. The subsystem necessary are body, front and rear suspension, front and rear tire, steering sub system and test rig. All the analyses currently available are based on the driving machine. Therefore, to perform open loop, closed loop and quasi static analysis it needs MDI_SDI_TEST RIG in the assemblies. The only analysis that is not based on the driving machine is the data driven analyses. It uses _MDI_TEST RIG. The figure (Fig 5.17) shows full vehicle assembly of Bajaj qute.

5.5.4 ESTIMATION OF INERTIAL PROPERTIES AND THEIR EFFECTS ON FULL VEHICLE MODEL

Basic vehicle dynamics have been traditionally subdivided into lateral/directional dynamic modes including yawing and rolling motions. The basic input for these dynamics is steering, and speed is a key operating point. Inertial properties affect the time constants of various response modes, and also the influence of control inputs. Inertial properties have known effects on vehicle dynamic responses. Key inertial variables relate to directional and roll mode stability issues. With the help of NHTSA inertia data base, the relationship between vehicle inertial properties and vehicle basic size dimensions are revealed in the paper [59]with the use of regression analysis.

Here, it is assumed that the moments of inertia of vehicle are general logarithmic function of key vehicle dimensions[59].

$$log\, I_{x,y,z} = log\, k1 + k2 * log\, l + k3 * log\, Tw + k4 * log\, Hr + K5 * log\, Wt \qquad equation\ 5.7$$

Where

$\mathrm{I}_{x,y,z}$ = principle moment of innertia

K1 − constant of proportionality or intercept

K2, K3, K4 − regression coffcient

l − wheel base(feet)

$Tw \quad -$ average track width(feet)

$Hr \quad -$ roof height (feet)

$Wt \quad -$ total weight (lbs)

The above equation (numbered, 5.7) is in the form that will allow multiple linear regression to be applied to the NHTSA inertia data base. Furthermore, if we take the antilogarithm of both side of the equation 5.7, we obtain the following expression for moment of inertia.

$$I_{x,y,z} = 10^{K1} * l^{k2} * Tw^{K3} * Hr^{K4} * Wt^{K5} \qquad \text{equation 5.8}$$

Regression analysis results are summarized for roll, pitch and yaw moment of inertia in[59].

Roll: - The coefficient on the trackwidth (Tw) dimension is almost 2 as expected, but roof height has a small coefficient. This probably represents the wide variations in roof height between passenger cars and SUVs that does not represent much difference in moment of inertia. There is also a small negative coefficient on wheelbase (l) which decreases roll moment of inertia at longer wheel bases.

$$\log I_x = -2.1363 - 0.1596 * \log l + 1.9406 * \log Tw + 0.3629 * \log Hr + 0.9421 \quad \log Wt \qquad equation\ 5.9$$

$$\log I_x = -2.1363 - 0.1596 * \log 6.3 + 1.9406 * \log 4.3 + 0.3629 * \log 5.42 + 0.9421 \quad \log 1455.05$$

$$\log I_x = 2.211 \quad , Ix = 162.56 lbft^2 = 7{,}067{,}826$$

Pitch: - Wheelbase is the dominant coefficient, but is somewhat less than 2. Roof height is the second dimension in the pitch plane, but its effect is not statistically reliable (p>.05). Trackwidth (Tw) which is not in the pitch plane does have a statistically reliable, albeit small, effect.

$\log I_y = \log(-2.0024) + 1.5315 * \log l + 0.2526 * \log Tw + 0.1009 * \log Hr + 1.0206 * \log Wt \qquad equation\ 5.10$

$\log I_y = -2.0024 + 1.5315 * \log 6.3 + 0.2526 * \log 4.3 + 0.1009 * \log 5.42 + 1.0206 * \log 1455.05$

$\log I_y = 2.6869\ , Iy = 486.3 lbft^2 = \ 21{,}143{,}478$

Yaw: - Both wheelbase (l) and trackwidth (Tw) are the yaw plane dimensions. Wheel base has a coefficient that is somewhat less than expected, while trackwidth has a significantly lower coefficient. The roof height coefficient is negligible, and not statistically reliable.

$\log I_z = -1.799 + 1.4316 * \log 6.3 + 0.3811 * \log 4.3 + 0.0188 * \log 5.42 + 0.98 * \log 1455.05$

$\log I_z = \ 2.7\ , Iz = 501.187 lbft^2 \quad = 21{,}790{,}739$

From our calculation we can understand that the ranges of the pitch and yaw moments of inertia are quite similar as might be expected since the mass distribution is similar in each case.

5.5.5 TESTING MANEUVERS

NHTSA_has created various testing maneuvers for vehicle roll over testing[60]. The maneuvers are designed to test and quantify certain aspects of vehicle properties. In general, there are two types of maneuvers to test for vehicle roll over propensity[60]. Quasi static maneuver tests the likelihood of vehicle to rollover in steady state running while dynamic maneuver provokes transient vehicle properties that are caused by weight transfer and suspension parameter effects.

5.5.5.1 QUASI-STATIC MANEUVER

Quasi-static rollover testing is composed of maneuvers that test a vehicle's propensity for rollover with a model that removes the effects of transients. Maneuvers that fall under the quasi-static realm include the constant radius and the steadily increasing steer. These maneuvers gradually increase the vehicle's steer angle or velocity, causing a semi- static rollover. Although, the quasi-static maneuvers incorporate the main factors that affect vehicle rollover, they do not include effects of vehicle roll due to suspension configurations and other transient properties. So that this will not be discussed in this paper.

5.5.5.2 DYNAMIC MANEUVER

Real world vehicle rollovers are mainly caused by dynamic behavior of a car. Testing dynamic maneuver incorporates the effects created by vehicle transients. The maneuvers defined by NHTSA are created to excite certain vehicle dynamics that are not taken into account in the static and quasi-static testing procedures. The maneuvers included in NHTSA's testing for transient maneuver are the J-turn, the fishhook, and the double lane change. The J-turn maneuver is a result of a step steer angle applied during a constant velocity run. The fishhook maneuver simulates a road edge recovery maneuver that emulates a sinusoidal steering input that greatly increases the vehicle's chances for rollover. The double lane chance maneuver is quite similar to the fishhook maneuver, in that it requires two steer angles, but it does not excite the vehicle dynamics as much as the fishhook maneuver. In many ways' fishhook is better testing maneuver to perform real road edge emulations.

5.5.6 FISHOOK MANEUVER SIMULATIONS IN ADAMS CAR

To gain insight into the dynamic events leading to vehicle roll over and in to the effective way of decreasing the roll over, full Bajaj qute model is used. To perform a complete full vehicle simulation analysis, fishhook maneuver is selected. Because none of the maneuvers excites the vehicle dynamics as much as fishhook maneuver[60].

NHTSA uses slowly increasing steer tests to measure linear range and maximum quasi-static lateral acceleration. While maximum lateral acceleration data is interesting, it is not a required metric when determining a vehicles NCAP (new car assessment performance) rollover resistance rating. For this reason, NHTSA recommends use of an "abbreviated" Slowly Increasing Steer maneuver[61]. The handwheel angles used in this abbreviated procedure only steer the vehicle enough to assess its linear range lateral acceleration performance.

Analyses of Slowly Increasing Steer tests output overall average handwheel position at a specified lateral acceleration. When lateral acceleration data collected during Slowly Increasing Steer tests is plotted with respect to time, a first order polynomial best-fit line accurately describes the data from 0.1 to 0.55 g. A simple linear regression is used to determine the best-fit line. As shown in Fig 5.19, the lateral acceleration outputs have linear relation with respect to time at the very beginning of the maneuver.

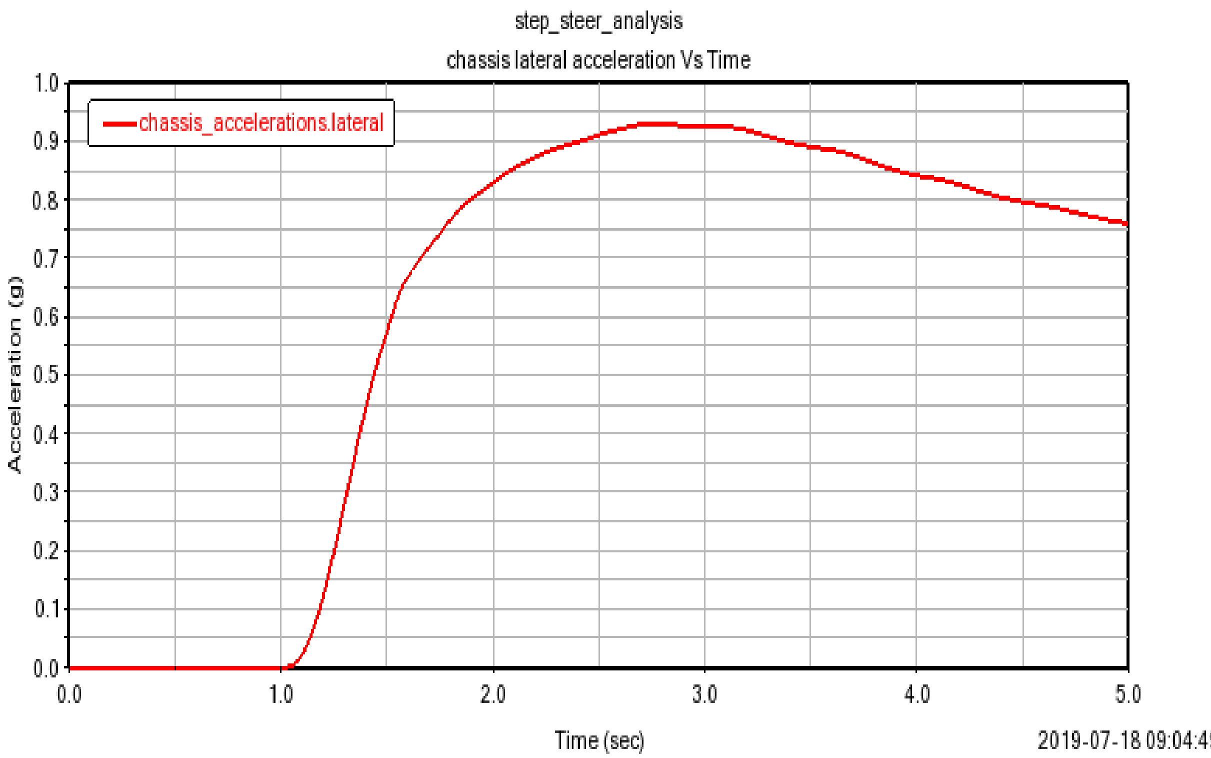

Figure 5. 20 Chassis lateral acceleration from step steer analysis

Fishhook maneuver handwheel angles are calculated with lateral acceleration and hand wheel angle data collected during slowly increasing steering analysis. Using the slopes of these regression lines (Fig 5.19), the handwheel angle at 0.3g determined for the test.

The Fishhook maneuver steering angles are calculated by multiplying $\delta_{0.3g}$ overall by a steering scalar (SS). The default steering scalar is 6.5[61].

$$\delta_{\text{fishhook default}} = 6.5 * \delta_{\text{0.3g over all,from step steer}} \quad \text{equation 5.11}$$

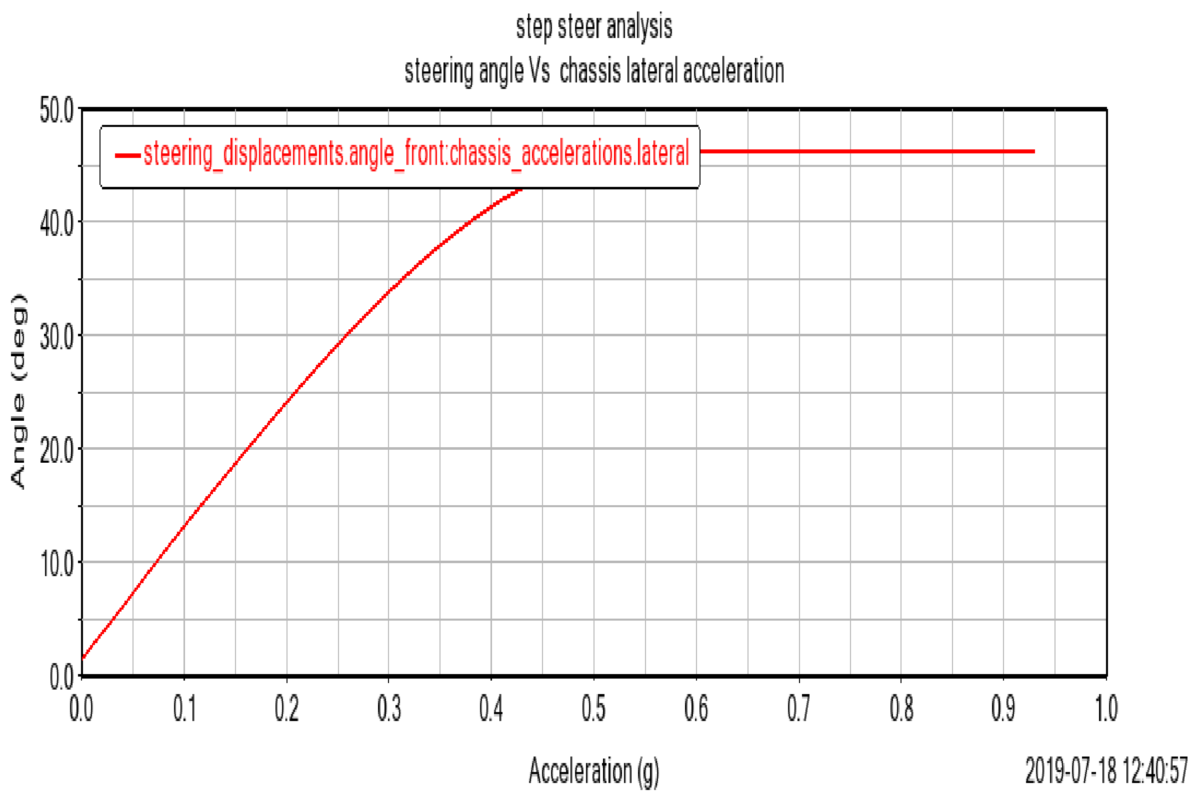

Figure 5. 21 Steering angle vs chassis lateral acceleration

For the developed full vehicle model, the steering angle of 34 degrees produces 0.3g lateral acceleration. Multiplying the result by scalar of 6.5 gives 221 degree which is the initial input for fishhook maneuver. A fixed timing fishhook consists of an initial steering input followed by a dwell time of 650 ms [21]. Then, a counter steering input of equal magnitude follows after that, which is again followed by a 3.423 s pause, as shown in Fig 5.21 and Fig 5.22.

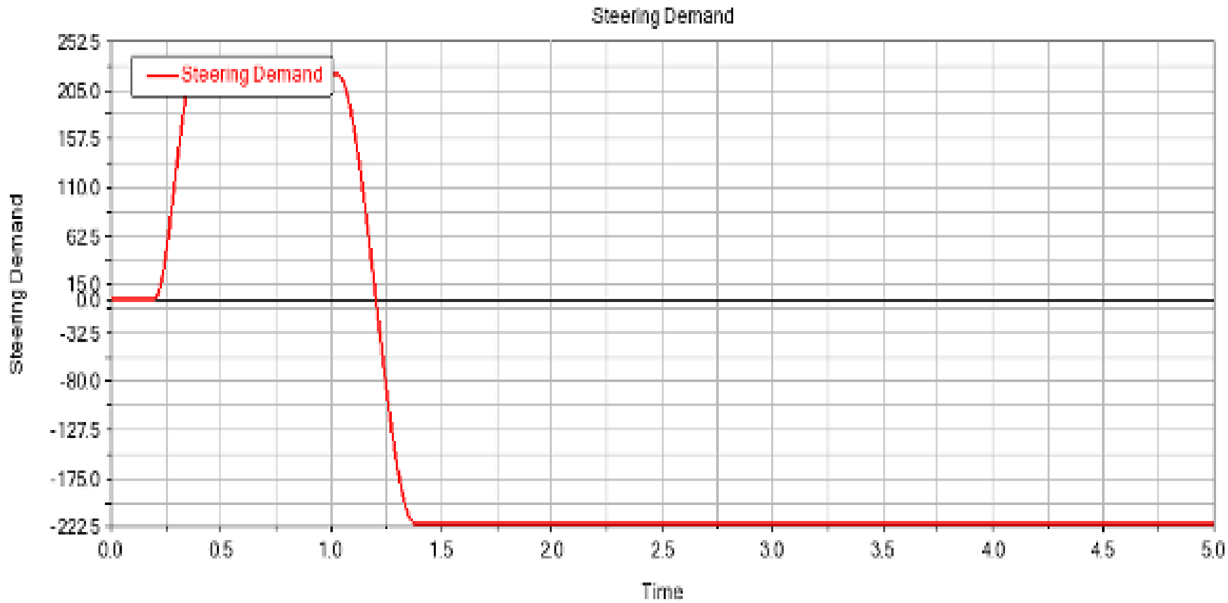

Figure 5. 23 steering angle Vs time

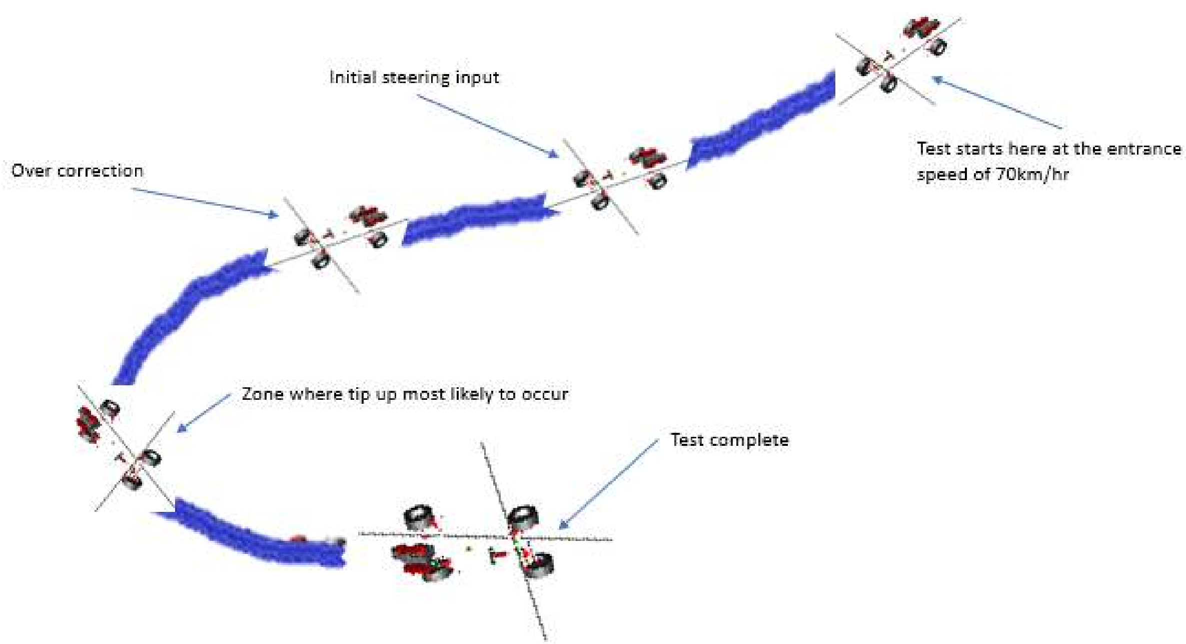

Figure 5. 22 Fishhook trailers of the car

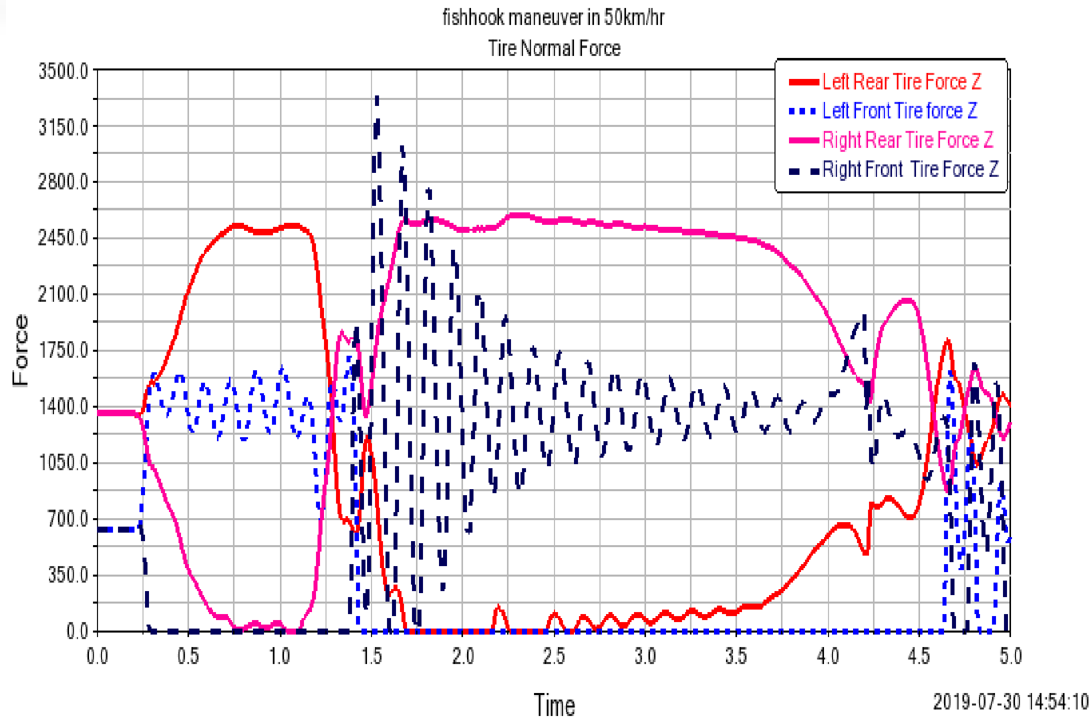

Figure 5. 24 Tire normal force in fishhook maneuver

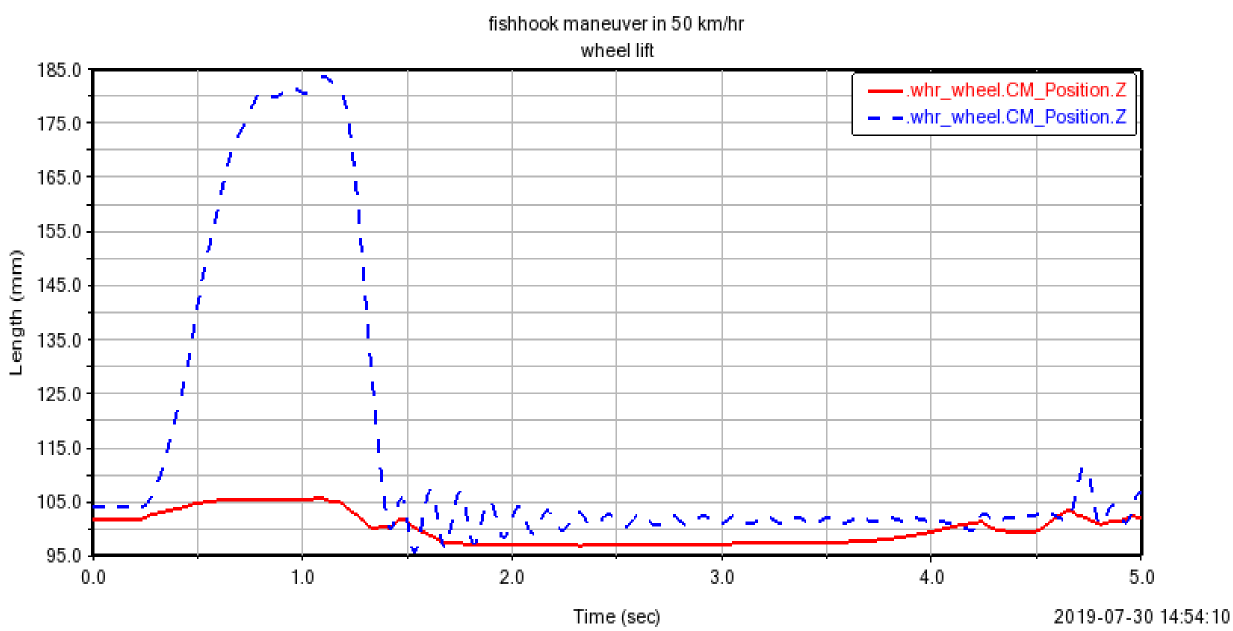

Figure 5. 25 wheel lift Vs time in fishhook maneuver @50km/hr

Maneuver entrance speed is measured at the initiation of the first steering ramp and is increased until termination condition is satisfied. The order of termination speed is increased by 5km/hr. However, when a maneuver entrance speed of greater than 45 km/hr is used the severity of response produced in a vehicle increase substantially from that observed at lesser entrance speeds. This is especially true if a vehicle has a propensity to oscillate in roll, and/or is able to produce two- wheel lift slightly less than NHTSA's threshold criterion of two inches (Fig 24). Normal force of the inside wheels was evaluated to check whether the wheel lifts of or not. If both normal forces go to zero as shown in the Fig 5.23 and also markers were created to measure the wheel lift during the maneuver in the vehicle model. Since the wheel center vertical displacement is more than 50.8mm, the wheel is considered to lift off as shown in the Fig 5.24.

5.6 EFFECT OF SUSPENSION DESIGN PARAMETERS ON LATERAL BEHAVIOR OF ACAR

Suspension geometry is primarily characterized by five dominant parameters: toe, camber and roll center height for both front and rear suspensions, and caster and kingpin inclination (KPI) angles for the front suspension. All these parameters and their changes in wheel travel (bump/rebound) affect dynamic response of the vehicle in roll or handling or both. The location of hardpoints determines static values and change in wheel travel for these suspension parameters. Hardpoints are the most elementary building blocks in ADAMS/Car that define and parameterize all key locations in the model [22]. The primary objective of this paper is to investigate the influence of these suspension parameters on roll stability and to adjust the dominant parameters by changing hardpoints to maximize fishhook lift-off speed without significantly affecting vehicle understeer. This was accomplished in three major stages and the steps involved in the process are explained in the flowchart in Fig 5.26.

5.7 DESIGN OF EXPERIMENT

Design of Experiments (DOE) techniques enables designers to determine simultaneously the individual and interactive effects of many factors that could affect the output results in any design. DOE also provides a full insight of interaction between design elements; therefore, it helps turn any standard design into a robust one. Generally, DOE helps to pin point the sensitive parts and sensitive areas in designs that cause problems in Yield. Designers are then able to fix these problems and produce robust and higher yield designs prior going into production[25].

DOE is increasingly used for identification and optimization of design parameters to improve system performance. Using DOE tool ADAMS/Insight, all suspension hardpoints were assessed for their influence on suspension design parameters (toe, camber, roll center height, etc.). The effects of individual suspension hardpoints on these design parameters are evaluated and the most dominant hardpoints are identified.

The type of experiment used for screening depends on the number of factors employed and number of levels (two-level, quadratic, cubic, etc.). The full factorial experiment is the most thorough approach for screening, but is rarely used for screening high number of factors, as was the case in this study. Fractional factorial experiment is a variation of full factorial design, where only a subset of the runs is made. Factorial Method considers the limiting values within a statistically influential range for each significant parameter considering approximately linear responses. Fractional Factorial method reduces the number of runs without compromising the interactive possibilities predicted. The approach employed is called as "Confounding", where the last main effect factor(s) is associated (Aliased) with the highest order interaction. No two columns in the design matrix must have the same level signatures of high (+) and low (-) in the same block, i.e. the columns should be orthogonal. This principled method is used to obtain a balanced design of the model. In this manner, although the number of runs is reduced, maximum information about the process is obtained with a little compromise on the accuracy of the otherwise cumbersome Full Factorial method[62]. Fractional factorial design is adopted in this paper.

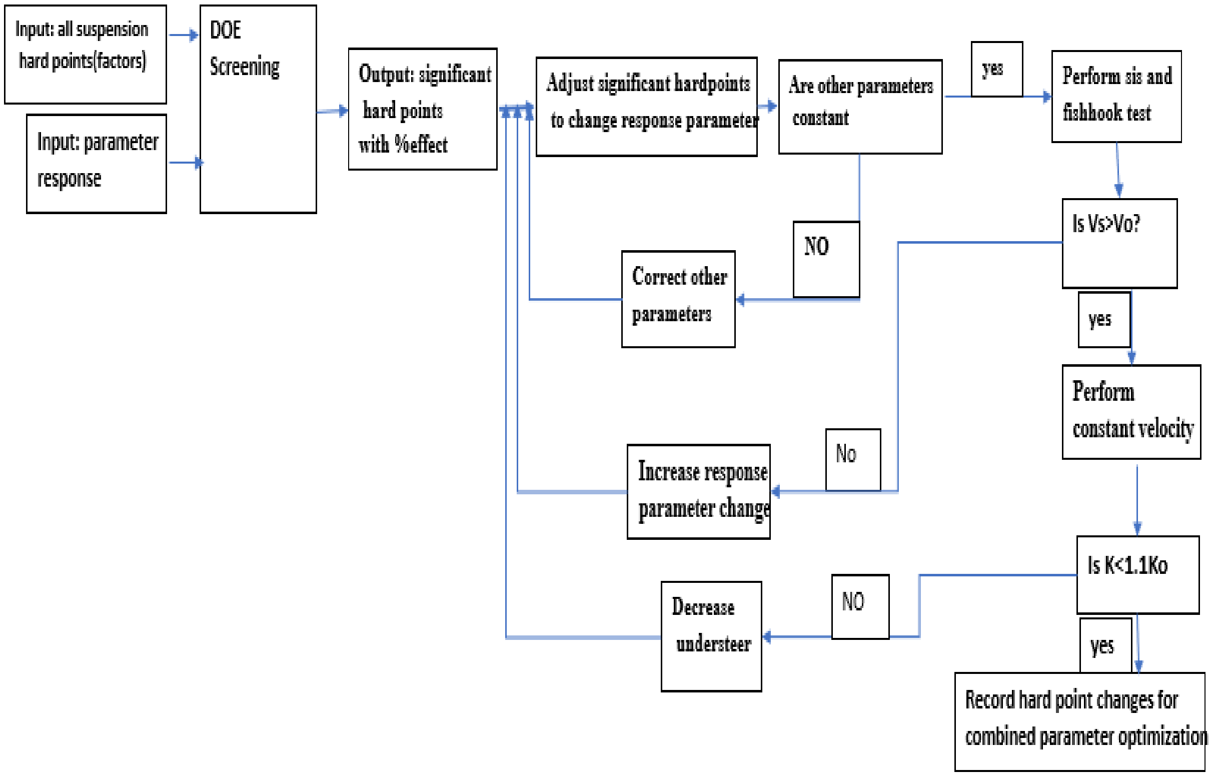

Figure 5. 26 Dynamic optimization flow charts

5.8 SUSPENSION PARAMETER OPTIMIZATION IN ADAMS/INSIGHT

Once significant improvement is observed in fishhook response by varying the suspension parameters, the degree of change is optimized to result in best fishhook response, i.e. highest lift-off speed (Vs). Understeer gradient (K) in constant velocity test is simultaneously monitored to ensure that it increases less than 10% of its original value. Response surface methods (RSM) available in ADAMS/Insight was used for optimization. A response surface is a mathematical surface represented by a series of polynomials. It gives an approximate value of the response (dependent variable or objective) as a function of the factors (independent variables or Design Variables). The techniques you use to create and analyze response surfaces are collectively called Response Surface Methodology (RSM). RSM is widely used for developing and optimizing processes and products of all kinds. The first step in RSM is to find an approximation for the functional relationship between response and the set of independent factors. ADAMS/Insight uses the method of least squares to estimate the parameters in the polynomial. R2 (R-Squared) indicates how well the response surface represents the results. It is the square of the multiple correlation coefficient (R). R2 is the fraction of variability in the data for which the model accounts. The larger it is, the better the fitted equation explains variations in the data. R2 is between 0 and 1. If R2 = 1, the equation exactly matches the data. A high R2 (.9 for example) indicates a good, but not exact, fit. A low R2 (.3 for example) indicates a poor fit.

5.9 MULTI OBJECTIVE PARAMETER OPTIMIZATION

If there are more than one response set to Min or Max, then you are performing a multi-objective optimization.

The targets and weight values are used to adjust the relative importance of the responses. Using these values, Adams Insight computes a cost for each response and combines these into an overall cost. Adams Insight then minimizes the overall cost. The response cost is the difference between the response value and the target value multiplied by the weight. The target value acts as the desired value, and the weight scales the response relative to other responses. The weight should reflect both different units or scales among the responses, as well as increased or decreased importance.

All hard points of front suspension system are used as factors for fractional factorial design and two levels are set for each factor. The critical (dominant) hardpoints obtained from DOE screening are then adjusted to produce the suspension characteristics that improve vehicle roll stability during fishhook maneuver.

5.9.1 BUMP STEER

Bump steer is a complex phenomenon. It is basically the self-steering action of any automobile in response to lateral acceleration and consists of slip angle changes due to , toe change and the inertias of the sprung mass[63].also the brake force and cornering behavior of a car affect the toe angle of the car.

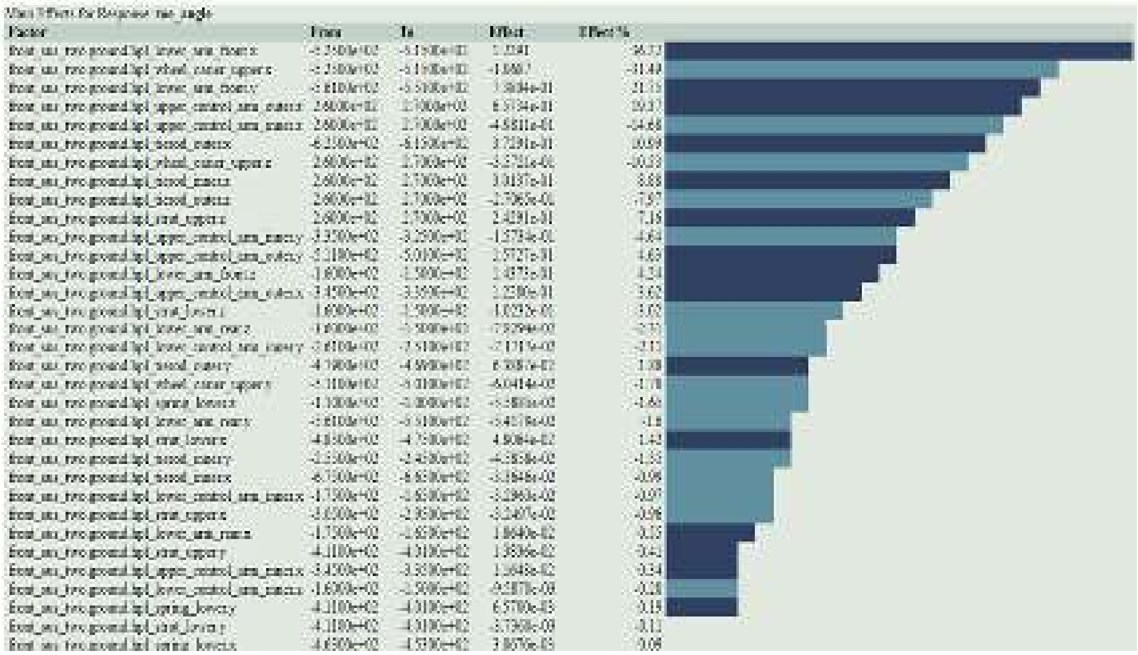

Figure 5. 27 Pareto charts for hard point sensitivity for toe angle

To increase the accuracy of the analysis it is required to decrease the number of selected factors as per the percent of their effects in the respective parameter as shown in Table 5.3 and finally it is combined for the multi objective analysis.

Table 5. 3 critical hard points which affect toe angle

Critical hard points	**Effect %**
Front_sus_two.ground.hpl_lower_arm_front.x	36.22
Front_sus_two_ground.hpl_wheel_carier_upper.x	-31.49
Front_sus_two.ground.hpl_lower_arm_front. y	21.75
Front_sus_two_ground.hpl_upper_control_arm_outer. z	19.37
Front_sus_two_ground.hpl_upper_control_arm_inner. z	-14.68
Front_sus_two_ground.hpl_tierod_outer.x	10.99
Front_sus_two_ground.hpl_wheel_carier_upper. z	-10.53

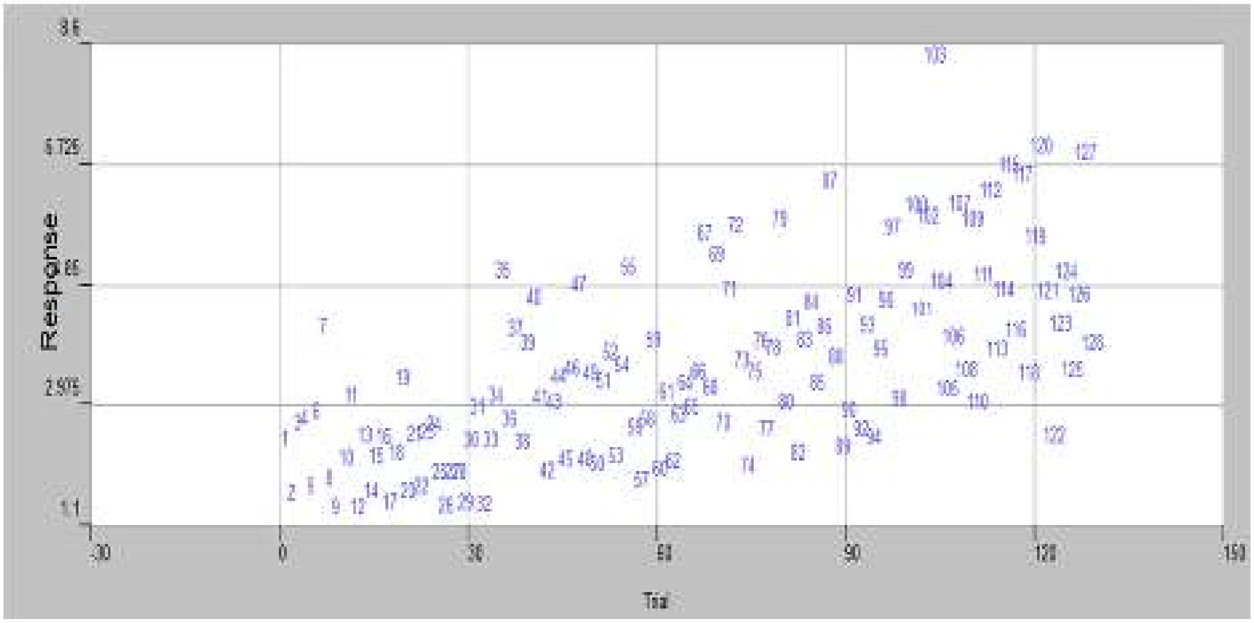

Figure 5. 28 Scatter point distribution for objective response

After iterative simulation, ADAMS/INSIGHT to standard variance (ANOVA) tools to fit the simulation results shown in the scatter diagram (fig 5.27), the degree of fitting is good (a Goodness of fit) check the fitting, the fitting results are shown in table 5.4. The greater the R2 said the better the fitting, R2adj is usually less than R2, when the value of 1 indicates that the fitting very well; P value indicates whether useful items in a fitting expressions, the smaller the value, the more useful items; R/V model calculation value and the relationship between the original data points, the higher the value, the better, at the same time, more than 10 R/V shows that model has a good prediction results[54] . Table 3 shows hard point coordinate position before and after optimization for the combined parameter optimization. It explains fitting is verified the correctness of the relationships between variables and the design goal.

Table 5. 4 Fit for regression "toe angle"

	DOF	SS	MS	F	P
Model	8	254	31.8	202	1.84e-65
Error	119	18.7	0.157		
Total	127	273			
R2	0.931				
R2adj	0.927				
R/V	66.7				

5.9.2 CAMBER

The proper camber angle can ensure the handling stability of the tire. If the angle changes too much, it will reduce lateral adhesion of tire, so that it need to minimize the change of the camber angle[64]. The data from pareto chart (Fig 5.28) shows the effect of each hard point on the camber angle. The most significant hard points are selected for the combined parameter optimization as shown in table 5.5. The result achieved from the ANOVA table are evaluated as per the criteria for the regression fitting. The scatter point diagrams are the response s for each and every trial in the screening of significance. The green color in the table 5.5 (green) implies that the fitting in the response surface method is accurate, so that it is very confidential to predict the response for other trials.

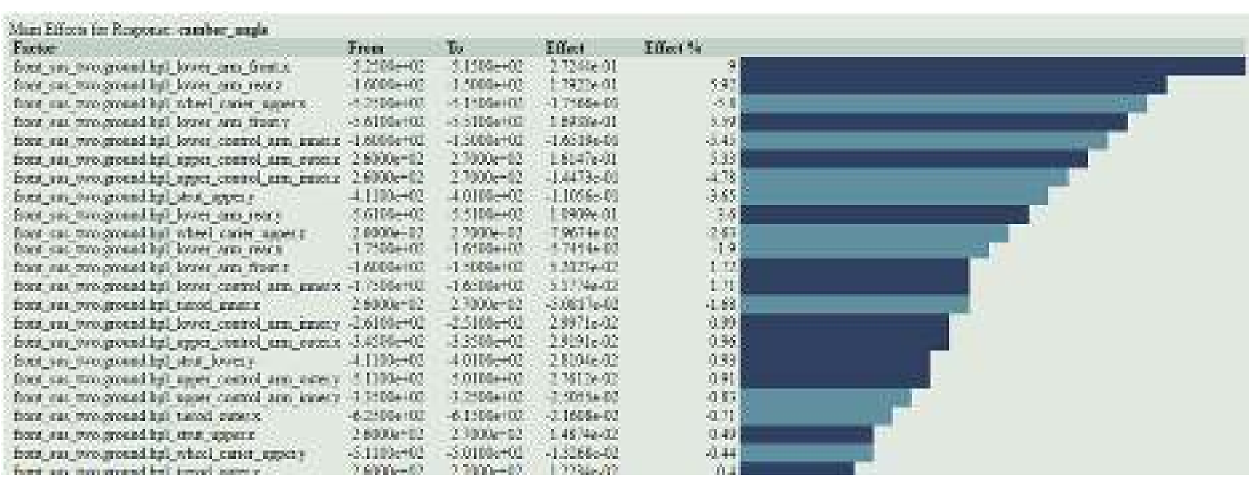

Figure 5. 29 Pareto chart for camber angle

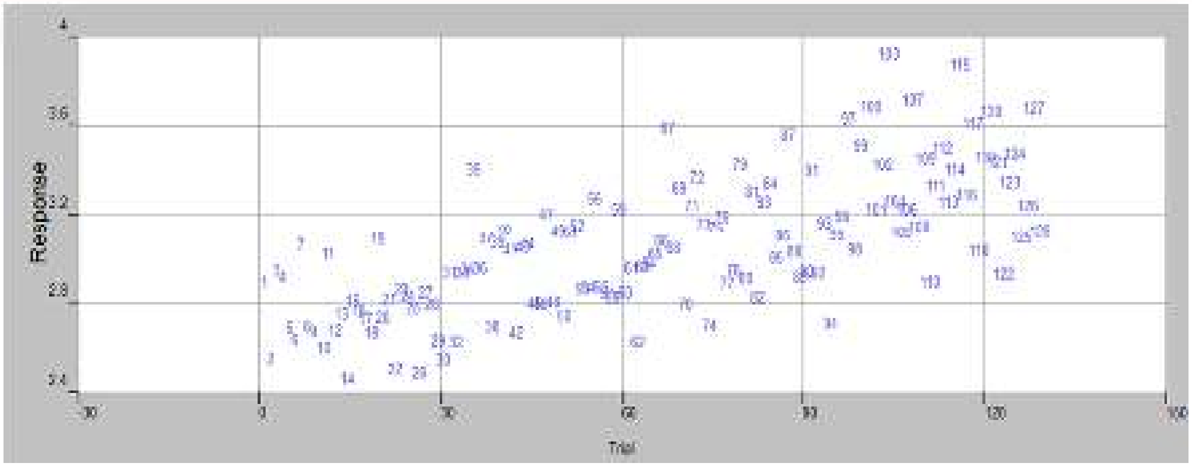

Figure 5. 30 Scatter point diagram of response for each trial

Table 5. 5 Critical hard points which affect camber angle

Critical hard points	Effect in %
Front_sus_two_ground.hpl_lower_arm_front.x	9
Front_sus_two_ground.hpl_lower_arm_rear. z	5.92
Front_sus_two_ground.hpl_wheel_carier_upper.x	-5.8
Front_sus_two_ground_hpl_lower_arm_front. y	5.59
Front_sus_two_ground.hpl_lower_control_arm_inner. z	-5.45
Front_sud_two_ground.hpl_upper_control_arm_outer. z	5.33

Table 5. 6 Fit for regression camber angle

	DOF	SS	MS	F	P
Model	8	111.9	1.49	488	3.84e-87
Error	119	0.362	0.00305		
Total	127	12.2			
R2	0.97				
R2adj	0.968				
R/V	97.7				

5.9.3 CASTER ANGLE

The hard points assessed in the screening for caster angle shows that only some of them have significant effect. The factor Wheel_carier_upper.x has the highest effect in the variation of caster angle. Lower arm_front_x and Wheel_carier_upper. y follows wheel carier_upper.x. The most significant hard point factors are selected for combined parameter optimization from pareto chart (fig 5.30). Table 5.5 describes the selected factors for better effect in caster angle change. The ANOVA table description is put down in table 5.6. All the evaluation parameters meet the requirement for the regression analysis. The green spot in the table 5.6 shows that the magnitude for the parameter is in the required and optimal setting.

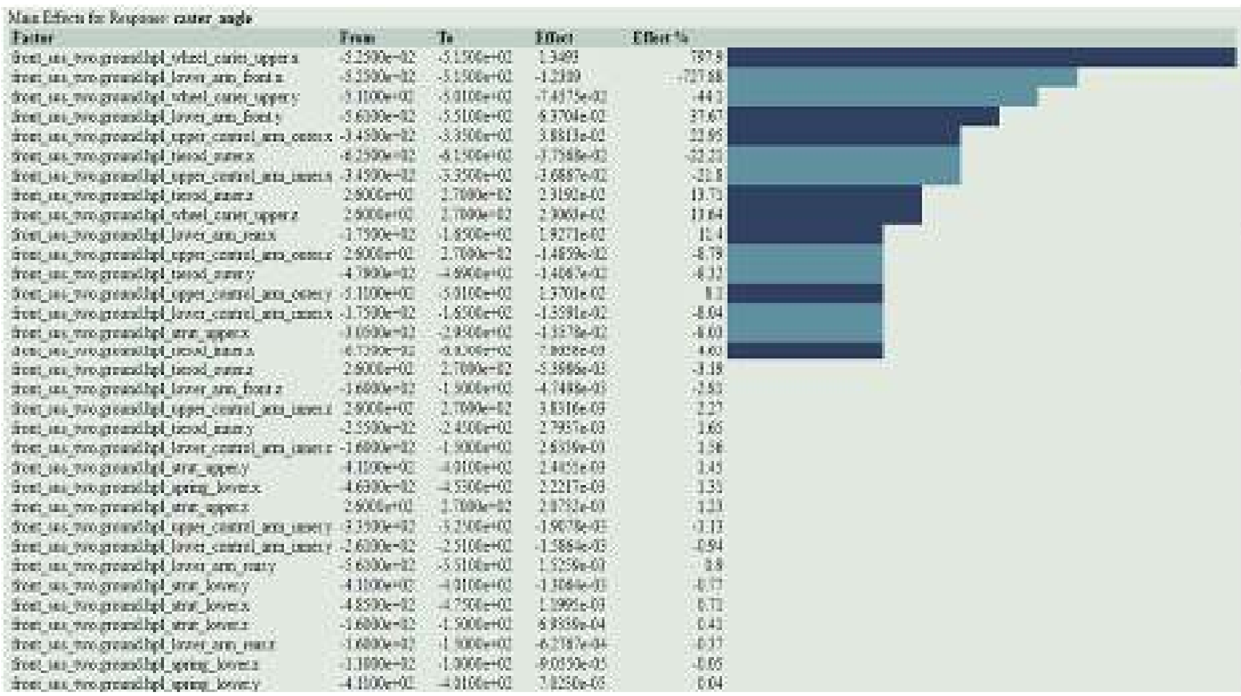

Figure 5. 31 Pareto charts for caster angle

Table 5. 7 effect of critical hard points in caster angle

Critical hard points	Effect in %
Front_sus_two_ground.hpl_wheel_carier_upper.x	797.9
Front_sus_two_ground.hpl_lower_arm_front.x	-727.88
Front_sus_two_ground.hpl_wheel_carier_upper. y	-44.1
Front_sus_two_ground.hpl_lower_arm_front. y	37.67
Front_sus_two_ground.hpl_upper_control_arm_outer.x	22.95
Front_sus_two_ground.hpl_tierod_outer.x	-22.21
Front_sus_two_ground.hpl_upper_control_arm_inner.x	-21.8

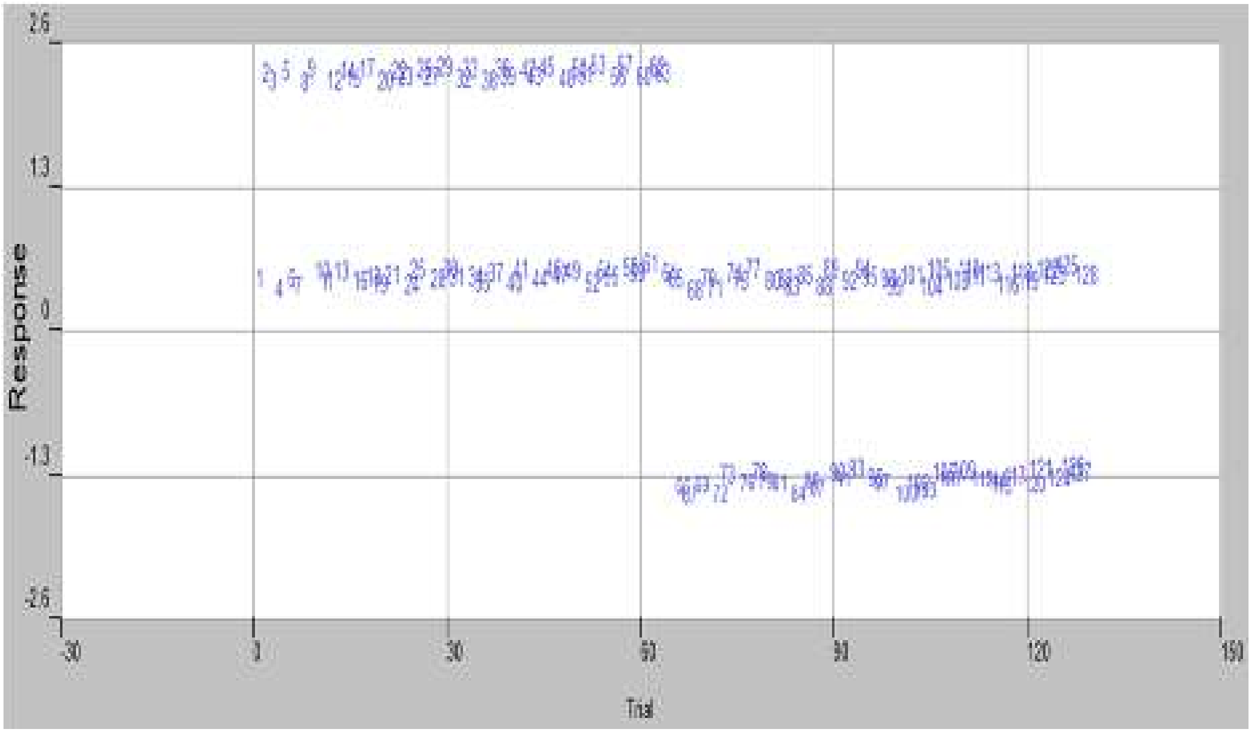

Figure 5. 32 Scatter point diagram for caster angle response for each trial

Table 5. 8 Fit for regression "caster angle"

	DOF	SS	MS	F	P
Model	8	215	26.9	6.45e+04	1.46e-212
Error	119	0.0497	0.000417		
Total	127	215			
R2	1				
R2adj	1				
R/V	714				

5.9.4 KINGPIN INCLINATION ANGLE In this part only two hard point factors (Table 5.7) are selected from the screening. The pareto chart shows that Wheel_carier_upper. y has 15.39% and Lower_arm_front.y. y has absolute value of 13.59%.all the other factors haven't any significant effect or the effect is very small (Fig 5.32). The variance of response depicted from Fig 5.32 is very small.

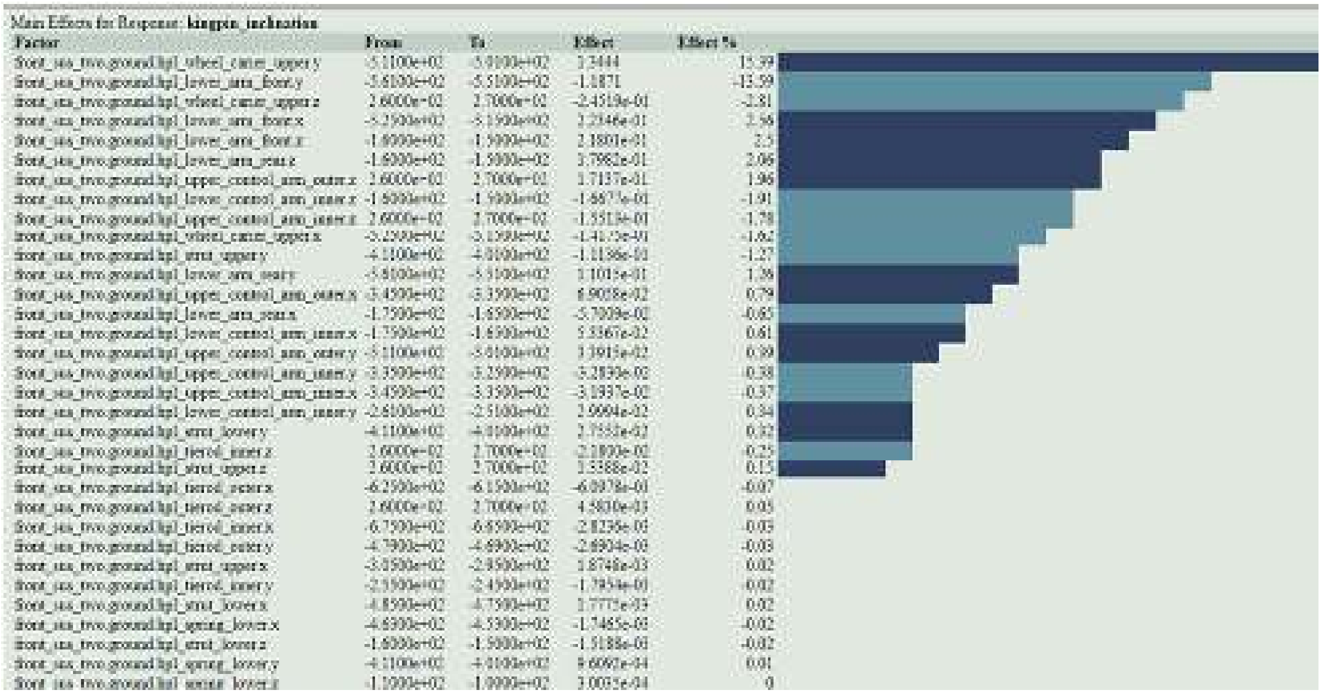

Figure 5. 33 Pareto charts for kingpin inclination angle

Table 5. 9 effect of critical hardpoints for kingpin inclination angle

Critical hard points	Effect in %
Front_sus_two_ground.hpl_wheel_carier_upper. y	15.39
Front_sus_two_ground.hpl_lower_arm_front. y	-13.59

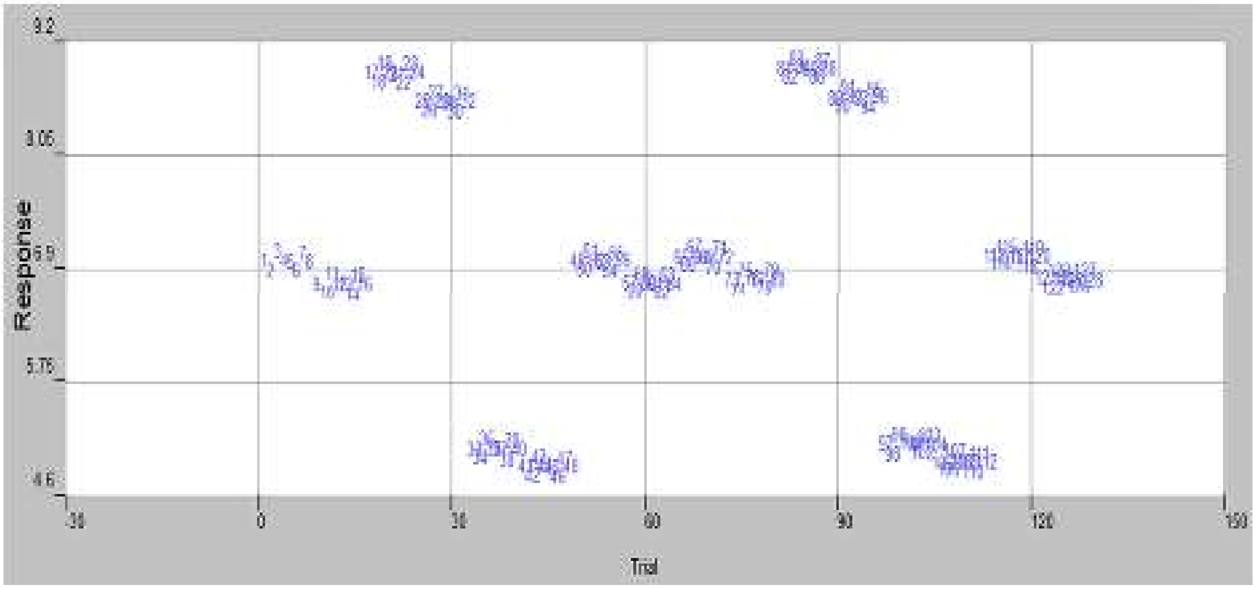

Figure 5. 34 Scatter point diagram of response for each trial in kingpin inclination angle

Table 5. 10 Fit for regression “kingpin Inclination angle"

	DOF	SS	MS	F	P
Model	8	227	28.4	5.81e+04	7.85-210
Error	119	0.0582	0.000489		
Total	127	227			
R2	1				
R2adj	1				
R/V	719				

5.10 COMBINED PARAMETER OPTIMIZATION

Finally, from all the above suspension parameter optimization the most significant and the better mode effect are selected for parameter optimization. Fig 5.34 implies that the selected hard point factors from all suspension parameter screening are significant for combined parameter optimization. After developing polynomial of from the response surface method the trial which have the better result are selected. From combined parameter optimization, (Fig 5.34).

Term significances for model "Model_03"

	toe_angle	camber_angle	caster_angle	kingpin_inclination	Term
1	2.6983e-21	1.5528e-38	2.7339e-18	6.7628e-31	1 (constant)
2	2.3071e-48	3.0725e-70	1.6834e-200	1.5802e-21	lower_arm_front.x
3	1.4939e-28	2.1268e-48	1.1327e-11	2.6516e-197	lower_arm_front.y
4	0.0044393	0.17457	5.2662e-13	1.8285e-197	wheel_carier_upper.y
5	5.7563e-14	2.3721e-22	8.2499e-34	2.5382e-90	wheel_carier_upper.z
6	1.0986e-10	0.0019497	3.9124e-05	0.0096297	tierod_outer.x
7	2.513e-24	1.7879e-45	1.8106e-44	4.2796e-48	upper_control_arm_outer.z
8	4.4504e-15	1.4727e-40	0.00010873	3.7223e-45	upper_control_arm_inner.z
9	8.4229e-41	8.037e-50	3.6351e-200	0.2032	wheel_carier_upper.x

Figure 5. 35 Term of significance for combined parameter optimization

There are six trials in addition to the original one to select and compromise for the better behavior of the car. The result and way of compromising is discussed in the next chapter. Actually, we have many trials as shown in Table 5.9, which have parameter of in optimal setting. But for such kinds of trial, the judgement is due another vehicle property like roll over and lateral behavior of the car.

Table 5. 11 Selected optimized trials for additional analysis

No	Factors and responses	original	1st trial	2nd trial	3rd trial	4th trial	5th trial	6th trial
1	Lower_arm_front.x	-520	-524.2	-526.43	-526.76	-526.77	-526.77	-526.77
2	Lower_ arm_ front. y	-556	-561.76	-562.77	-562.77	-562.77	-562.77	-562.77
3	Wheel_carier_upper. y	-506	-503.48	-503.48	-505.16	-506	-509.36	-511.78
4	Wheel_carier_upper. z	265	266.68	267.52	269.2	270.04	271.09	271.1
5	Tie rod_outer.x	-620	-618.32	-616.64	-614.96	-614.22	-613.9	-613.9
6	Upper_control_arm_outer. z	265	263.32	261.64	259.96	259.22	258.9	258.9
7	Upper_control_arm_inner. z	265	271.75	271.77	271.77	271.77	271.77	271.77
8	Wheel_carier_upper.x	-520	-515.8	-513.75	-513.89	-513.9	-513.9	-513.9
9	Max absolute value of toe angle	3.5209	1.6884	1.0453	0.92157	0.87688	0.87186	0.90657
10	Max absolute value of camber angle	3.047	2.6159	2.4634	2.4135	2.3938	2.3825	2.3846

11	Average value of caster angle	0.4664 1	1.5722	2.1452	2.1871	2.1934	2.1912	2.1879
12	Average value of kingpin inclination	6.8714	7.8803	7.9799	7.7133	7.5811	7.1109	6.7861

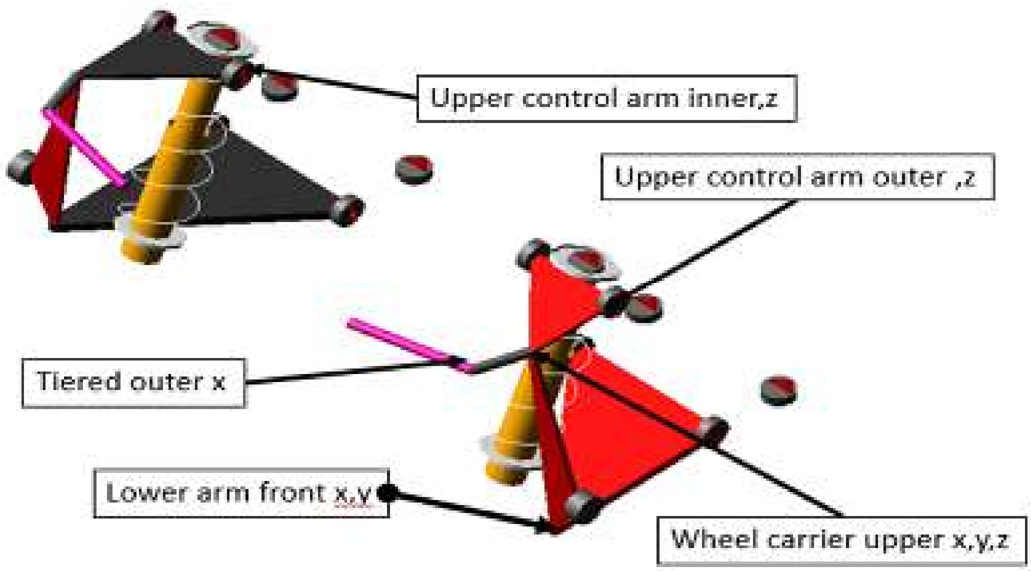

Figure 5. 36 Description of optimized parameters

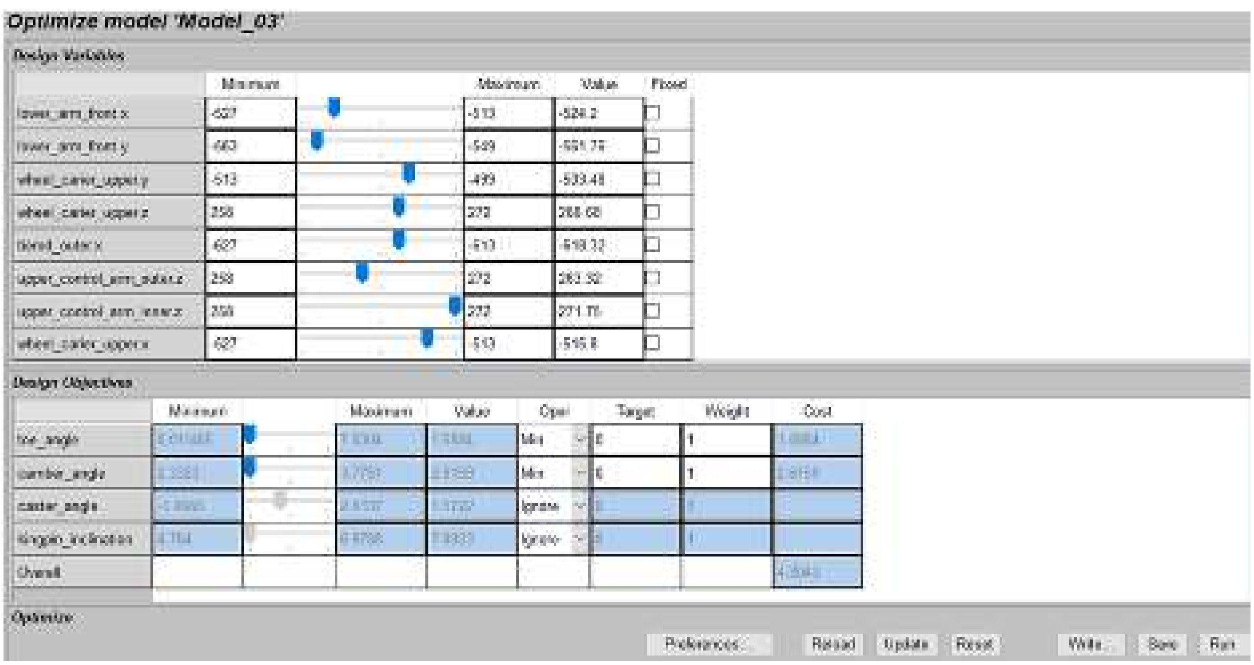

Figure 5. 37 Optimization of suspension parameter

CHAPTER SIX
RESULT AND DISCUSSION FOR DYNAMIC ANALYSIS

6.1 SUSPENSION PARAMETER OPTIMIZATION

A wide range of suspension parameters may be evaluated. Change in one Suspension parameter usually affects the other parameters[23]. but here, the most critical and principal parameters are analyzed and optimized. The principal ones being bump steer, bump camber, caster angle and kingpin inclination angle. Knowledge of these parameter values and characteristics is an essential tool to a thorough understanding of a vehicle's performance in terms of ride, impact isolation, steering and handling and lateral behavior.as we discussed in the previous chapter, these all parameter are optimized in order to get better vehicle performance. The optimization was based on hard point modification. Because, Kinematic design of a suspension system involves determining the positions of hardpoints or kinematic design points. Suspension static design factors such as toe, camber and caster are decided by the location of hardpoints. All cars have suspension static design factor in order to compromise the problem in the working condition. The optimal setting can be achieved by putting the hardpoints in the correct position at the suspension designing stage. This approach helps the car manufacture to save resources in multi direction.

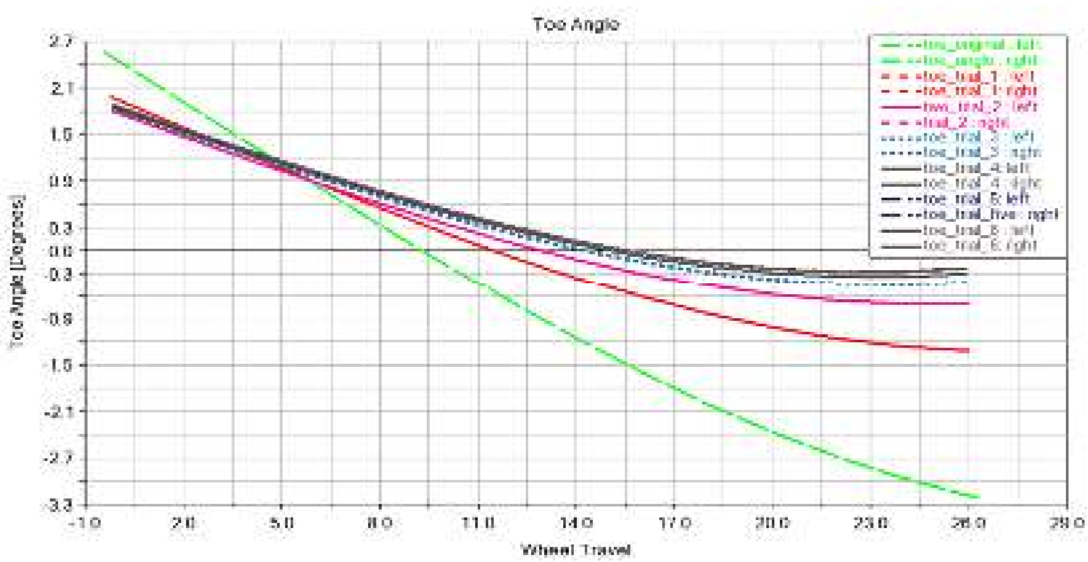

Figure 6. 1 Toe angle after optimization for the selected trial

Six trials (table 5.11) which have better results and minimum variation are selected for optimization and compromization as per multi objectives. Figure 6.1 depicts change in toe angle for all trials selected. Actually, all the six trials have better response relative to the original toe angle analysis. The original front suspension system toe angle varies from 2.7 degree of toe out to 3.1 degree of toe in. The variation is 5.8. This makes the car very difficult to control in off-road and also when there are potholes in the road. Trial-1 toe angle varies from -1.5 degrees to 2 degrees. It has better performance relative to original suspension system. Trail-4 and Trial-6 variance is very small relative to others. Trail-4 varies from 0 to 1.9 degrees. Trial-6 varies from 1.8 degrees to 0.2 degrees. Trail three is less in performance relative to trial-4 and trial-6.

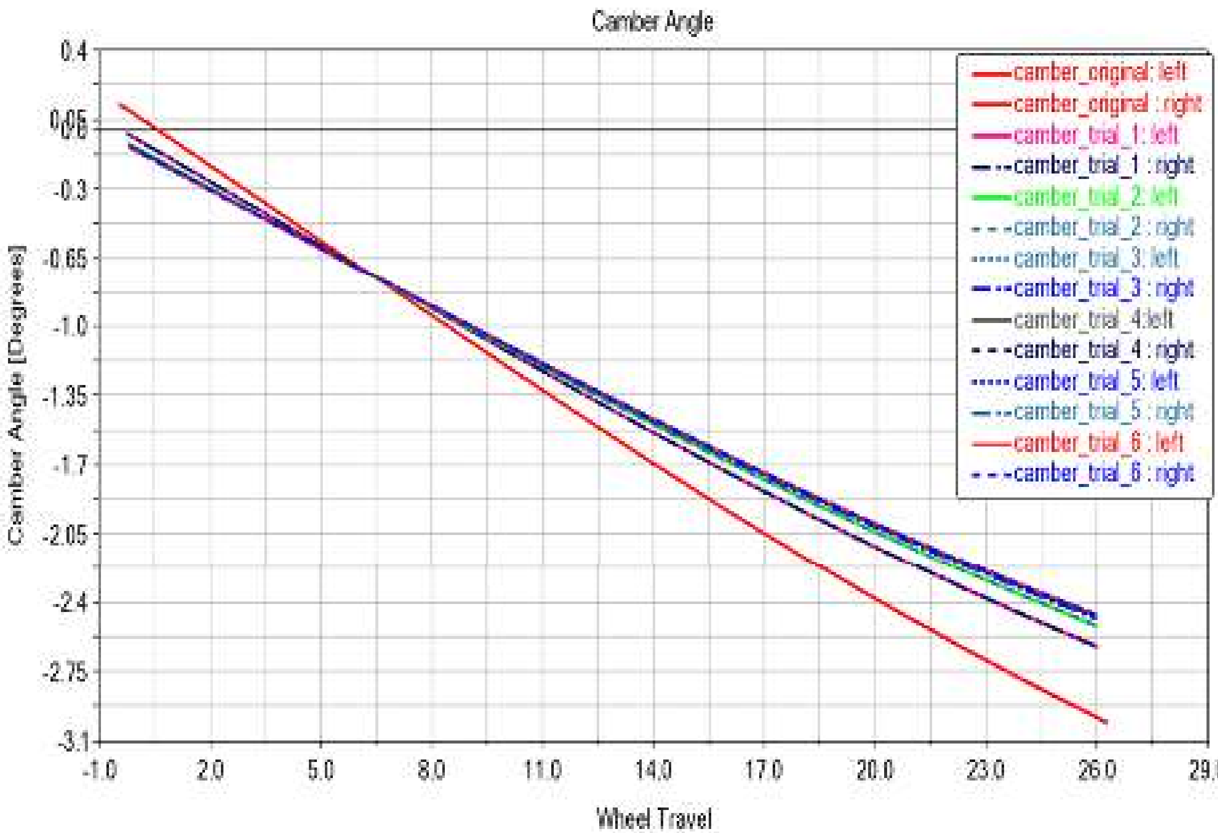

Figure 6. 2 camber angle after optimization for selected trial

Car manufactures use -1(optional) degree of static setting to compromise the camber out behavior in the working condition. When the car turns around weight transfers laterally to the external part of the car due to centrifugal force. This force makes the external tire to cary more load than the interior one. At that time if the tire to ground contact is small the traction force of the car decreases.

This behavior generally affects the cornering performance of a car. If negative camber is applied initially, the tire becomes in full grip of the road when cornering .so that the car can have better cornering performance.

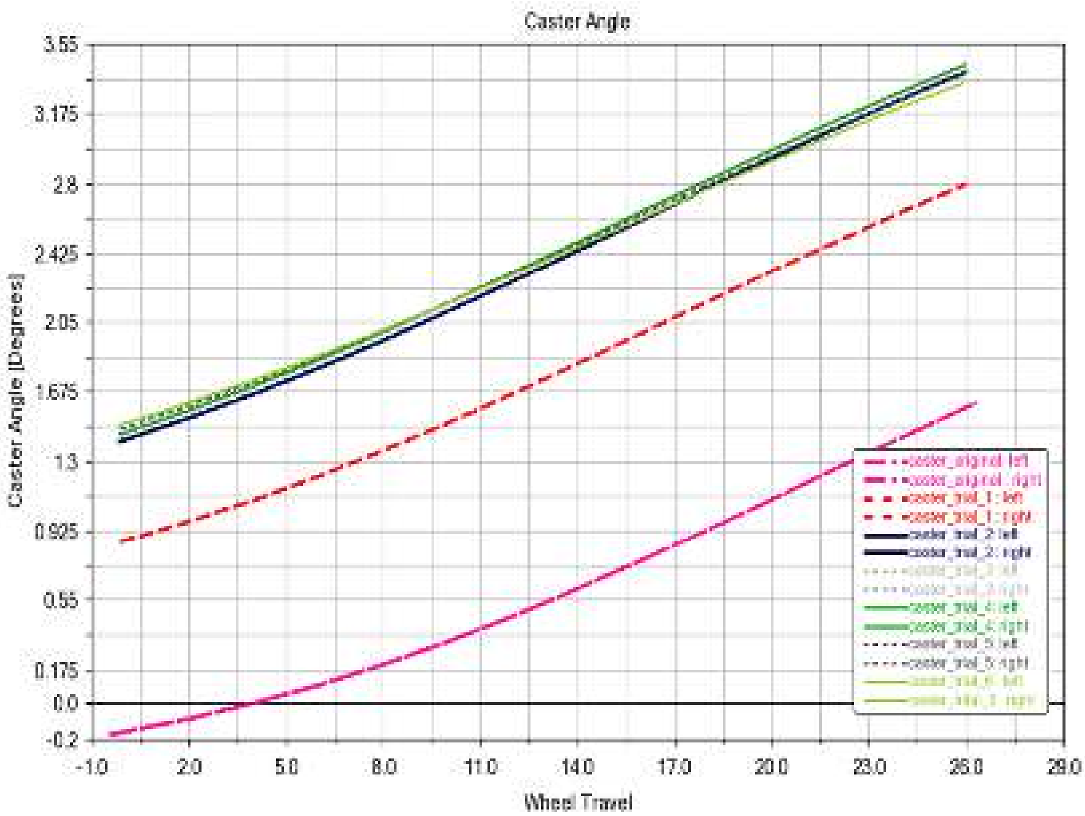

Figure 6. 3 Caster angle after optimization for selected trials

Fig 6.2 shows the camber angle result for each trial. The response converges to approximate value. The original suspension system camber angle varies from -3.1 to 0.3 degrees. As it is discussed previously that initially at static setting the camber angle of front suspension system was -1 degrees. When the wheel bumps in the first stage it starts to toe out which decrease the initial camber angle setting of -1 degrees to 0.3 and returns back at the rebound stages rebound. Trail 1 variation in camber angle is from -2.6 degrees to 0 degree. This trial shows that most of the time the tire is in the camber in position. This makes the outside of the tire to lean out. This is also the case for all other trials, but trials other than original, Trial-1 and Trial-2 have better camber orientation which is from -2.4 degrees to 0 degrees.

Caster angle behavior and its orientation effect is discussed in the previous chapter. Caster angle optimal result varies from car manufactures to manufacturers. This is because it is arranged as per their target objectives. if the caster is too negative and equal, the steering of the car becomes very light. So that the car becomes uncontrollable even in straight line maneuver. Because, if the tire hits either bump, rebound or pot holes, the steering system gives reaction at that time the car becomes out of control. If the caster angle is too positive and equal, the steering system becomes heavy to maneuver and it is difficult to make controlled maneuver. But using negative caster is not recommended.

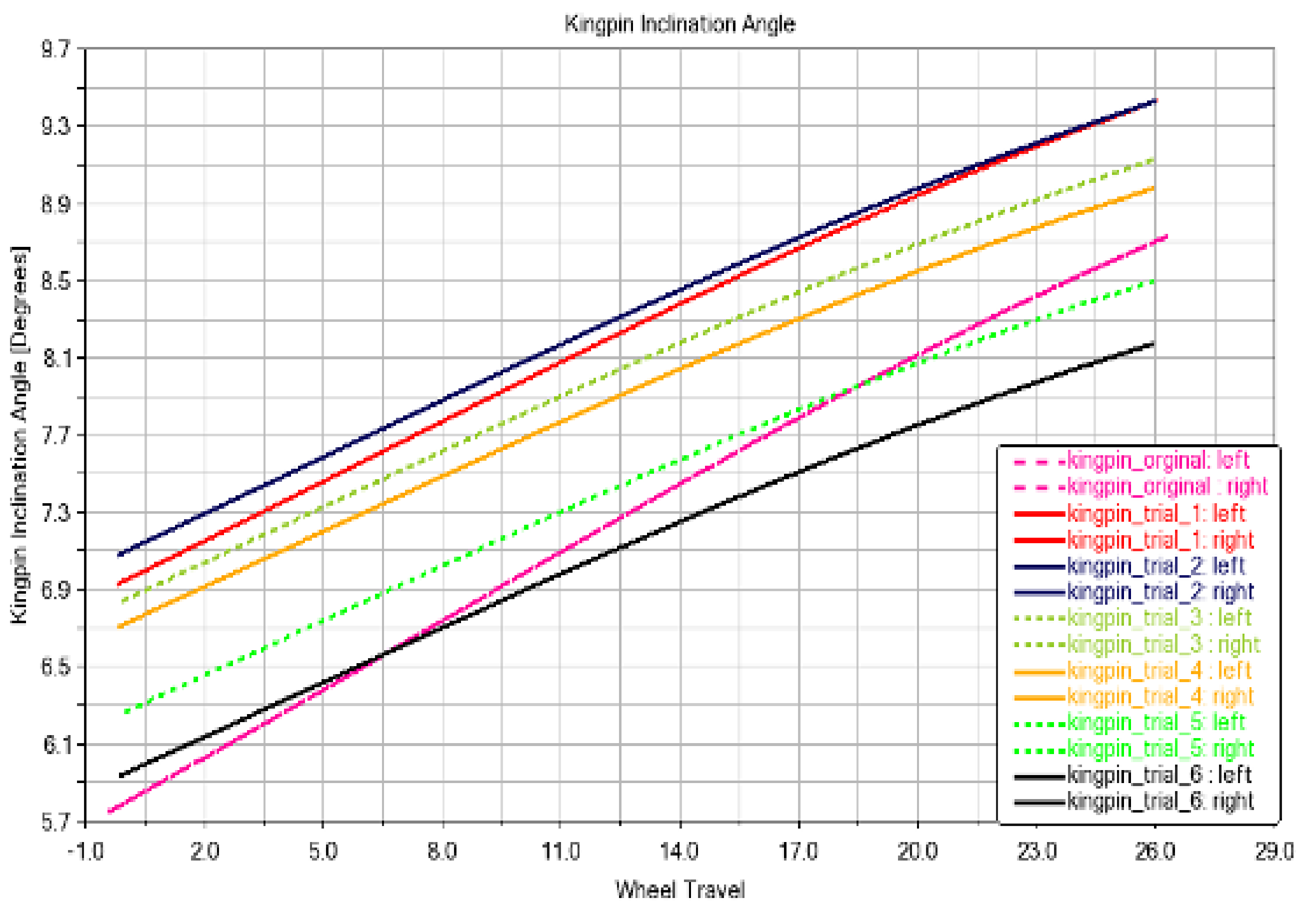

Figure 6. 4 Kingpin inclination after optimization selected trials

The original suspension system caster angles have negative value in some extent. This is not advisable. The caster angle varies for original suspension system from -0.2 to 1.6 degrees. Most of the time car manufacturer uses caster angle of 1.5 to 3 degrees. Some other car manufactures like Citroën C5, Audi A4, Renault Clio II, Peugeot 307, Volkswagen Tourane uses 3.1, 3.4,2.1 ,4.6, 7.5 respectively. Trail-1 caster angle is in between 0.8 to 2.8. it is better than the original value of suspension system. Trial-2 varies (Fig 6.3) from 1.4 degrees to 3.4 degrees. The caster angle for all other trials are approximately the same. Actually, caster angles have less effect in tire friction.

Kingpin inclination angle helps the car for self-centering. Kingpin inclination decrease the amount of force required to turn the car round. From the figure 6.4 we can see that all the trials, the original as well as the remaining trials kingpin inclination angle is in optimum setting. The original kingpin inclination angle varies in between 5.7 degrees and 8.7 degrees. The variation is 3. Trial-6 varies from 5.9 degrees to8.25 degrees. The variation is calculated as 2.35 degrees. Trial-2 has varied from 7.1 to 9.5 degrees. The difference in variation is 2.4. almost all of trials have approximately equal variation. But in some extent Trial-6 and Trail-3 have minimum variations.

6.2 ROLL OVER OPTIMIZATION

The main target of the paper was to minimize the roll over propensity of a car to increase the lateral performance of the vehicle. The paper done on the stability behavior of a car recommends to make analysis on stability of a vehicle base on lateral behavior affecting parameters. Obviously as it is discussed in the previous chapter, suspension parameters certainly affect the lateral behavior of a car. Camber angle, caster angle, kingpin inclination, and toe angle variation in the working condition of car increase and at some time decrease roll over performance of a car. To get significant roll over stability behavior the most functional trial is selected for additional roll over optimization.

6.2.1 EFFECT OF SUSPENSION PARAMETER ON ROLLOVER BEHAVIOR OF THE CAR

Suspension parameter directly affects the lateral behavior of a car. Significance of parameter for roll over varies from parameter to parameter. Our target but ideal statement is that "making the wheel in working condition in full grip and traction position".

A car performs many maneuvers even in normal conditions. The turning of the car directly creates lateral load distribution pot holes, tactile movements, bump, and rebound changes the value of the suspension parameter. For example, when the driver wants to brake the wheel movement the wheel becomes in toe out conditions .so it affects the stability of the car. To compensate this there is static setting of toe in condition. Camber angle has better direct relation with lateral behavior of a car. Because camber angle decides the amount of contact patch between the wheel and the ground. Amount of contact patch decides the amount of traction force and the ability to grip the road. The performance of a car to resist the centrifugal force comes from traction force of the wheel.

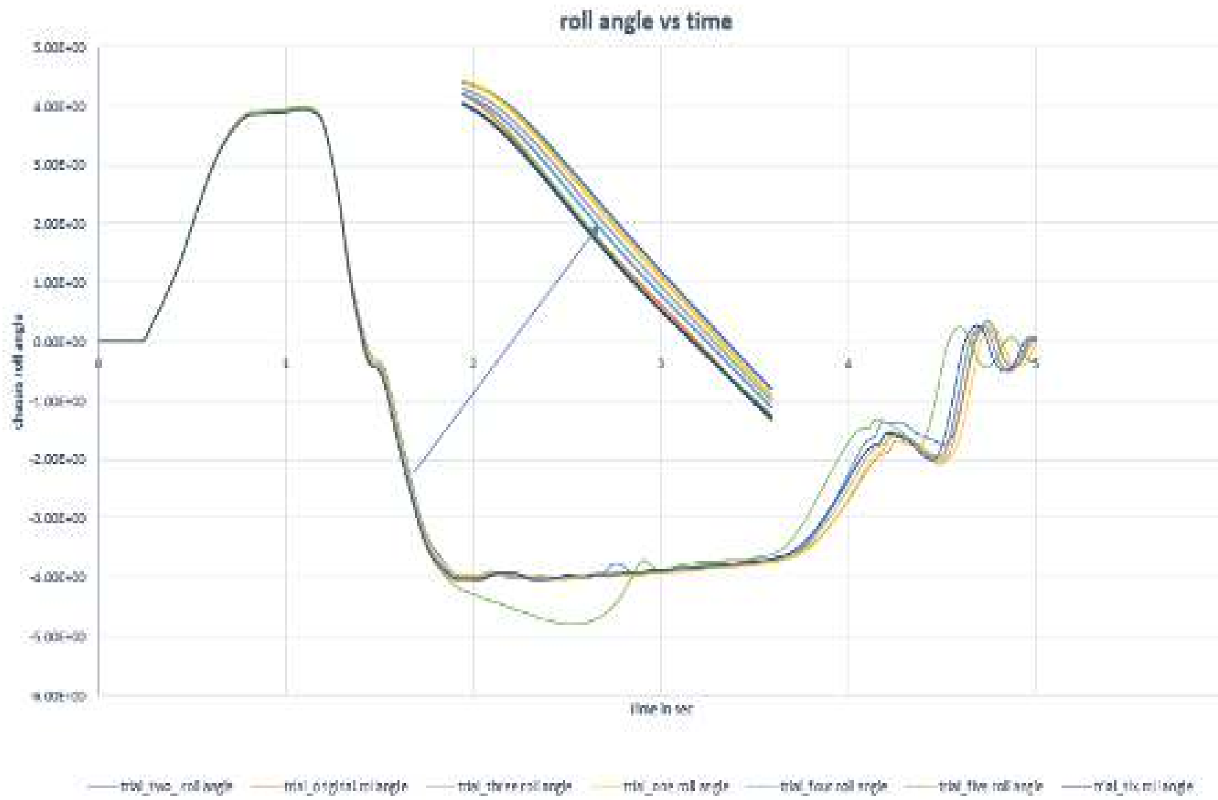

Figure 6. 5 Effect of suspension parameter optimization on roll over

The diagram (Fig 6.5) discusses effect of suspension parameter on roll over behavior of a car. In the previous topic it is discussed about the optimization of suspension parameter. It is not depicted their effect on roll over (lateral behavior of a car). The above diagram (fig 6.5) helps us to visualize the parameters significance on the lateral behavior. Suspension parameter optimization result shows that optimized suspension parameters are better than the original one in rollover performance. Table 6.1 describes the maximum roll angle for each trial when the car is in left and right fishhook maneuver. Actually, except trial-five all the other trials roll angle have related result.

Trial-five turning to the left in fishhook maneuver recorded maximum roll angle is 3.905, but in the second right turn maneuver the maximum roll angle reaches to 4.7992. it is very high relative to other trials.

Table 6. 1 Maximum roll angle for suspension parameter optimized trials

Trials	original		Trial-1		Trial-2		Trial-3		Trial-4		Trial-5		Trial-6	
Directions	left	right	left	right	left	right	left	right	left	right	left	right	left	right
Rollover results	3.964	4.0036	3.9819	4.052	3.9854	4.0234	3.6965	4.0157	3.9612	4.0157	3.9509	4.7992	3.9447	4.0528

Trial -3,4, and Trial-6 have better results relative to the original fishhook results. From the previous suspension optimization discussion, Trial-6 has better in all parameters. The toe, camber, caster, and kingpin inclination variation of trial- 6 is minimum. As result trial-6 is selected for better advanced fishhook performances and rollover optimization.

6.22 ROLL OVER OPTIMIZATION AND ITS EFFECT IN FISHOOK SPEED

Cornering capacity of the tires is influenced by: suspension geometry, vehicle load transfer characteristics, vehicle downforce size, and characteristics of the tires and the vehicle gross weight[63] .the influence of vehicle suspension geometry on cornering capacity is selected for the analysis.

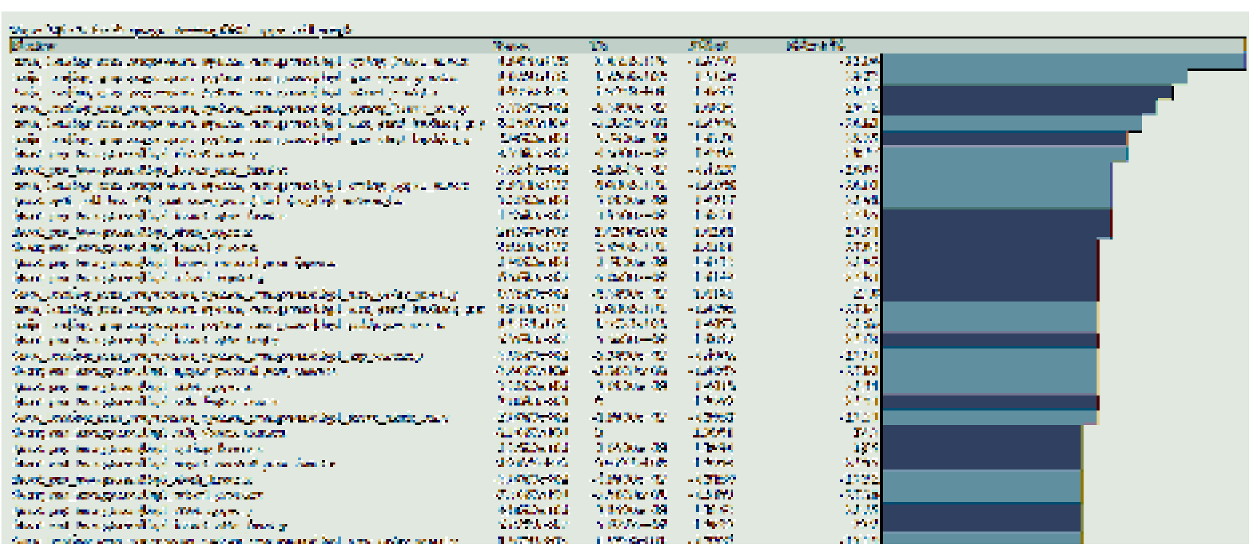

Figure 6. 6 Effect of hardpoint factors on roll angle optimization of the car

Hard points are the building block for suspension system. In the same manner which is described in the suspension parameter hard points are used as factor to optimize roll angle of car. Adams insight which is robust software for design of experiment used for optimization. Most of the optimization factors have equal effect on rollover angles of the car (shown in fig 6.5). because of this from the 255 trials, the arrangement with better roll angles are selected for the analysis. the result modified are listed in the appendix B. All the five trials have different roll angle optimization. Selecting the minimum roll angle trial may help the car to turn in minimum roll angles. But it is not enough to put and only upgrade roll over behavior of the car irrespective of understeer gradients. This is because, when we minimize the roll angle, it is mandatory to check the understeer gradient of a car. Understeer gradient (K) in swept steer test is simultaneously monitored to ensure that it increases less than 10% of its original value. Minimizing roll in fishhook maneuver is not the only objective, but also the vehicle understeer is the deciding factor and should be within the acceptable range.

Fig 6.6 shows the roll angle value of the optimized trials. Trial-4 has better roll over optimization angle. So that if the understeer gradient of Trial-4 is less than 10 %, optimization result on Trial-4 is acceptable.

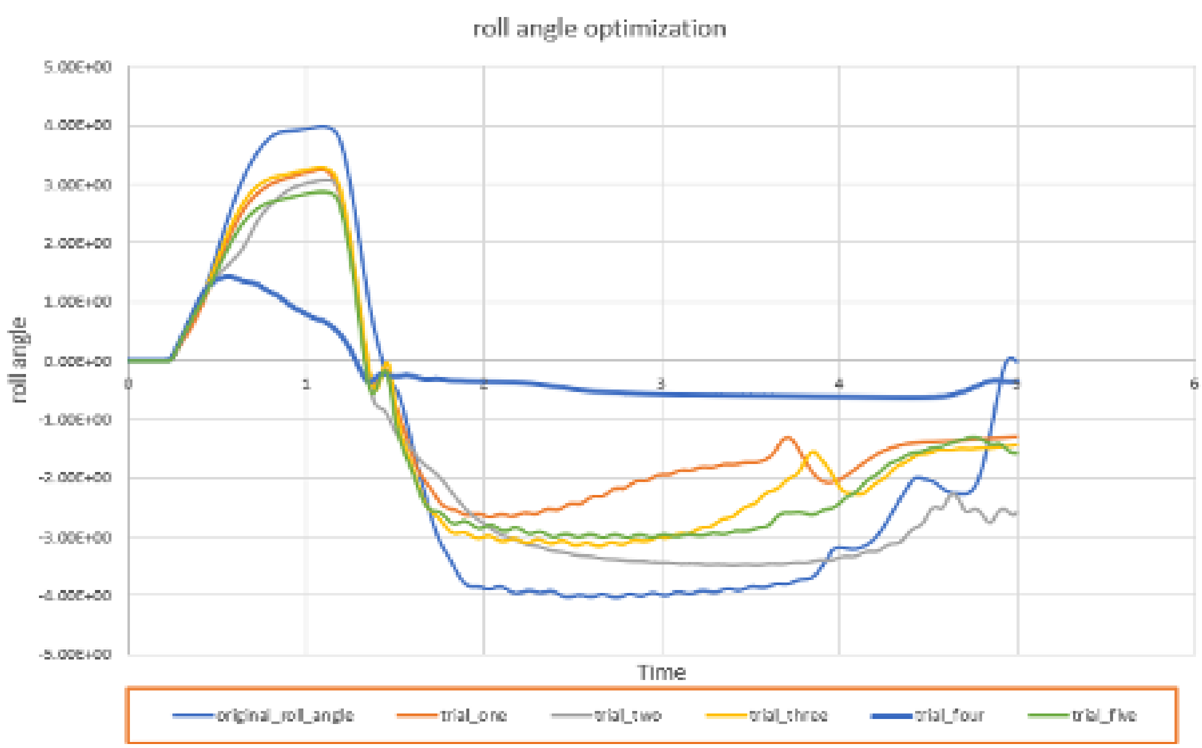

Figure 6. 7 Roll angle Vs time for optimized trials

As a result, the fishhook maximum speed will be assessed for this angle. But, if the understeer gradient of Trial-4 is greater than 10% then we will go to the next minimum roll angle from the optimization trial.

The fishhook speed of the previous unoptimized car was 50 km/hr (as shown in the Fig 5.22). According to the NHTSA standard, with a steering angle of 220 degrees at a speed of 50km/hr, the cars wheel lifts of from the ground. So, the work required here is to check whether the optimized roll angle system increase the lift of speed or not.

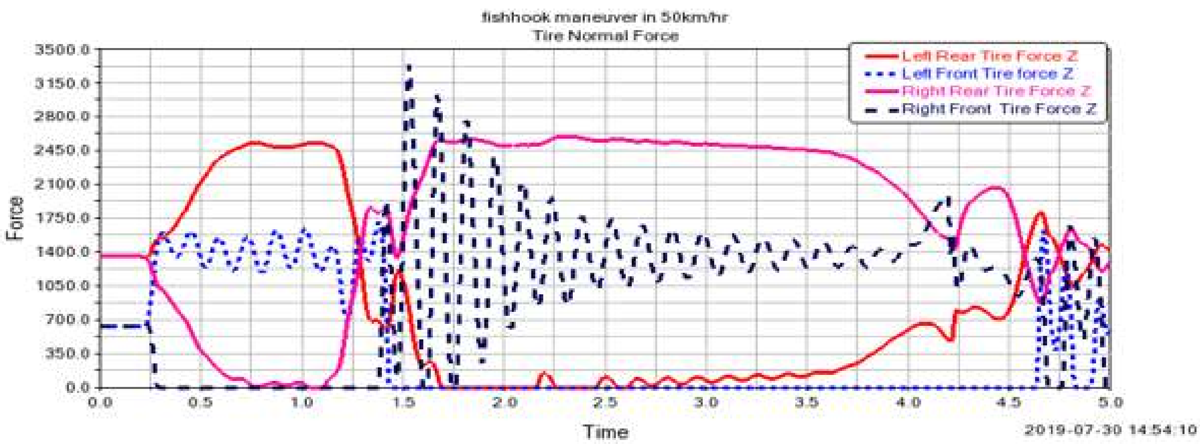

(a)

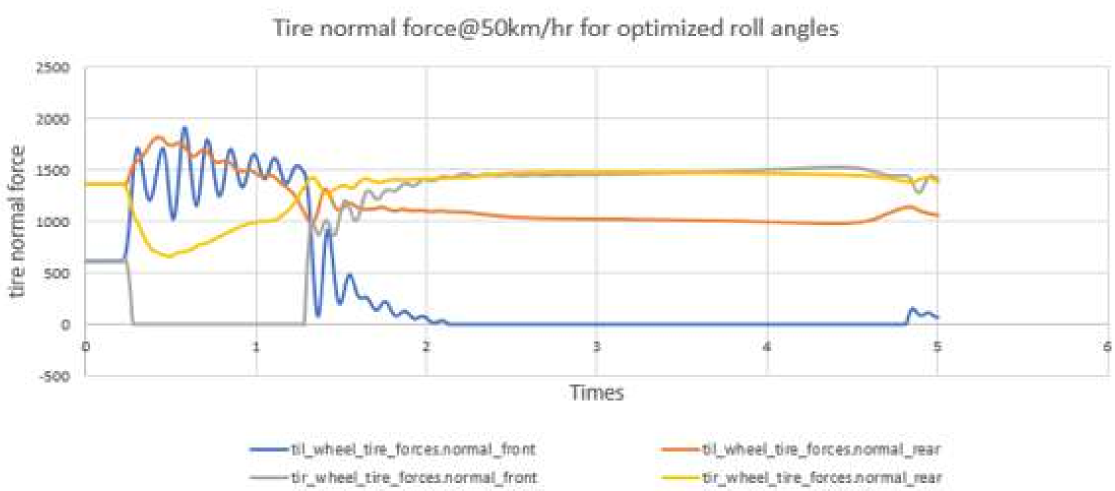

(b)

Figure 6. 8 Tire normal force at speed of 50km/hr (a) before optimization (b) after optimization.

Figure 6.8 shows the tire normal force at 50km/hr before and after optimization. The optimized model stops lifting of the wheel according to NHTSA. Because, the tire normal force for the rear wheel minimum force is about 500N. The force distribution before and after optimization varies. The force distribution in the optimized model is better and there is no disturbance. However, in the original model the car has a sinusoidal movement and disturbance. Figure 6.9 describes the wheel lift from the ground before and after optimization at 50 km/hr. The wheel lift is decrease from 85mm to 35 mm. the optimized model doesn't lift of at 50 km/hr. According to NHTSA the car is in lift of speed, if the two wheels lift of and the wheel lift of height is greater than 50.8mm.

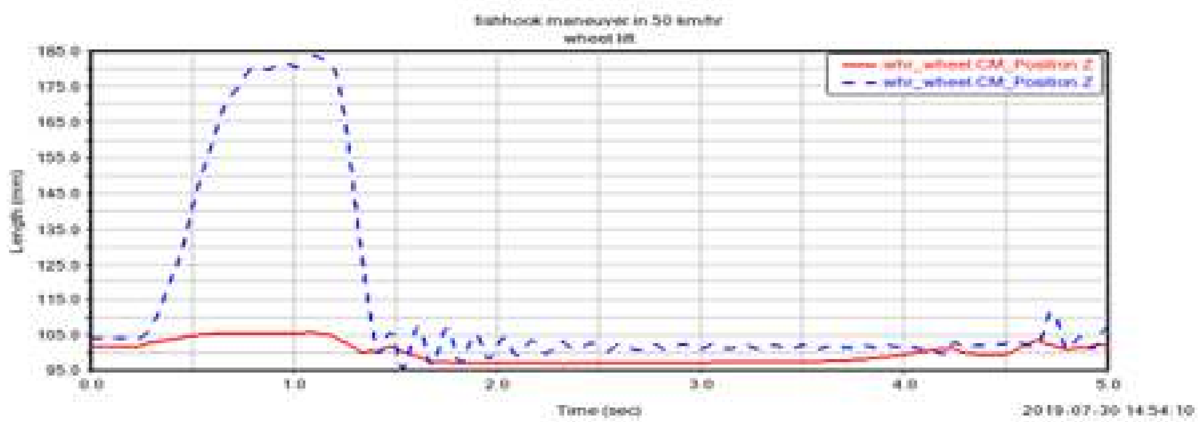

(a)

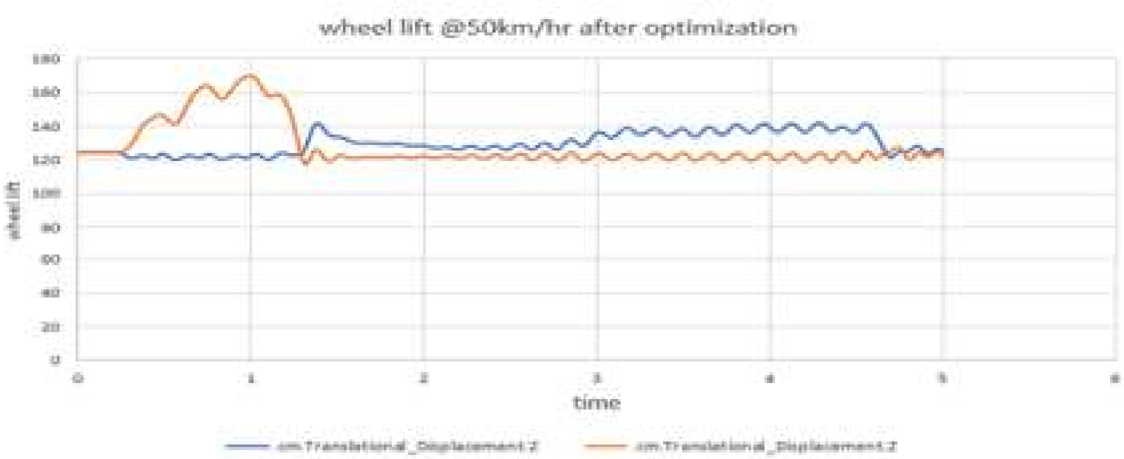

(b)

Figure 6. 9 wheel lift at 50km/hr before and after optimization

The optimized models wheel lift is checked at 60 km/hr and also at 65 km/hr. Still the car is not in fishhook at 60 km/hr. But the car reaches wheel lift of limit at 65 km/hr. Even the car wheel lift is around 53mm in front side, rear wheel doesn't lift of the ground. From Fig 6.9-wheel lift magnitude is plotted with a speed of 60 km/hr and 65 km/hr. NHTSA recommends that if there is sinusoidal movement or vibration even if the fishhook lifts of criteria is not attained, it is not recommended to drive with that speed. Figure 6.9 depicts that the car fishhook lift of speed can be greater than 65km/hr. The maximum designed speed of the four-wheeler bajaj qute car is 70 km/hr. Before checking for 70 km/hr, it is needed to evaluate tire normal force at 65 km/hr. If the tire normal force is normal, that means if there is no sinusoidal movement, it implies that the car fishhook lifts off speed can be greater than 65 km./hr. So, it may has possibilities of 70 km/hr fishhook lift of speed.

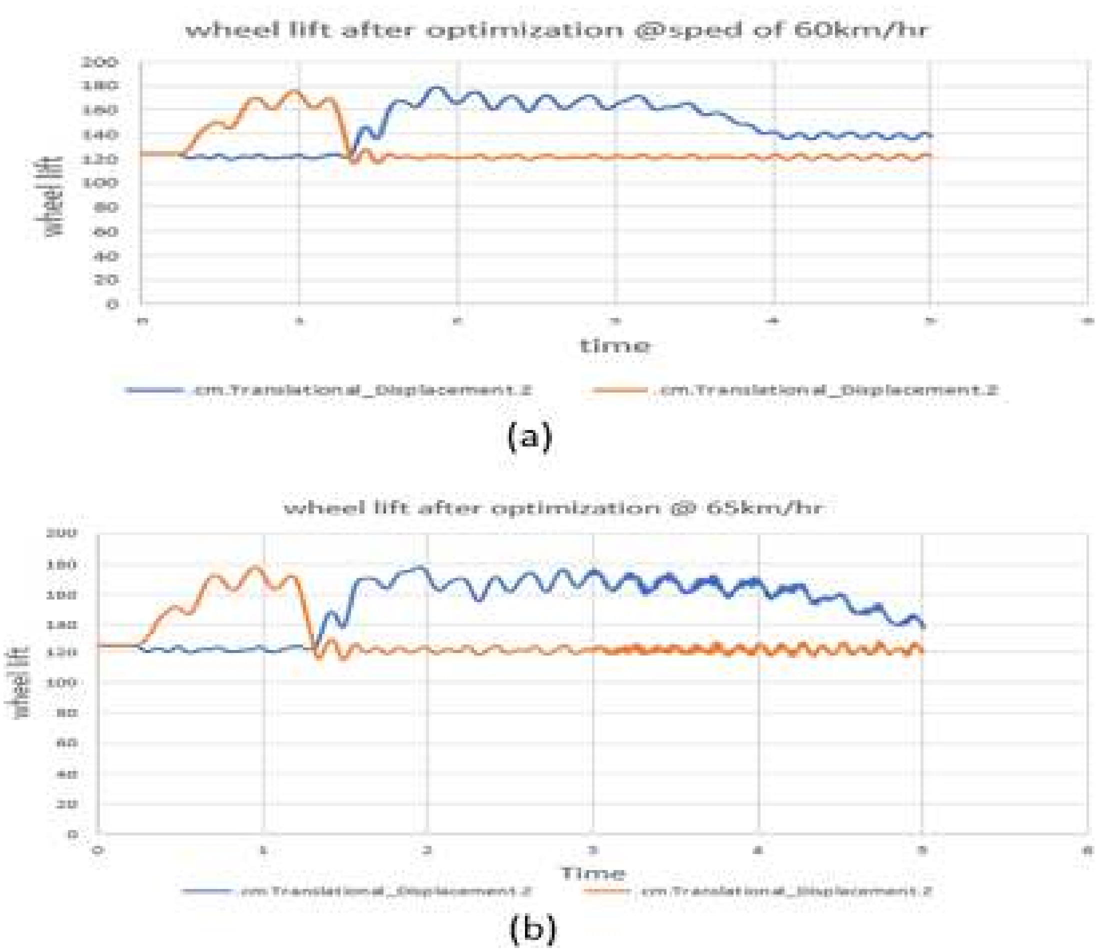

Figure 6. 10 Wheel lift off after optimization (a) with speed of 60 km/hr (b) 65km/hr

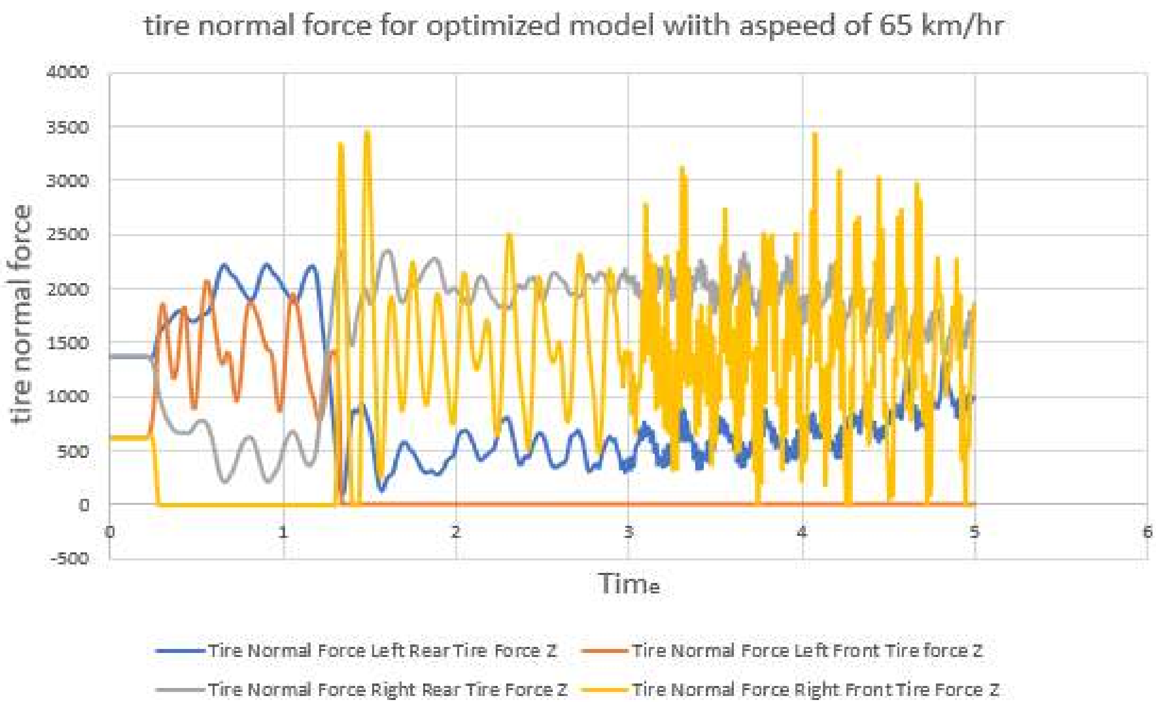

Figure 6. 11 Tire normal force for optimized model at speed of 65km/hr

Tire normal force for all wheels is described in fig 6.11. From the figure we can understand that the car is at high sinusoidal movement. The magnitude of the forces varies significantly, which affects the stability of the vehicle. As a result, even if the NHTSA criteria shows us that the fishhook lift of speed of four wheeler bajaj qute speed is greater than 65 km/hr, it is not recommended to drive it for fishhook with greater speed of 65 km/hr. the normal value to drive in fishhook maneuver is 60 km/hr but up to 65 km/hr it is acceptable.

6.2.3 CHECK FOR UNDERSTEER GRADIENT

The understeer gradient of a vehicle can greatly influence by how a vehicle handles its stability in turning. The value is dependent upon vehicle and tire properties and suspension characteristics.

$$\text{KUS} = \frac{\partial\delta}{\partial ay} \qquad \textit{equation } 6.1$$

Where KUS understeer gradient

$\partial\delta$ steering angles in rad

∂ay lateral acceleration

In reality, K_{US} is a function of several vehicle properties since the cornering stiffness is a function of suspension, load, and other vehicle parameters. With the above equation, the understeer gradient is in terms of the change in steer angle over the change in lateral acceleration.

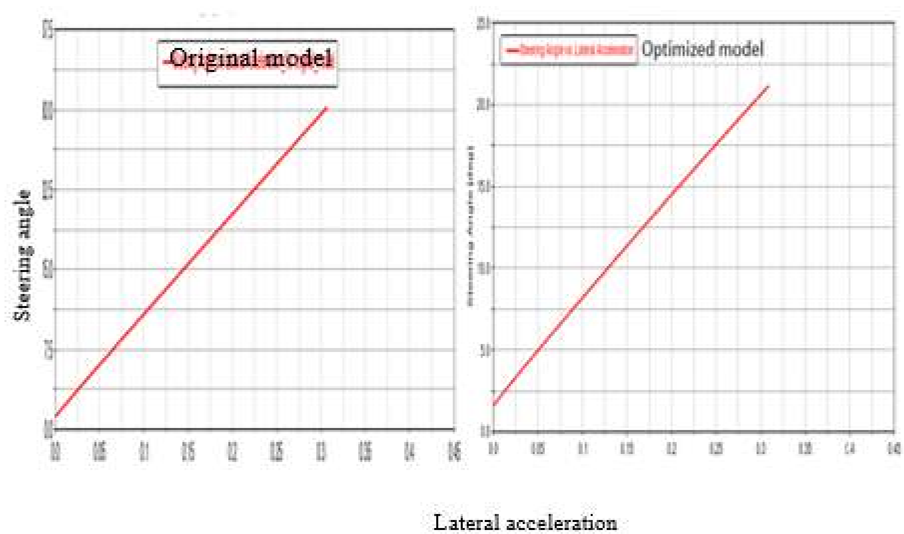

Figure 6. 12 Steering angle vs lateral acceleration (a) before optimization (b) after optimization

Vehicles can be described as understeer when the understeer gradient, Kus, is greater than zero. In a constant radius turn, an understeer vehicle requires an increasing steer angle with an increase in speed to maintain the constant radius turn. Most passenger cars are designed to be understeer, in order to allow the everyday driver to be able to handle the vehicle in evasive maneuvers[60].

Vehicles can be described as oversteer when the understeer gradient, Kus, is less than zero. An oversteer vehicle will want to turn more when the vehicle's velocity is increasing (the back end wants to slide out). Vehicles are not usually designed to be oversteer due to driving difficulties associated with the setup. In the constant radius test, the steer angle in an oversteer vehicle would have to be decreased as the longitudinal velocity increases to maintain the swept steer turn.

Vehicles can be described as neutral steer when the understeer gradient, Kus, is equal to zero. A neutral steer vehicle would optimize the handling characteristics during turning; however, a slightly understeer configuration is actually desired in production vehicles due to handling requirements[65].

Fig 6.12 shows average change of steering input per unit of lateral acceleration (in terms of g). the model before optimization has understeer gradient of 94 deg/g. This shows that the vehicle is in understeer condition, since the understeer gradient is greater than zero. After optimization the understeer gradient of the optimized model is 74deg/g of unit lateral acceleration. Even if the vehicle is still in understeer condition but the understeer gradient is decrease with 20 % of the original value. Even though commercial vehicles are designed to understeer condition for handling purpose. Only a slightly understeer configuration is enough. Finally, a car with a minimum but greater than zero understeer configuration is desirable for commercial vehicles.

CHAPTER SEVEN

RIDE COMFORT VERIFICATION

Passenger comfort is a very important parameter in design and manufacturing of automobiles. Suspension system carries the weight of the vehicle structure, driver, and passenger and it absorbs the vibrations passing to the vehicle body from the road. These vibrations are mainly due to irregularities in road surface, aerodynamic forces, and non-uniform wheel assembly. And among these, surface irregularities are predominant[16].

Ride comfort (RC) is defined as the condition where the passenger experiences no or minimum shocks that are transferred by the road surface. Changes in vehicle mass, suspension configuration and suspension characteristics will have an effect on the sprung mass and wheel hop frequencies[66]. So, minimum in the sprung mass acceleration has maximum in the RC. Ride Comfort is defined by the ISO 2631-1-1997(Table 7.1). Ride comfort is measured in terms of sprung mass acceleration. There are many harmful effects on body due to vehicle vibrations.

For the vehicle ride comfort studies, experimental research and theoretical analysis methods are generally used to simulate the vehicle ride comfort. The test research method on real vehicle test uses “design-trial production-test improvement-further trial production” process to simulate the vehicle ride comfort. This method is greatly influenced by objective factors and the test results feedback slowly, needing high cost and long cycle. The theoretical analysis method simplifies real vehicle model result in many important characteristics of vehicle that cannot be accurately analyzed[18].

Numerous studies have been conducted on the description and improvement of ride comfort. Four methods to evaluate ride comfort (human response to vibration) objectively are used throughout the world at present. The parameters, which are indicative of ride comfort (e.g. vertical acceleration), have been described and levels of acceptance laid down in standards such as ISO 2631, BS 6841, VDI 2057 and Average Absorbed Power (AAP).

Table 7. 1 Acceptability range of sprung mass vertical acceleration[37]

Range: Rms of vertical acceleration	Acceptability
<0.315	Not uncomfortable
0.315-0.63	A little uncomfortable
0.5-1	Fairly uncomfortable
0.8-1.6	uncomfortable
1.25-2.5	Very uncomfortable
>2	Extremely uncomfortable

Due to the fact that the geometry of a suspension system is optimized based on lateral stability, handling and road holding, the geometry of a suspension system has not been taken into account as a design variable for ride comfort. In fact, ride quality mostly depends on the characteristics of rear and front springs and dampers[67][68][68],but geometry of suspension system, and wheel assembly have great significance on the ride comfort of a vehicle.

In daily life, most people are exposed to vibrations that affect the human beings' health. Many researchers revealed those vibrations may cause the loss of performance on working people[69]. In this chapter, motion in vertical direction is normally considered for the quantification of discomfort. RMS acceleration of sprung mass gives a measure of Ride Comfort for passenger vehicles. Acceptability of measured value Rms acceleration of sprung mass is described in the ISO 2631 as shown in the Table 7.1[37]. The maximum limiting acceptable value of ride comfort is 1.6m/sec^2. Full vehicle is modelled as shown in Figure 7.1 to compute sprung mass vertical

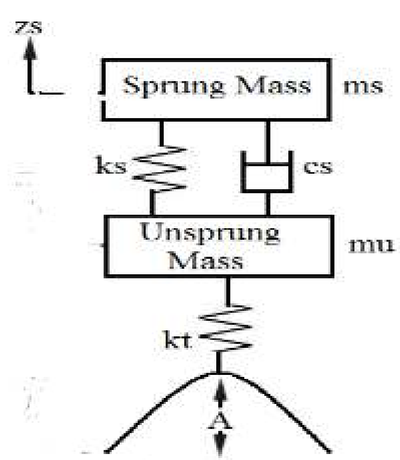

Figure 7. 1 full vehicle modelling for ride comfort verification

acceleration[16].

To the author's knowledge, no literature was found that is directly applicable to the ride comfort vs. handling decision as applied to off-road vehicles or controllable springs, although some of the concepts proposed by different authors are worth exploring [70].

To compute the ride comfort of the Bajaj qute, both original and optimized model are used for analysis. For both model the Rms value of sprung mass acceleration is calculated with different speed. Speed ranging from 10km/hr to 60 km/hr are used to compute vertical sprung mass accelerations. The mode of acceleration is the same but the Rms value of the acceleration different for both model at the same speed.

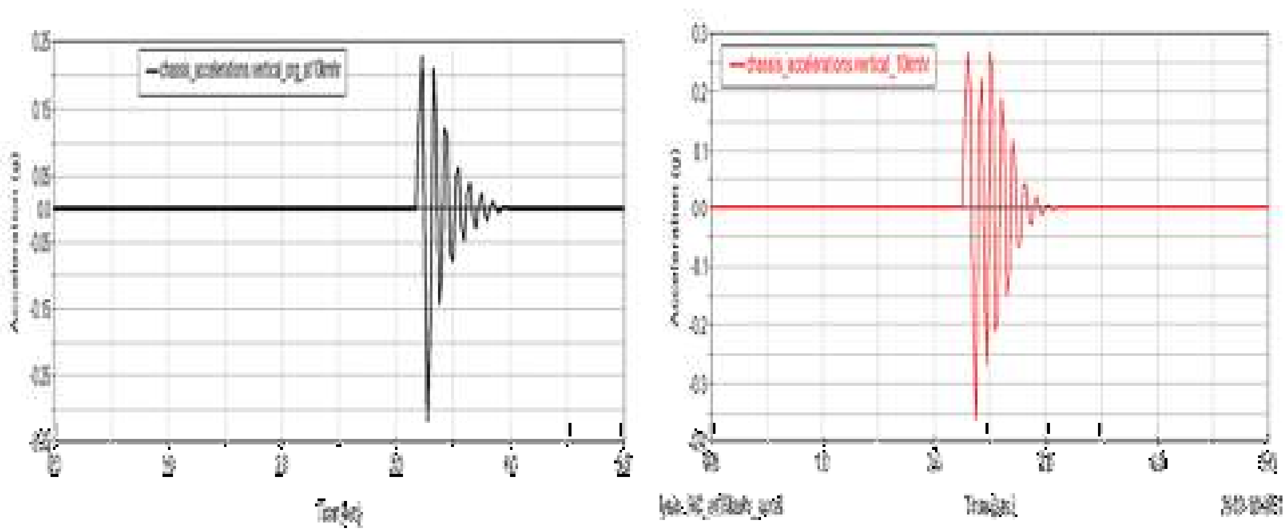

(a) (b)

Figure 7. 2 Sprung mass vertical acceleration at 10km/hr (a) original model (b) optimized model

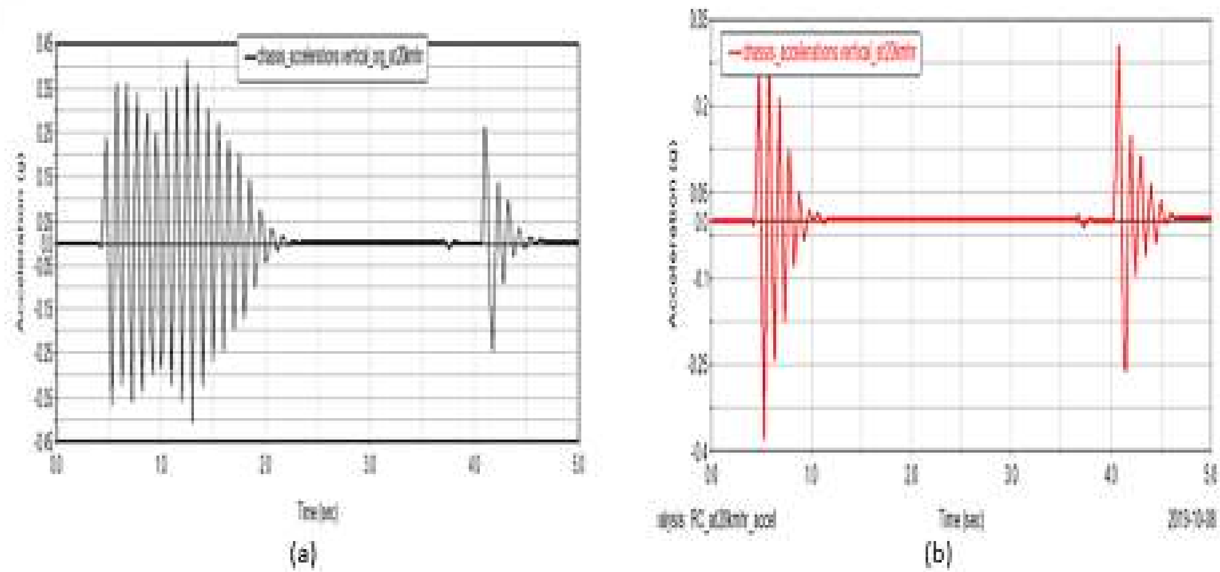

Figure 7. 3 Sprung mass vertical acceleration at 20 km/hr (a) original model (b) optimized model

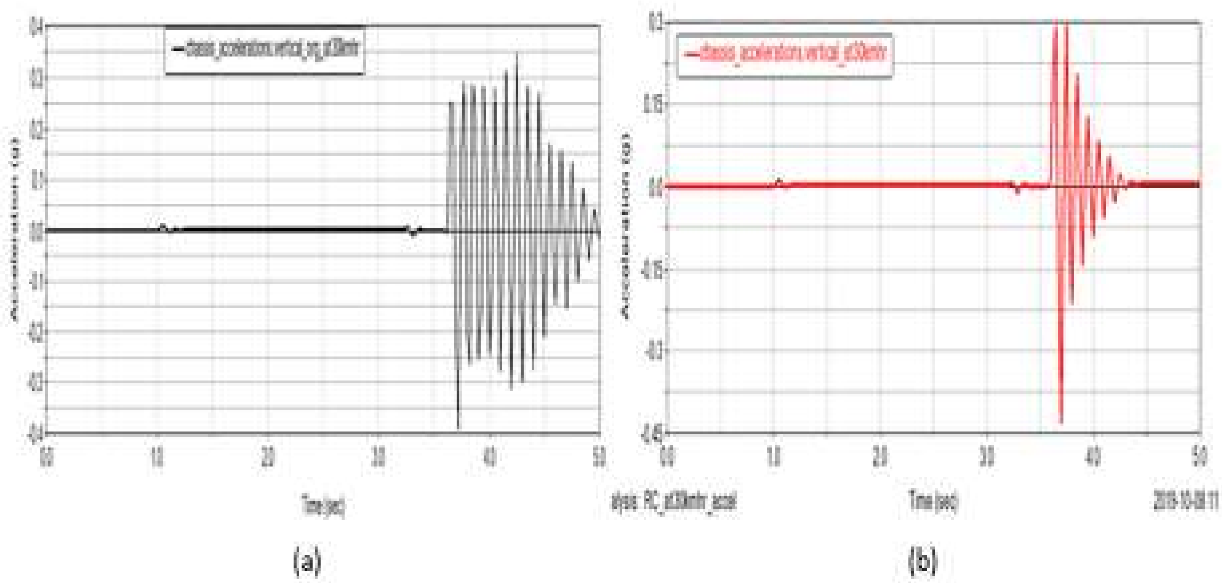

Figure 7. 4 Sprung mass vertical acceleration at 30 km/hr (a) original model (b) optimized model

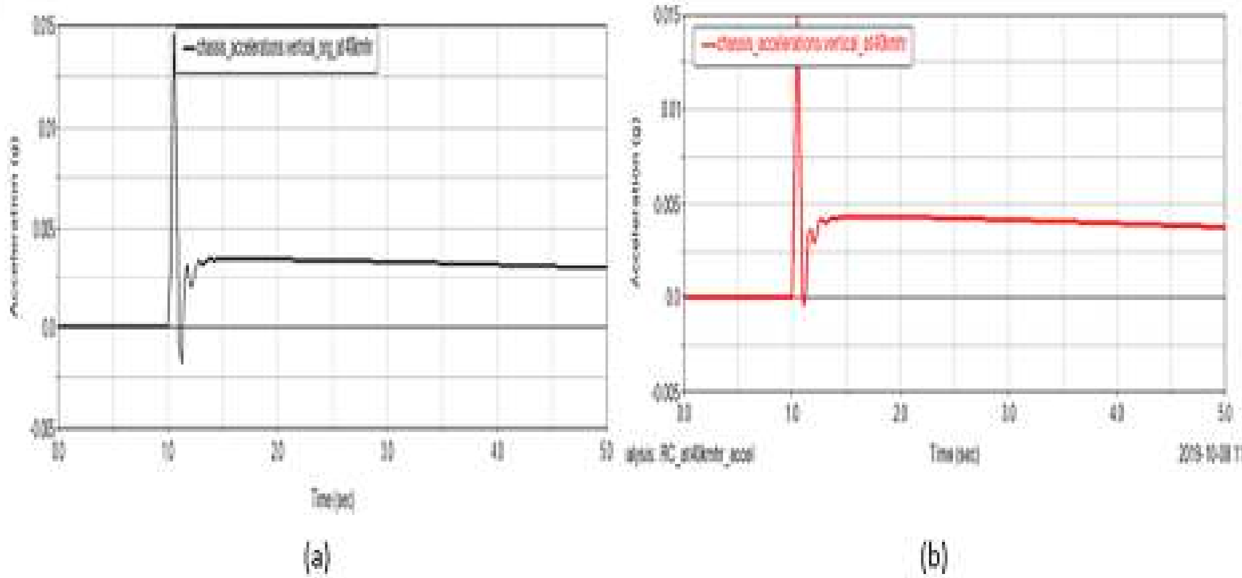

Figure 7. 5 sprung mass vertical acceleration at 40 km/hr (a) original model (b) optimized model

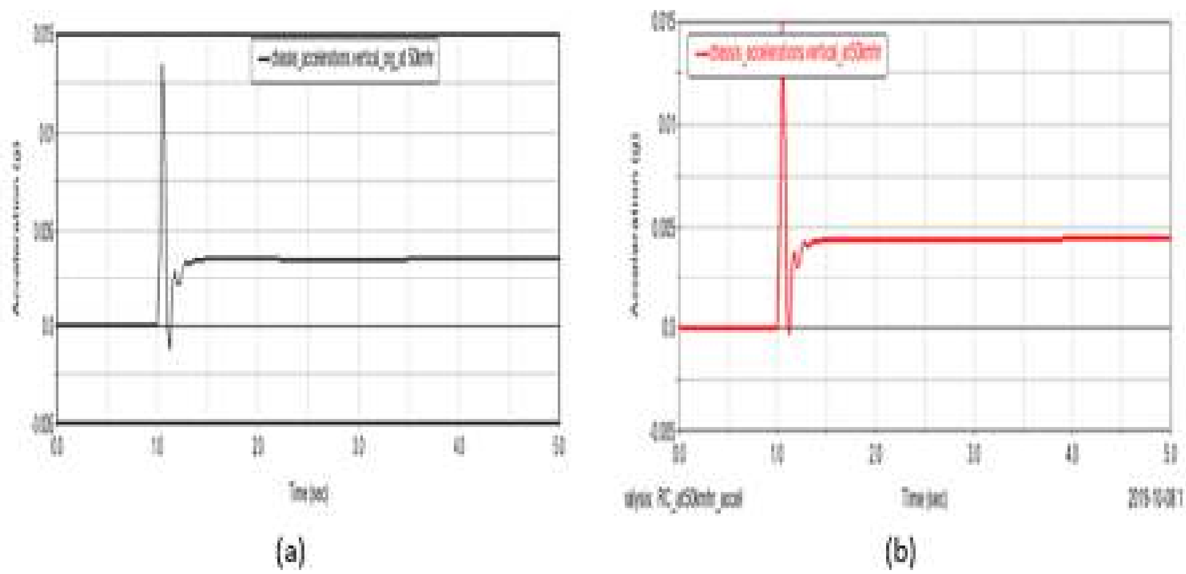

Figure 7. 6 Sprung mass vertical acceleration at 50 km/hr (a) original model (b) optimized model

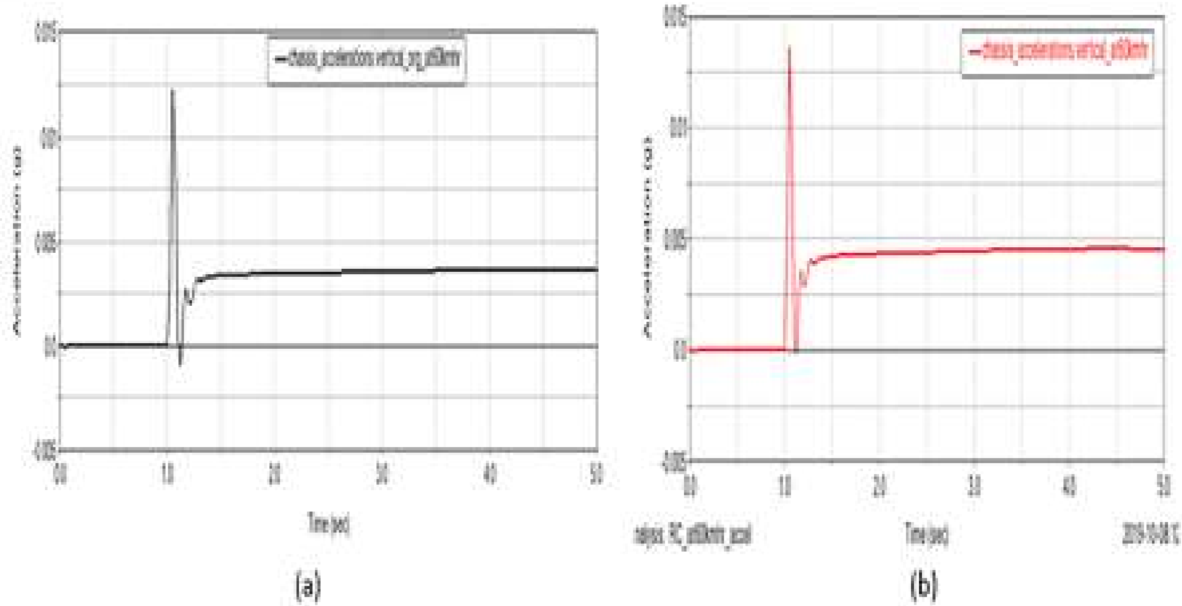

Figure 7. 7 Sprung mass vertical acceleration at 60km/hr (a) original model (b) optimized model

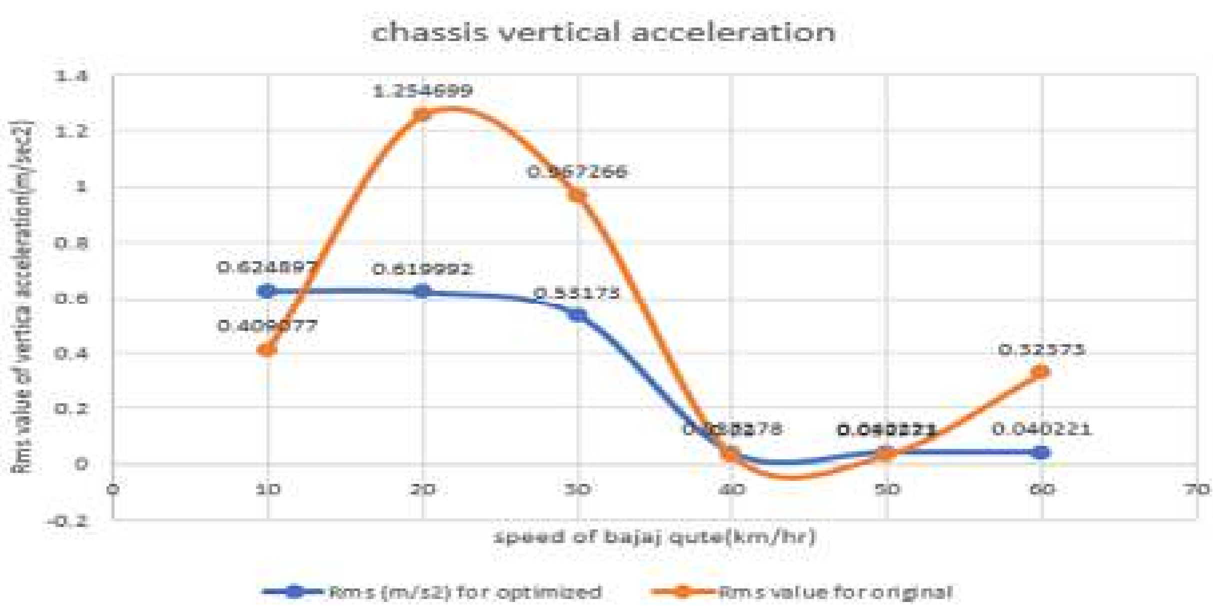

Figure 7. 8 Rms value of sprung mass vertical acceleration Vs speed of bajaj qute

From fig 7.1 up to 7.6 the vertical sprung mass of Bajaj qute relative to times are displayed. With an initial speed of 10km/hr of Baja qute, the Rms acceleration of original Bajaj qute was better than the optimized. The rms value of the original model at10km/hr initial speed is 0.409077m/sec^2. But the rms value of the optimized model is 0. 624897. When we go to 20km/hr, and 30km/hr of the initial speeds, the ride comfort of the original model is significantly better than the original model. The Rms value for optimized model is 0.619992 m/sec^2, and 0.53172 m/sec^2 for 20km/hr and 30 km/hr respectively. But, the rms value of original model is 1.254699 m/sec^2, and 0.967266 m/sec^2 for 20 km/hr and 30 km/hr, respectively. For 40km/hr up to 60 km/hr the value of Rms value for both models are approximately the same. However, the graph shows that after 60 km/hr, the ride comfort for optimized model is better than the original. In general, Rms vertical acceleration Vs speed of the Bajaj qute is depicted in the Fig 7.7 that the ride comfort behavior of the optimized model is much better than the original model even though both models' vertical sprung mass Rms acceleration is in the limiting range. Note that the road used in this work is standard flat road.

CHAPTER EIGHT
CONCLUSION AND RECOMMENDATION

Under this topic the main objective of the thesis and the result brought by the analysis are discussed. Future works are recommended for better approach which are not addressed in this paper or approaches which helps us to virtualize the analysis.

CONCLUSION

As a conclusion, suspension parameters have significant effect on lateral behavior and ride comfort quality of motor vehicles. The structural analysis done on lower control arm of front suspension also shows that the Bajaj qute lower control arm carry more strength than the required. The results relating with specific objectives are discussed as follows.

I. Literatures shows that control arm of cars carry more strength than the required. FEA is applied to make analysis whether lower control arm of front suspension system can withstand the applied load by using maximum von mises stress, deformation, and fatigue life. The result showed that the load applied is significantly less than the strength of arm. Topology optimization is made with constant fatigue life (fatigue life as constraint) to optimize the weight of the lower control arm.

II. Rollover propensity of Bajaj qute is analyzed based on suspension parameters optimizations in order to improve lateral behavior and cornering performance. Initially, the original modeled Bajaj qute fishhook speed was 50km/hr. The optimization analysis for roll behavior of bajaj qute implied that it can make fishhook maneuver up to 65km/hr. However, the bajaj qute movement becomes sinusoidal and it may have an effect on the structure and can create unprecedent accidents. Hence, the fishhook speed of the bajaj qute is limited to 60km/hr.

III. Ride comfort and road holding are two parameters which has to be studied side by side. Changing of one parameter affects the other. There is no cut-off decision which used to decide road holding behavior of a car. But the reality is, increasing the roll over performance of bajaj qute increases the road holding behavior of bajaj qute. Hence, to verify the ride comfort of bajaj qute for the original and optimized model by using standard ISO 2635, Rms value of sprung mass vertical acceleration is calculated for both models.

From the Rms chart we can understand that the optimized model is more comfortable than the original one.

RECOMMENDATIONS

There are different kinds of suspension parameter which have effect on rollover behavior of bajaj qute. In this paper toe, camber, caster, and kingpin inclination are used for analysis. Roll center height still also have significant effect on the roll over behavior, but it is not including on this analysis. Because the above listed parameter are wheel alignment parameters but roll centers are related to geometry of suspension in designing of the suspension system and it is more primary. Hence, it is better to work for roll center height.

Now a day's loads applied are not regularly cyclic or the amplitude is not constant. In this paper constant amplitude fatigue life analysis is done. To make the result more realistic, it is better to model for variable amplitude. The ride comfort of bajaj qute is verified based on ISO 2635. ISO standards are designed for on road vehicles (flat road), but in our country (Ethiopia) most passenger cars are off road. So, the applicability standards for off road vehicles should be studied.

REFERENCES

[1] A. C. Mitra, T. Soni, and G. R. Kiranchand, "Optimization of Automotive Suspension System by Design of Experiments: A Nonderivative Method," *Adv. Acoust. Vib.*, vol. 2016, 2016.

[2] A. Hac, "Rollover Stability Index Including Effects of Suspension Design," *SAE World Congr.*, vol. 2002, no. 724, 2002.

[3] M. Walz, "Trends in the static stability factor of passenger cars, light trucks, and vans," *NHTSA Tech. Reportwashingt.*, no. June, p. 37, 2005.

[4] A. Debebe, "Stability Analysis of Four Wheeler Bajaj (Bajaj Qute)," no. November, 2018.

[5] E. Sert and P. Boyraz, "Optimization of suspension system and sensitivity analysis for improvement of stability in a midsize heavy vehicle," *Eng. Sci. Technol. an Int. J.*, vol. 20, no. 3, pp. 997–1012, 2017.

[6] T. Shim and P. C. Velusamy, "Improvement of vehicle roll stability by varying suspension properties," *Veh. Syst. Dyn.*, vol. 49, no. 1–2, pp. 129–152, 2011.

[7] J. R. Wilde, G. J. Heydinger, D. A. Guenther, T. Mallin, and A. M. Devenish, "Experimental Evaluation of Fishhook Maneuver Performance of a Kinetic Suspension System," vol. 2005, no. 724, 2018.

[8] S. S. Jambukar and C. Sujatha, "Study of the effects of caster offset and kingpin offset on kinematics and lateral dynamics of long wheelbase solid axle bus STUDY OF THE EFFECTS OF CASTER OFFSET AND KINGPIN OFFSET ON," no. March 2019, 2017.

[9] C. Constant, "Suspension design: definitions and effects on vehicle behavior 16," pp. 1–10, 2019.

[10] L. X. Long and L. Van Quynh, "Study on the influence of bus suspension parameters on ride comfort," no. February, 2019.

[11] A. Fahmi, M. Riduan, and N. Tamaldin, "Review on active suspension system," vol. 02008, pp. 1–8, 2018.

[12] A. Goodarzi and A. Khajepour, "Vehicle Suspension System Technology and Design," pp. 2–4, 2017.

[13] G. N. Jazar, R. Alkhatib, and M. F. Golnaraghi, "Root mean square

optimization criterion for vibration behaviour of linear quarter car using analytical methods," *Veh. Syst. Dyn.*, vol. 44, no. 6, pp. 477–512, 2006.

[14] M. Kazemi, K. Heydari Shirazi, and A. Ghanbarzadeh, "Optimization of semi-trailing arm suspension for improving handling and stability of passenger car," *Proc. Inst. Mech. Eng. Part K J. Multi-body Dyn.*, vol. 226, no. 2, pp. 108–121, 2012.

[15] S. Banerjee, V. Balamurugan, and R. Krishnakumar, "Ride Comfort Analysis of Math Ride Dynamics Model of Full Tracked Vehicle with Trailing Arm Suspension," *Procedia Eng.*, vol. 144, pp. 1110–1118, 2016.

[16] A. C. Mitra, G. J. Desai, S. R. Patwardhan, P. H. Shirke, W. M. H. Kurne, and N. Banerjee, "Optimization of Passive Vehicle Suspension System by Genetic Algorithm," *Procedia Eng.*, vol. 144, pp. 1158–1166, 2016.

[17] D. R. Naidu and P. P. D. Rao, "Design and Analysis of Coilspring for Two and Three Wheelers," no. Xxxix, pp. 182–187.

[18] J. Gao and K. Chen, "Frequency-domain simulation and analysis of vehicle ride comfort based on virtual proving ground," *Int. J. Intell. Eng. Syst.*, vol. 4, no. 3, pp. 1–8, 2011.

[19] Z. Chi, Y. He, and G. F. Naterer, "Design Optimization Of Vehicle Suspensions With A Quarter-Vehicle Model," *Trans. Can. Soc. Mech. Eng.*, vol. 32, no. 2, pp. 297–312, 2008.

[20] I. O. P. C. Series and M. Science, "Investigating the effects of roll center height in simulation , for safety- margin research Investigating the effects of roll center height in simulation , for," 2018.

[21] J. Zhang, J. Pei, and J. Zhang, "The Optimization Study of the Front Suspension Structure Parameters for the Mine Truck Based on Adams / car," no. Icvmee, 2016.

[22] V. Goga and M. Kl'Účik, "Optimization of vehicle suspension parameters with use of evolutionary computation," *Procedia Eng.*, vol. 48, pp. 174–179, 2012.

[23] Dhurai Prabhahar, "Optimization and Effects of Suspension Parameter on Front Suspension of SAE Baja Vehicle using ADAMS," *Int. J. Eng. Res.*, vol. V5, no. 09, pp. 83–87, 2016.

[24] J. Yang and M. Dong, "Research on Vibration of Automobile Suspension

Design," vol. 04008, pp. 3–6, 2018.

[25] Example, "Design of Experiments Tutorial," 2017.

[26] A. T. Guide, "Using ADAMS / Insight with ADAMS / Chassis."

[27] C. Du, B. Zhu, H. Wang, X. Mai, and T. Qin, "Design and Optimization of Front Suspension of FSAE based on ADAMS Simulation," vol. 136, no. Icsma, pp. 538–543, 2017.

[28] R. Larsson, "Methodology for topology and shape optimization: Application to a rear lower control arm," 2016.

[29] U. Schramm, H. Thomas, and M. Zhou, "Manufacturing Considerations and Structural Optimization for Automotive Components," *SAE Tech. Pap. Ser.*, vol. 1, no. 724, 2010.

[30] J. Marzbanrad and A. Hoseinpour, "Structural optimization of MacPherson control arm under fatigue loading," *Teh. Vjesn. - Tech. Gaz.*, vol. 24, no. 3, pp. 917–924, 2017.

[31] H. Singh and G. Bhushan, "Finite Element Analysis of a Front Lower Control Arm of LCV Using Radioss Linear," no. April 2012, pp. 121–125, 2016.

[32] J. Liu and Y. Ma, "Advances in Engineering Software A survey of manufacturing oriented topology optimization methods," *Adv. Eng. Softw.*, vol. 100, pp. 161–175, 2016.

[33] D. Detwiler, "DETC2017-68192," pp. 1–10, 2017.

[34] L. Zhao, J. Ma, T. Wang, and D. Xing, "Lightweight Design of Mechanical Structures based on Structural Bionic Methodology," *J. Bionic Eng.*, vol. 7, pp. S224–S231, 2010.

[35] K. Kadirgama, M. M. Noor, and R. Rejab, "Fatigue Life Prediction of Lower Suspension Arm Using Strain-Life Approach," no. May, 2009.

[36] A. M. Puranik, P. V. M. Bansode, P. S. N. Jadhav, and A. P. Y. C, "Durability Analysis and optimization of an Automobile Lower Suspension Arm Using FEA and Experiment Technique," pp. 1381–1389, 2018.

[37] L. X. Long, L. Van Quynh, and B. Van Cuong, "Study on the influence of bus suspension parameters on ride comfort," *Vibroengineering Procedia*, vol. 21, pp. 77–82, 2018.

[38] G. Dahanu and Prof.r.s.kattimani, "Comparision Study of Lower Control Arm With Different Material," *Int. Res. J. Eng. Technol.*, vol. 3, no. 10, pp. 702–708, 2016.

[39] L. Li and Q. Li, "Vibration Analysis Based on Full Multi-Body Model for the Commercial Vehicle Suspension System," *6th WSEAS Int. Conf. Signal Process. Robot. Autom.*, pp. 203–207, 2007.

[40] P. Andrea *et al.*, "Stress analysis of a suspension control arm To cite this version : HAL Id : hal-01916247," 2018.

[41] T. A. and P. N. Kale AR*, "Analysis and Optimization of Lower Control Arm_ Crimson Publishers," *Evol. Mech. Eng.*, vol. 1, pp. 1–6, 2018.

[42] A. Van Berkum, P. C. J. N. Rosielle, and M. Steinbuch, "Chassis and suspension design FSRTE02 Dutch summary," no. March, 2006.

[43] T. Optimization, "4. topology optimization 4.1," pp. 72–111.

[44] B. S. Lazarov, F. Wang, and O. Sigmund, "Length scale and manufacturability in density-based topology optimization Length scale and manufacturability in density based topology optimization," no. April, 2016.

[45] C. Groth and M. Evangelos, "ScienceDirect Automatic Automatic shape shape optimization optimization of of structural structural components components with with manufacturing constraints manufacturing constraints Thermo-mechanical modeling of a high pressure turbine blade airplane ga," *Procedia Struct. Integr.*, vol. 12, pp. 416–428, 2018.

[46] J. F. V. Vincent and D. L. Mann, "Systematic technology transfer from biology to engineering," *Philos. Trans. R. Soc. A Math. Phys. Eng. Sci.*, vol. 360, no. 1791, pp. 159–173, 2002.

[47] C. Mattheck and S. Burkhardt, "A n e w method of structural shape optimization based on biological growth," vol. 3, no. 3, pp. 185–190, 1990.

[48] B. Gadade and R. G. Todkar, "Design , analysis of A-type front lower suspension arm in Commercial vehicle," pp. 759–766, 2015.

[49] M. Fahrurrazi and B. Jubri, "Design and development of car suspension lower arm," no. December, 2015.

[50] M. Hafizi, A. Rahman, M. S. Salleh, M. Suffian, A. Razak, and M. R. Mohamad, "Design and Optimization of Front Lower Control Arm (FLCA)

for C - Segment Passenger Car," vol. 7, pp. 71–75, 2018.

[51] "ADAMS / Car."

[52] H. Adams, "Adams H.-Chassis Engineering _ Конструирование шасси.pdf." .

[53] M. Software, "Adams Car," 2017.

[54] B. Shuya zhi1, a Yang Luo2, "Car Suspension Simulation and Optimization Shuya zhi," vol. 529, pp. 636–640, 2014.

[55] A. Staniforth, "Competition_Car_Suspension.pdf." 1999.

[56] A. Postprocessor and A. A. Postprocessor, "Welcome to Adams / Post Processor."

[57] A. Goodarzi and A. Khajepour, *Vehicle Suspension System Technology and Design*. 2017.

[58] D. V. Wale, "Modelling and Simulation of Full Vehicle for Analysing Kinematics and Compliance Characteristics of Independent (Macpherson strut) and Semi Independent (Twist Beam) suspension system," pp. 16–20.

[59] R. W. Allen, D. H. Klyde, T. J. Rosenthal, and D. M. Smith, "Estimation of Passenger Vehicle Inertial Properties and Their Effect on Stability and Handling," vol. 2003, no. 724, 2018.

[60] S. Navigation and N. S. Route, "A Study of Vehicle Properties That Influence Rollover and Their Effect on Electronic Stability Controllers Except," vol. 2007, pp. 44–45.

[61] N. Car and A. Program, "Laboratory Test Procedure for Dynamic Rollover The Fishhook Maneuver Test Procedure," no. March, pp. 1–43, 2013.

[62] A. C. Mitra, T. Soni, G. R. Kiranchand, S. Khan, and N. Banerjee, "Experimental Design and Optimization of Vehicle Suspension System," *Mater. Today Proc.*, vol. 2, no. 4–5, pp. 2453–2462, 2015.

[63] M. Passmore, *Ground Vehicle Aerodynamics: Racecar Aerodynamics*. .

[64] J. Liang and L. Xin, "Simulation analysis and optimization design of front suspension based on ADAMS," *Mechanika*, vol. 18, no. 3, pp. 337–340, 2012.

[65] V. Thulasi, "Simulated Study on the Effect of Camber and Toe on the Handling Characteristics of a Car during Cornering," no. January 2013, 2016.

[66] P. S. Els, "The applicability of ride comfort standards to off-road vehicles," *J. Terramechanics*, vol. 42, no. 1, pp. 47–64, 2005.

[67] A. C. Mitra, M. V. Patil, and N. Banerjee, "Optimization of Vehicle Suspension Parameters for Ride Comfort Based on RSM," *J. Inst. Eng. Ser. C*, vol. 96, no. 2, pp. 165–173, 2015.

[68] P. E. Uys, P. S. Els, and M. Thoresson, "Suspension settings for optimal ride comfort of off-road vehicles travelling on roads with different roughness and speeds," *J. Terramechanics*, vol. 44, no. 2, pp. 163–175, 2007.

[69] A. Sezgin and N. Yagiz, "Analysis of passenger ride comfort," *MATEC Web Conf.*, vol. 1, no. May 2014, 2012.

[70] T. H. E. Ride, C. Vs, and H. Decision, "The ride comfort vs. handling decision," 2002.

APPENDIX A

ENGINE

Type	Four stroke, spark ignition, single cylinder engine, liquid cooled		Max. Speed	70km/h ,5th gear
Max. Power	9.9 kw at 5500Rpm		Displacement	217cc
Max. Torque	19.6Nm at 4000Rpm		Clutch	Wet Multi-Disc clutch

BRAKE AND TIRES

Brake Type	Hydraulic with H-split,right foot operated control	Front tire size(width and radius)	101mm/R203mm
Brake SIze	All drum, Dia. 180mm	Rear tire size(width and radius)	101mm/R203mm

VEHICLES

Frame type	Monocoque Chassis		Ground Clearance	180mm (this is the distance between the ground and the underside of the vehicle chassis)
Length*Width*Height	2752mm*1312mm*1652mm		Kerb Weight	399Kg (the weight of motor car without occupant)
Wheel Base	1925mm		Fuel tank (Reserve)	8L (including 1 liter reserve)

Suspension Front	Independent Suspension. Twin leading arm		Suspension Rear	Independent Suspension. Coil spring, semi-trailing arm.
Turning radius	3.5 meters		Front and Rear Track	1143mm

CAPACITY

Seating capacity	4(1+3)
Number of seating rows	2 rows
Number of doors	4 Doors
Boot space	44 litres

ELECTRICAL

System	12 volt DC –ve earth		Battery	12volt , 26AH
Head Lamps	35*35 WHS1		Tail Lamp	5/21 W
Side Indictor Lamp	10 W		Reverse Lamp	10W
Horn	12VDC_Dia 82		Wiper Motor	12volts, single speed

APPENDIX B Hardpoint modification and trials for rollover optimization

no	front_sus_two.ground.hpl_lower_arm_front.x	front_sus_two.ground.hpl_lower_arm_front.y	front_sus_two.ground.hpl_lower_arm_front.z	front_sus_two.ground.hpl_lower_arm_rear.x	front_sus_two.ground.hpl_lower_arm_rear.y	front_sus_two.ground.hpl_lower_arm_rear.z	front_sus_two.ground.hpl_lower_control_arm_inner.x	front_sus_two.ground.hpl_lower_control_arm_inner.y
1	-536.43	-572.77	-145	-180	-566	-165	-180	-246
2	-536.43	-572.77	-145	-180	-546	-145	-180	-246
3	-516.43	-572.77	-165	-180	-546	-165	-180	-266
4	-516.43	-572.77	-165	-160	-546	-145	-180	-266
5	-516.43	-552.77	-165	-180	-546	-145	-160	-246
6	-516.43	-552.77	-145	-180	-566	-145	-160	-246

front_sus_two.ground.hpl_lower_control_arm_inner.z	front_sus_two.ground.hpl_wheel_center.x	front_sus_two.ground.hpl_wheel_center.y	front_sus_two.ground.hpl_wheel_center.z	front_sus_two.ground.hpl_wheel_carrier_upper.x	front_sus_two.ground.hpl_wheel_carrier_upper.y	front_sus_two.ground.hpl_wheel_carrier_upper.z	front_sus_two.ground.hpl_tierod_outer.x	front_sus_two.ground.hpl_tierod_outer.y
-145	-530	-616	-65	-523.75	-493.48	257.52	-626.64	-464
-145	-530	-596	-45	-523.75	-493.48	257.52	-626.64	-484
-165	-530	-616	-45	-523.75	-513.48	257.52	-606.64	-484
-165	-530	-596	-45	-503.75	-513.48	257.52	-606.64	-464
-145	-510	-596	-45	-523.75	-513.48	277.52	-606.64	-464
-145	-510	-596	-65	-523.75	-493.48	277.52	-606.64	-464

front_sus_two.ground.hpl_tierod_outer.z	front_sus_two.ground.hpl_upper_control_arm_outer.x	front_sus_two.ground.hpl_upper_control_arm_outer.y	front_sus_two.ground.hpl_upper_control_arm_outer.z	front_sus_two.ground.hpl_upper_control_arm_inner.x	front_sus_two.ground.hpl_upper_control_arm_inner.y	front_sus_two.ground.hpl_upper_control_arm_inner.z	front_sus_two.ground.hpl_strut_lower.x	front_sus_two.ground.hpl_strut_lower.y
275	-330	-516	271.64	-330	-340	281.77	-490	-416
255	-330	-516	271.64	-350	-320	261.77	-470	-416
275	-330	-496	251.64	-350	-340	281.77	-470	-396
275	-350	-516	271.64	-350	-340	261.77	-490	-396
275	-330	-496	251.64	-350	-340	261.77	-490	-416
255	-350	-516	251.64	-350	-340	281.77	-470	-396

front_sus_two.ground.hpl_strut_lower.z	front_sus_two.ground.hpl_strut_upper.x	front_sus_two.ground.hpl_strut_upper.y	front_sus_two.ground.hpl_strut_upper.z	front_sus_two.ground.hpl_spring_lower.x	front_sus_two.ground.hpl_spring_lower.y	front_sus_two.ground.hpl_spring_lower.z	front_sus_two.ground.hpl_tierod_inner.x	front_sus_two.ground.hpl_tierod_inner.y
-165	-310	-396	255	-448	-396	-115	-660	-240
-165	-290	-416	275	-468	-396	-115	-660	-260
-165	-310	-416	275	-448	-396	-115	-680	-260
-165	-290	-396	275	-448	-416	-95	-660	-260
-165	-310	-416	255	-468	-416	-95	-660	-240
-145	-290	-396	255	-468	-416	-115	-680	-260

front_sus_two.ground.hpl_tierod_inner.z	front_sus_two.ground.hpl_sub_frame_inner.x	front_sus_two.ground.hpl_sub_frame_inner.y	front_sus_two.ground.hpl_sub_frame_inner.z	front_sus_two.ground.hpl_sub_frame_rear.x	front_sus_two.ground.hpl_sub_frame_rear.y	front_sus_two.ground.hpl_sub_frame_rear.z	front_sus_two.ground.hpl_droplink_external.x	front_sus_two.ground.hpl_droplink_external.y
275	-10	-246	-165	-10	-566	-165	-310	-410
255	-10	-266	-145	-30	-546	-165	-310	-410
275	-30	-266	-165	-10	-546	-145	-330	-410
255	-30	-246	-145	-10	-546	-165	-310	-390
275	-10	-246	-145	-10	-546	-145	-330	-410
275	-10	-246	-145	-30	-566	-165	-330	-410

front_sus_two.ground.hpl_droplink_external.z	twin_leading_arm_suspension_system_rear.ground.hpl_arm_outer_pivot.x	twin_leading_arm_suspension_system_rear.ground.hpl_arm_outer_pivot.y	twin_leading_arm_suspension_system_rear.ground.hpl_arm_outer_pivot.z	twin_leading_arm_suspension_system_rear.ground.hpl_arm_inner_pivot.x	twin_leading_arm_suspension_system_rear.ground.hpl_arm_inner_pivot.y	twin_leading_arm_suspension_system_rear.ground.hpl_arm_inner_pivot.z	twin_leading_arm_suspension_system_rear.ground.hpl_spring_lower_seat.x	twin_leading_arm_suspension_system_rear.ground.hpl_spring_lower_seat.y
-165	1515	-666	110	1535	-355	110	1855	-566
-145	1535	-666	110	1515	-375	110	1855	-586
-165	1535	-666	90	1515	-355	90	1855	-566
-165	1515	-666	90	1535	-355	110	1855	-586
-165	1515	-666	90	1515	-375	110	1855	-566
-165	1535	-646	110	1535	-375	90	1855	-566

twin_leading_arm_suspension_system_rear.ground.hpl_spring_lower_seat.z	twin_leading_arm_suspension_system_rear.ground.hpl_spring_upper_seat.x	twin_leading_arm_suspension_system_rear.ground.hpl_spring_upper_seat.y	twin_leading_arm_suspension_system_rear.ground.hpl_spring_upper_seat.z	twin_leading_arm_suspension_system_rear.ground.hpl_arm_strut_bushing.x	twin_leading_arm_suspension_system_rear.ground.hpl_arm_strut_bushing.y	twin_leading_arm_suspension_system_rear.ground.hpl_arm_strut_bushing.z	twin_leading_arm_suspension_system_rear.ground.hpl_top_mount.x	twin_leading_arm_suspension_system_rear.ground.hpl_top_mount.y
230	1855	-586	390	1855	-586	90	1835	-586
250	1835	-566	390	1855	-586	110	1855	-586
250	1835	-586	390	1855	-566	110	1835	-566
230	1835	-586	410	1835	-586	110	1855	-566
250	1855	-566	410	1835	-586	90	1835	-586
250	1835	-586	390	1835	-586	90	1855	-566

twin_leading_arm_suspension_system_rear.ground.hpl_top_mount.z	twin_leading_arm_suspension_system_rear.ground.hpl_subframe_front.x	rear.ground.hpl_subframe_front.y	rear.ground.hpl_subframe_front.z	rear.ground.hpl_subframe_rear.x	rear.ground.hpl_subframe_rear.y	rear.ground.hpl_subframe_rear.z	rear.ground.hpl_arm_strut_bushing_x.x	rear.ground.hpl_arm_strut_bushing_x.y
410	1372.5	-700	110	1942.5	-366	90	1752.5	-590
410	1352.5	-720	110	1942.5	-366	110	1772.5	-590
410	1372.5	-720	110	1942.5	-346	110	1752.5	-570
410	1352.5	-720	90	1942.5	-346	90	1752.5	-590
390	1352.5	-720	110	1942.5	-346	110	1772.5	-590
410	1372.5	-720	90	1942.5	-346	110	1752.5	-590

rear.ground.hpl_arm_strut_bushing_x.z	rear.ground.hpl_arm_strut_bushing_z.x	rear.ground.hpl_arm_strut_bushing_z.y	rear.ground.hpl_arm_strut_bushing_z.z	rear.ground.hpl_wheel_center.x	rear.ground.hpl_wheel_center.y	rear.ground.hpl_wheel_center.z	rear.ground.hpl_drive_shaft_inr.x	rear.ground.hpl_drive_shaft_inr.y
110	1752.5	-605	90	1915	-666	110	1892.5	-190
110	1752.5	-605	110	1935	-666	110	1892.5	-210
110	1752.5	-585	90	1935	-646	110	1892.5	-210
110	1752.5	-605	90	1915	-646	110	1872.5	-210
90	1732.5	-605	110	1935	-646	110	1892.5	-210
110	1752.5	-605	90	1935	-646	110	1872.5	-210

rear.ground.hpl_drive_shaft_inr.z	roll_angle
160	0.035504
140	0.050769
160	3.56786
140	3.61625
140	3.35923
160	3.43561